Kazakh Physical Society

KAZAKH KBTU BRITISH
TECHNICAL
UNIVERSITY

Second Annual Meeting of Kazakh Physical Society

June 6-8, 2019, Almaty

SECOND ANNUAL MEETING OF KAZAKH PHYSICAL SOCIETY

June 6-8, 2019, Kazakh-British Technical University

Chair: Prof. T. A. Kozhamkulov, President of KPS
Co-Chairs: Prof. T. S. Ramazanov, Vice-President of KPS, Al Farabi Kazakh National University,
Prof. K.A. Baigarin, Head of Nur-Sultan Branch of KPS, Nazarbayev University
Prof. M.T. Gabdullin, Head of Almaty Branch of KPS, Kazakh-British technical University

Scientific Program Committee:
KazNU: T.A. Kozhamkulov, T.S. Ramazanov, A.E. Davletov, M. E. Abishev, N.Zh. Takibayev, K.N. Dzhumagulova;
NU: K.A. Baigarin, A. Nurmukhanbetova, Z. Utegulov, A. Tikhonov, A. Desyatnikov, A. Zhumabekov, A. Bountis, M. Kaikanov;
ENU: R. Myrzakulov, A. K. Aryngazin;
KBTU: M.T. Gabdullin, K.Kh. Nussupov, N.B. Beisenkhanov, D.I. Bakranova;
KazNTU: S.E. Kumekov, R. Beisenov;
KazNPU: A.I. Kupchishin, V.N. Kosov;
NNC: E.G. Batyrbekov, M.K. Skakov;
INP: E. Kenzhin, N.T. Burtebayev, T. Zholdybayev, M. Zdorovets;
PTI: T.K. Sadykov, A. Serikkanov;
FAPI: L.M. Chechin, M. Dubovichenko;
ISR: Ch. Omarov;
II: V.M. Somsikov, O.N. Krikunova;
KSU: N. Ibrayev
TSHVNS: V.V. Zhukov
ZhSU: E.S. Andasbaev

Local Organizing Committee:
Almaty Branch of KPS
Kazakh-British Technical University

PROGRAM
SECOND ANNUAL MEETING OF KAZAKH PHYSICAL SOCIETY
Kazakh-British Technical University

Day 1
June 6, 2019

08:30 – 09:30	**REGISTRATION OF PARTICIPANTS OF THE CONFERENCE LONDON ROOM (404 ROOM)**
09:30 – 09:50	**ANNUAL MEETING OPENING** **Maratbek Gabdullin**, Head of Almaty Branch of KPS **Tolegen Kozhamkulov,** President of KPS **Kanat Baigarin,** Head of Astana Branch of KPS **Erlan Batyrbekov**, General Director of the RSE NNC RK **Bum-Hoon Lee,** President, Korean Physical Society
09:50 – 10:10	**Bum-Hoon Lee** Sogang University, Seoul, South Korea **Black Holes in the dilatonic Einstein-Gauss-Bonnet theory**
10:10 – 10:30	**Hernando Quevedo** National Autonomous University of Mexico, Mexico City, Mexico **Quasi-homogeneous black hole thermodynamics**
10:30 – 10:50	**Tlekkabul Ramazanov** Institute for Experimental and Theoretical Physics, Al-Farabi Kazakh National University, Almaty, Kazakhstan **Polarization and magnetic field effects in complex plasmas**
10:50 – 11:10	**Sergey Maiorov** Prokhorov General Physics Institute of the Russian Academy of Sciences, Moscow, Russia Joint Institute for High Temperature of the Russian Academy of Sciences, Moscow, Russia **On the ion drift in cold gas**
11:10 – 11:30	**Anton Desyatnikov** Nazarbayev University, Nur-Sultan, Kazakhstan **Optical vortex rings in nonlinear media**
11:30 – 11:50	**Alexander Shepetov** P.N.Lebedev Physical Institute (LPI), Tien-Shan Mountain Cosmic Ray Station, Moscow, Russia **Simultaneous observation of lightning emission in different wave ranges of the electromagnetic spectrum in Tien Shan mountains**
11:50 – 12:10	**Nassurlla Burtebayev** Institute of Nuclear Physics, Almaty, Kazakhstan **The interaction processes of the charged particles and light ions**

	with the p- and sd-shell nuclei for astrophysical and thermonuclear applications
12:10 – 12:30	**Alexandr Vurim** NNC RK (National Nuclear Center of the Republic of Kazakhstan), Kurchatov, Kazakhstan **Experimental Researches to Ensure Nuclear Power Safety at the Base of NNC RK Facilities**
12:30 – 14:00	**LUNCH BREAK**
14:00 – 14:15	**Nurzhan Beisenkhanov** Kazakh-British Technical University, Almaty, Kazakhstan **Physical Properties of Epitaxial Silicon Carbide Films, Grown by Atomic Substitution on the High-resistance (111) Oriented Silicon**
14:15 – 14:30	**Askhat Jumabekov** Department of Physics, Nazarbayev University, Nur-Sultan, Kazakhstan **Semitransparent Back-Contact Perovskite Solar Cells**
14:30 – 14:45	**Vladimir Kossov** **Olga Fedorenko** Abai Kazakh National Pedagogical University, Almaty, Kazakhstan **Special Regimes under Diffusion in Gaseous Mixtures**
14:45 – 15:00	**Askar Davletov** Al-Farabi Kazakh National University, Almaty, Kazakhstan **Roton structure of dust-acoustic wave spectrum of complex plasmas with finite-size particles**
15:00 – 15:15	**Vladimir Dzhunushaliev** Institute for Experimental and Theoretical Physics, Al-Farabi Kazakh National University, Almaty, Kazakhstan **Non-Abelian Proca-Dirac-Higgs theory: particle-like solutions and a mass gap**
15:15 – 15:30	**Vladimir Messerle** Combustion Problems Institute of Ministry of Education and Science of Kazakhstan, Almaty, Kazakhstan **Plasma Application for Uranium-Containing Solid Fuels Processing**
15:30 – 16:00	**COFFEE BREAK**
16:00 – 16:15	**Nurgali Takibayev** al-Farabi Kazakh National University, Almaty, Kazakhstan **Induced Processes and Reactions in Neutron Star Crusts**
16:15– 16:30	**Alma Dauletbekova** L.N. Gumilyov Eurasian National University, Nur-Sultan, Kazakhstan **Synthesis of nanocrystals in SiO2/Si track template by**

	electrochemical deposition of Zn"
16:30 – 16:45	**Leonid Chechin** Fesenkov Astrophysical Institute, Almaty, Kazakhstan **Ergali Kurmanov** Al-Farabi Kazakh National University, Almaty, Kazakhstan **On the theory of light propagation in the non-stationary gravitational lens. Problem formulation**
16:45 – 17:00	**Alexandr Ustimenko** Institute for Experimental and Theoretical Physics, Al-Farabi Kazakh National University, Almaty, Kazakhstan **Plasma Technology for Biomedical Waste Processing**
17:00 – 17:15	**Karlygash Dzhumagulova** Department of Physics, al–Farabi KazNU, Almaty, Kazakhstan **Optical reflectivity and dynamical conductivity of the dense semiclassical plasma on the basis of the effective potentials**
17:15 – 17:30	**Vyacheslav Somsikov** Physics of the geo-cosmos relation, Almaty, Kazakhstan **Nature of the determinism in physics**
17:30 – 17:45	**Zhandos Moldabekov** Institute for Experimental and Theoretical Physics, Al-Farabi Kazakh National University, Almaty, Kazakhstan **Dynamical structure factor of strongly coupled ions in warm dense matter**
17:45 – 18:00	**Alexander Tikhonov** Nazarbayev University **New high-current pulsed ion INURA accelerator facility at Nazarbayev University: new opportunities for advanced materials, nano science, plasma and charged beams physics**
18:00 – 18:15	**Koblandy Yerzhanov** L.N.Gumilyov Eurasian National University, Nur-Sultan, Kazakhstan **F(R,T,X,ϕ) cosmology solution involving one arbitrary function**
18:15 – 18:30	**Turlan Sadykov, Yernar Tautayev** Satbayev University, Institute of Physics and Technology, Almaty, Kazakhstan **Investigation of structures in the distribution of particles from the central area of extensive air showers on Hadron-55 installation**
18:30 – 18:45	**Aizhan Kuratova** Al-Farabi Kazakh National University, Almaty, Kazakhstan **Observation of CTA 102 Blazar on Tien-Shan Astronomical Observatory**
18:45 – 19:00	**Ruslan Irkimbekov** National Nuclear Center of the Republic of Kazakhstan, Kurchatov, Kazakhstan **IVG.1M research reactor conversion**

PROGRAM

SECOND ANNUAL MEETING OF KAZAKH PHYSICAL SOCIETY

Kazakh-British Technical University

Day 2
June 7, 2019

09:00 – 09:15	**Maratbek Gabdullin** Kazakh-British Technical University, Almaty, Kazakhstan **Dynamical and structural properties of dense plasmas**
09:15 – 09:30	**Medeu Abishev** Al Farabi National University, Almaty, Kazakhstan **Propagation of gravitational and electromagnetic waves through the magnetic field of the magnetar**
09:30 – 09:45	**Nurlan Tokmoldin** Institute of Physics and Technology, LLP, Satbayev University, Almaty, Kazakhstan **Heterojunction silicon solar cells**
09:45 – 10:00	**Zhandos Utegulov** Nazarbayev University, Nur-Sultan, Kazakhstan **Elastic property assessment of nanoscale-thick refractory metal films by nanosecond laser acoustics**
10:00 – 10:15	**Mukhit Muratov** NNLOT, Al-Farabi Kazakh National University, Almaty, Kazakhstan **Grain Surface Heating in Cryogenic Environment**
10:15 – 10:30	**Sandybek Kunakov** Al Farabi National University, Almaty, Kazakhstan **Fission fragments' and electrons'coupled Boltzmann equations and degradation energy spectra formation in a weakly ionized plasma irradiated by fission fragments**
10:30 – 10:50	**COFFEE BREAK**
10:50– 11:05	**Bolysbek Utelbayev** Kazakh-British Technical University, Almaty, Kazakhstan **The Hypothesis about Mechanism of Heat Transfer and The Nature of Its Carrier**
11:05 – 11:20	**Didar Batryshev**

	Al Farabi National University, Almaty, Kazakhstan **Investigation of carbon nanowalls synthesis by pecvd method**
11:20 – 11:35	**Daniele Malafarina** Nazarbayev University, Nur-Sultan, Kazakhstan **Observable properties of a black hole mimicker**
11:35 – 11:50	**Essen Suleimenov** Kazakh-British Technical University, Almaty, Kazakhstan **Effect of Non-Stationary Electric Current on The Oxide Meline System - Gas Phase**
11:50 – 12:05	**Chingiz Akniyazov** Fesenkov Astrophysical Institute, Almaty, Kazakhstan **Space debris cloud evolution; De-orbiting small space debris**
12:05 – 12:20	**Almasbek Utegenov** Institute for Experimental and Theoretical Physics, Al-Farabi Kazakh National University, Almaty, Kazakhstan **Properties of the Complex Plasma in the Radiofrequency Discharge With Imposed DC Field**
12:20 – 12:35	**Aigerim Tazhen** Institute for Experimental and Theoretical Physics, Al-Farabi Kazakh National University, Almaty, Kazakhstan **Experimental investigation of the properties of plasma-dust formations on pulsed plasma accelerator**
12:35 – 14:00	**LUNCH BREAK**
14:00 – 14:15	**Sagi Orazbayev** Institute for Experimental and Theoretical Physics, Al-Farabi Kazakh National University, Almaty, Kazakhstan **Synthesis of carbon nanoparticles in plasma medium and their application**
14:15 – 14:30	**Farid Umarov** Kazakh-British Technical University, Almaty, Kazakhstan **Particle-solid surface interactions**
14:30 – 14:45	**Gulzipa Sataeva** L.N. Gumilyov Eurasian National University, Nur-Sultan, Kazakhstan **Nanostructured Potassium Sulfate Crystals**
14:45 – 15:00	**Saken Toktarbay** Department of Theoretical and Nuclear Physics, Al-Farabi Kazakh National University, Almaty, Kazakhstan **Investigation of the stability of orbits by using the adiabatic theory of motion in General Relativity.**
15:00 – 15:15	**Nurlan Bakranov** Kazakh National Research Technical University after K.I. Satpayev, Almaty, Kazakhstan **Photoelectrochemical Application of Heterostructured Semiconductors**
15:15 – 15:30	**Timur Kulsartov** IETP, Al-Farabi Kazakh National University, Almaty, Kazakhstan Kazakh-British Technical University, Almaty, Kazakhstan

	Simulation of hydrogen isotopes absorption by metals under uncompensated pressure conditions
15:30 – 16:30	**COFFEE BREAK** **POSTER PRESENTATIONS** **Tour of KBTU (Center of Alternative Energy and Nanotechnologies and Round Hall)**
16:30 – 16:40	**Yerbolat Ussenov** NNLOT, Al-Farabi Kazakh National University, Almaty, Kazakhstan **Diagnostics of dusty plasmas with nanoparticles**
16:40 – 16:50	**Oxana Lyakhova** Branch "Institute of Radiation Safety and Ecology" NNC RK, Kurchatov, Kazakhstan **System of radiation monitoring of water and air environment on the Semipalatinsk Test Site**
16:50 – 17:00	**Askar Kassymov** Shakarim State University of Semey, Semey, Kazakhstan **Quantum concentration of the liquid**
17:00 – 17:10	**Kuralay Nurgaliyeva** Al Farabi National University, Almaty, Kazakhstan **Regular effects of non-equilibrium atmospheric gas – solar radiation system in theory and experiment**
17:10 – 17:20	**Ayan Mitra** Nazarbayev University, Nur-Sultan, Kazakhstan **Probing Uncertainty Relations in Non-Commutative Space through space based laser system: the case of nano- and pico-satellites fleet**
17:20 – 17:30	**Aiymgul Markhabayeva** Al-Farabi Kazakh National University, Almaty, Kazakhstan **Improved pseudocapacitive performance of w@wo3 structure**
17:30 – 17:40	**Yessenbek Aldakulov** Institute for Experimental and Theoretical Physics, Al-Farabi Kazakh National University, Almaty, Kazakhstan **Impact of neutral shadowing force on dust particles' structural and dynamical properties in cryogenic environment**
17:40 – 17:50	**Dina Bakranova** Kazakh-British Technical University, Almaty, Kazakhstan **Structural Properties of Epitaxial Silicon Carbide Films, Grown by Atomic Substitution on the Silicon**
17:50 – 18:00	**Kuralay Dyussebayeva** NNLOT, Al-Farabi Kazakh National University, Almaty, Kazakhstan **Study of the mechanisms of formation of modulation effects in the angular distributions of differential cross sections of elastically scattered alpha particles on light multi-cluster nuclei**
18:00 – 18:10	**Farida Kapsalamova** Kazakh-British Technical University, Almaty, Kazakhstan **Structural and phase transformations in wear resistant Fe-Ni-Cr-Cu-Si-B-C coatings**
18:10 – 18:30	**AWARDING CEREMONY** **ANNUAL MEETING CLOSING**

Black Holes in the dilatonic Einstein-Gauss-Bonnet theory

Bum-Hoon Lee
Sogang University
e-mail: bhl@sogang.ac.kr

Abstract : We investigate the properties of the Einstein-Gauss-Bonnet theory, in which the Gauss-Bonnet term is nonminimally coupled to the dilaton field. Hairy black holes with spherical symmetry seem to be easily constructed with a positive Gauss-Bonnet (GB) coefficient α within the coupling function, f(φ), in an asymptotically flat spacetime, i.e., no-hair theorem seems to be easily evaded in this theory. We study the properties of the black hole solution. Also, we iinvestigate whether this construction can be expanded into the case with the negative coefficient α. In this paper, we numerically present the dilaton black hole solutions with a negative α, and we analyze the properties of GB term through the aspects of the black hole mass. We construct the new integral constraint allowing the existence of the hairy solutions with the negative α. Through this procedure, we expand the evasion of the no-hair theorem for hairy black hole solutions.

References:

1. Expanded evasion of the black hole no-hair theorem in dilatonic Einstein-Gauss-Bonnet theory / Bum-Hoon Lee, Wonwoo Lee, Daeho Ro, Phys.Rev. D99 (2019) no.2, 024002

2. Phase transition for black holes in Dilatonic Einstein-Gauss-Bonnet theory of gravitation / Sunly Khimphun, Bum-Hoon Lee, Wonwoo Lee,**Phys.Rev. D94 (2016) 104067**

Quasi-homogeneous black hole thermodynamics

Hernando Quevedo
Institute of Nuclear Sciences – National Autonomous University of Mexico
e-mail: quevedo@nucleares.unam.mx

Abstract: Although the fundamental equations of ordinary thermodynamic systems are known to correspond to first-degree homogeneous functions, in the case of non-ordinary systems like black holes the corresponding fundamental equations are not homogeneous. We present several arguments, indicating that black holes should be described by means of quasi-homogeneous functions of degree different from one. In particular, we show that imposing the first-degree condition leads to contradictory results in thermodynamics and geometrothermodynamics of black holes. As a consequence, we show that in generalized gravity theories the coupling constants like the cosmological constant, the Born-Infeld parameter or the Gauss-Bonnet constant must be considered as thermodynamic variables.

Polarization and magnetic field effects in complex plasmas

T.S. Ramazanov, S.K. Kodanova, N. Kh. Bastykova, A. R.Abdirakhmanov, Zh.A. Moldabekov, M.K.Dosbolayev, M.T.Gabdullin

Institute for Experimental and Theoretical Physics, Al-Farabi Kazakh National University, 71 Al-Farabi ave., 050040 Almaty, Kazakhstan

e-mail: ramazan@physics.kz

The plasmas with micro- and/or nano-sized dust particles is referred to as complex (dusty) plasmas [1]. The investigation of the dynamics of strongly coupled system of charged particles, synthesis of nanoparticles, materials surface modification, contamination of thermonuclear fusion reactors are the examples of the active research problems in complex plasmas. In all this examples, plasma and dust particles polarization effects as well as external fields effects are important research topics [2-6].

As a rule, the laboratory complex plasmas are in a stationary non-equilibrium state. This leads to a different plasma polarization around charged dust particle than that of in equilibrium plasmas. The flow of ions relative to dust particles results in a dipole type interaction between particles. To account for this effect in a screening medium we have developed an analytical approach referred to as – multipole expansion in plasmas [2]. On the basis of the developed approach, we have studied the scattering processes in complex plasmas and found new interesting effects as zero angle scattering [3, 4].

To study the dust particles dynamics in partially magnetized complex plasmas, the experiments on dust particles rotation in the DC glow discharge in an external magnetic field were performed. In these experiments, the dust particles rotation direction is shown to depend on the angle between the magnetic field induction and electric field. Particularly, for the first time, the rotation due to the radial component of the magnetic field was observed. A simple analytical model describing the experimental observations is presented [5].

Furthermore, PIC/MCC simulation was used to study dust particles charging in plasmas in an external magnetic field. We found that an external magnetic field leads to the decrease of the density of electrons and ions in the vicinity of the dust particle. It was shown that at a strong magnetic field, the dust particle charge is significantly reduced and the charging time is extended. In the case B=4 T, which was recently realized on MDPX setup [65], the external magnetic field diminishes the dust particle (with the radius a = 8 μm and a = 4 μm) charge by more than 90 %. At such a strong magnetic field, the electrons are trapped along the magnetic field induction lines. This leads to the decrease of the electron flux on the surface of the dust particle. As the consequence, the absolute value of the dust particle charge also decreases, but the sign of the dust particle charge remains negative. Therefore, ions are weaker attracted to the dust particle in comparison to the case B=0.

References

1. V. E. Fortov and G. E. Morfill, Complex and Dusty Plasmas (CRC Press, 2010).
2. T.S. Ramazanov, Zh. A. Moldabekov, M.T. Gabdullin, Physical Review E 93, 053204 (2016).
3. S. K. Kodanova, T. S. Ramazanov, N. Kh. Bastykova, Zh. A. Moldabekov, IEEE Transaction on Plasma Science 44, 568 (2016).
4. N.Kh. Bastykova, S.K. Kodanova, T.S. Ramazanov, Zh.A. Moldabekov, Contribution to Plasma Physics 58, 198 (2018).
5. A. R. Abdirakhmanov , Zh. A. Moldabekov , S. K. Kodanova , M. K. Dosbolayev , and T. S. Ramazanov, , IEEE Transaction on Plasma Science (2019), doi 10.1109/TPS.2019.2906051 .
6. E. Thomas, Jr. U. Konopka, R. L. Merlino, M. Rosenberg, Phys. Plasmas 23, 055701 (2016).

On the ion drift in cold gas

S.A. Maiorov[1,2]

[1]*Prokhorov General Physics Institute of the Russian Academy of Sciences, Moscow, Russia*
[2]*Joint Institute for High Temperature of the Russian Academy of Sciences, Moscow, Russia*
e-mail: mayorov_sa@mail.ru

The problem of ion drift in such a strong electric field that the ion drift velocity significantly exceeds the thermal velocity of atoms is considered. In the case where the ion massis identical to the gas particle mass, scattering is isotropic in the center-of-mass system and the ion scattering cross section is independent of the collision velocity (hard sphere model). In the known solution to this problem [1], the ion velocity distribution function was set as the shifted two-temperature Maxwellian distribution

$$f_0\left(\bar{\mathrm{v}}\right)=\left(\frac{m}{2\pi T_i}\right)^{3/2}\exp\left(-\frac{m(u-W)^2}{2T_{||}}-\frac{m(\mathrm{v}^2+w^2)}{2T_{\perp}}\right), \qquad (1)$$

where $T_i=(T_{||}T_{\perp}^{\,2})^{1/3}$, and $T_{||}$ and $T_{\perp}$ - are the temperatures along and across the field, respectively. The parameters for the ion distribution function (1) were found from integral relations for average ion characteristics [1] and are written as $W=1.07\left(eE\lambda/m\right)^{1/2}$, $T_{||}=0.555eE\lambda$, $T_{\perp}=0.294eE\lambda$, where $\lambda=1/\sigma n$ is the mean free path, σ is the cross section of ion_atom collisions, and *n* is the numerical atomic density.

Table lists the results of Monte Carlo calculations of the drift velocity, longitudinal and transverse temperatures, the average ion energy, and diffusion coeffcients in longitudinal and transverse directions. We choose the quantities $u_\lambda=(eE\lambda/m)^{1/2}$ and $\varepsilon_\lambda=eE\lambda$ as characteristic velocities and energies, respectively. As a characteristic value of the diffusion coeffcient, we choose $D_\lambda=\lambda(eE\lambda/m)^{1/2}$, then the Chapman-Enskog diffusion coefficient for hard spheres is written as $D_{C-E}/D_\lambda=3\sqrt{\pi}/8\approx 0.66466$.

	W/u_λ	$\langle\varepsilon\rangle/\varepsilon_\lambda$	$T_{||}/\varepsilon_\lambda$	$T_{\perp}/\varepsilon_\lambda$	$D_{||}/D_\lambda$	$D_{\perp}/D_\lambda$
[1], approximate solutions	*1.07*		*0.555*	*0.294*		
[1], exact solution	*1.14*	*1.170*	*0.454*	*0.293*		
Monte Carlo [2]	*1.1467*	*1.1723*	*0.4431*	*0.2933*	*0.324*	*0.477*

The ion velocity distribution function is calculated by the Monte Carlo method, its characteristics and diffusion coeffient are determined. A comparison with known numerical and analytical solutions is performed. It is found that average characteristics (drift velocity, longitudinal and transverse temperatures) are in very good agreement with the values obtained from integral relations for the two-temperature Maxwellian distribution; however, the ion velocity distribution itself differs signiffcantly from the shifted two-temperature Maxwellian distribution.

This work was supported by the RFBR grant No. 19-08-00611a.

[1] B. M. Smirnov, *Physics of Weakly Ionized Gas in Problems with Solutions* (Nauka, Moscow, 1988)
[2] S. A. Maiorov, Bulletin of the Lebedev Physics Institute **46**, No. 1, pp. 9-12 (2019).

Optical vortex rings in nonlinear media

Anton S. Desyatnikov
Department of Physics and Center of Excellence for Fundamental and Applied Physics, School of Science and Technology, Nazarbayev University
e-mail: anton.desyatnikov@nu.edu.kz

Abstract: We study numerically vortex rings and vortex lines emerging during propagation of self-trapped wave beams in nonlocal nonlinear media. Together with spontaneous generation of a regular set of vortex rings at the periphery of radially perturbed solitons we observe the emergence of additional internal vortex-antivortex pairs nucleating from the edge-ring phase dislocation of perturbed higher-order soliton.

In nonlinear optical media, longitudinal dynamics of paraxial envelope $\psi(x,y,z)$ of a monochromatic laser beam is described by a Schrödinger-type equation [1] with the potential term proportional to the changes in the refractive index self-induced by a laser beam via Kerr-type effect,

$$i\partial\psi\partial z+\Delta\perp\psi+F(I)\psi=0\ ,\ (1)$$

here $\Delta\perp=\partial x2+\partial y2$ is transverse Laplacian and $I=|\psi|2$ is the intensity of a laser beam. The last term describes nonlinear modulation of the refractive index (I), e.g. $F(I)=I$ for pure Kerr nonlinearity, $F(I)=I/(1+I)$ for saturable and $F(I)=I-I2$ for cubic-quintic nonlinearities. In general, (I) can be nonlocal and anisotropic. For example, in thermal optical media $(I)=\theta(x,y,z)$ describes temperature perturbation coupled to intensity

$$\alpha\theta+\Delta\perp\theta=I,\ (2)$$

with the parameter α characterizing spatial extent of nonlocal response of the medium. Eq. 1 supports formation of spatial optical solitons [2] as well as nonlinear interaction between different waves. At the same time, in any system with multiple-wave interference, the so-called optical vortices appear naturally at points of total destructive interference, revealing twisted light and optical orbital angular momentum. In three dimensions vortex lines emerge as "threads of darkness"; these threads can be closed in loops and knots [3]. It is the nonlinear phase of the self-trapped light beam that breaks the wave front into a sequence of optical vortex rings, see Fig. 1(a). Similar conclusions regarding the nature of spontaneous vortex nucleation were reached in recent experimental observations of the spatiotemporal optic al vortex rings [4].

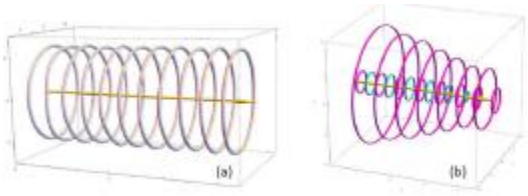

Fig. 1. (a) Spontaneous generation of a regular set of vortex rings around perturbed fundamental soliton; all vortices have the same direction of the twist [3, 5]. (b) Similar to fundamental soliton the external vortex rings are generated spontaneously around perturbed radial-mode soliton. However, the internal edge dislocation splits into sequence of alternating vortex-antivortex pairs [5].

Recently we confirmed [5] the generic nature of this phenomenon by demonstrating theoretically that vortex rings can be generated at the periphery of a fundamental soliton propagating in media with nonlocal modulation of the refractive index given by Eq. 2. A remarkable topological feature of radially perturbed higher-order solitons is the emergence of additional internal vortex antivortex ring pairs perpendicular to the optical axis, see Fig. 1(b). These vortex-antivortex pairs nucleate from the edge phase dislocation, or the dark intensity ring, and thus preserve conservation of topological charge and orbital angular momentum.

Vortex rings play a crucial role in the decay of superflow and in quantum turbulence in condensed-matter physics. Therefore, our findings may find use in other areas of physics as well as enrich our understanding of the role of topology in nonlinear dynamics.

[1] T. Uakhitov, A. Issakhanov, N. Ozat, and A. S. Desyatnikov, *Paraxial laser beams as versatile tool for modern photonics*, First Annual Meeting of Kazakh Physical Society, Nazarbayev University, Astana, 10-13 October (2018).

[2] A. S. Desyatnikov, Yu. S. Kivshar, and L. Torner, *Optical Vortices and Vortex Solitons*, Progress in Optics **47**, 291 (2005).

[3] A. S. Desyatnikov, D. Buccoliero, M. R. Dennis, and Yu. S. Kivshar, *Spontaneous knotting of self-trapped waves*, Scientific Reports **2**, 771 (2012)

[4] N. Jhajj, I. Larkin, E. W. Rosenthal, S. Zahedpour, J. K. Wahlstrand, and H. M. Milchberg, *Spatiotemporal Optical Vortices*, Phys. Rev. X **6**, 031037 (2016); **7**, 049901(E) (2017).

[5] V. Biloshytskyi, A. Oliinyk, P. Kruglenko, A. S. Desyatnikov, and A. Yakimenko, *Vortex nucleation in nonlocal nonlinear media*, Phys. Rev. A **99**, 043835 (2019).

Simultaneous observation of lightning emission in different wave ranges of the electromagnetic spectrum in Tien Shan mountains

A.L.Shepetov

P.. N. Lebedev Physical Institute of the Russian Academy of Sciences (LPI), Leninsky pr., 53, Moscow 119991, Russia

e-mail: ashep@tien-shan.org

Abstract: Simultaneous registration of electromagnetic emission generated by atmospheric lightning discharges in the radio-frequency (f = 0.1–30 MHz), infrared (λ = 610–800 nm), ultraviolet (λ = 240–380 nm), and in the soft energy gamma-radiation (Eγ = 0.1–4 MeV) ranges of electromagnetic spectrum was made synchronously in mountain conditions with complex detector system of the Tien Shan Mountain Cosmic Ray Station. We discuss preliminary results of these measurements and the perspectives of future application of the developing multispectral investigation technique to the study of the effects of thunderstorm activity..

1. Introduction

The photons of electromagnetic radiation seem to be most promising as information messengers on the phenomena which develop at the time of lightning initiation since they are abundantly generated in this process, and being electrically neutral they can reach rather significant distances from the discharge region. Presently, we attempt to detect the electromagnetic radiation generated by lightning with a set of radio, optic, and gamma ray detectors simultaneously to test the capabilities of multispectral investigation method in its application to the study of various kinds of lightning discharge. Preliminary results of this multispectral observation approach are the subject of the publication [1], as well as a discussion of the perspectives which the newly obtained experience in optic signal registration technique opens for the next stage of our thunderstorm investigation activity.

2. Results

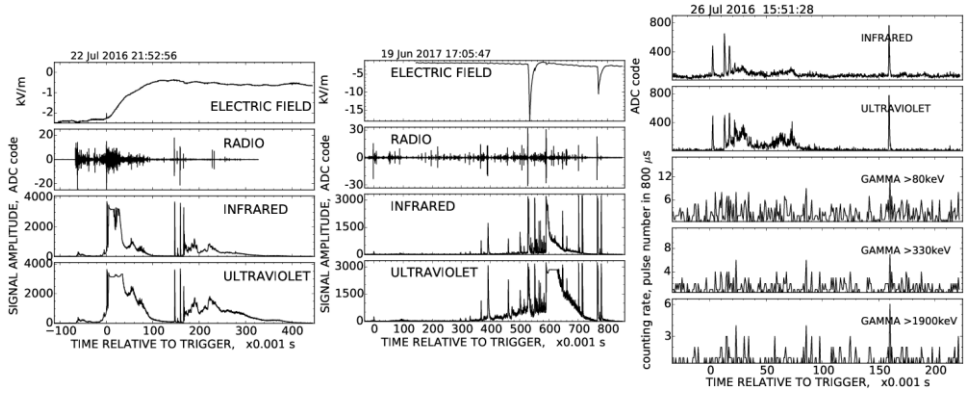

Fig. 1. A sample of the radiation intensity time series taken shortly after an atmospheric electric discharge: the 1-10MHz electromagnetic waves (*RADIO*), the 610–800 nm (*INFRARED*) and 240–380 nm (*ULTRAVIOLET*) wavelength light flashes, and the soft gamma ray emission with different energy thresholds (*GAMMA*). Zero point of the time axes coincides with the discharge moment.

It was found that mostly the development patterns of the infrared and ultraviolet flash from a lightning discharge correlate well both with each other and with that of the radio emission signal, but a variety of peculiar atmospheric discharge types has been revealed (see the Fig.1): (1) the" dark" electric discharges without significant optic radiation; (2) prolonged continuous optic flashes which last uninterruptedly about some milliseconds and "fill" the gaps between separate radio pulses from succeeding discharges; (3) short-time intensive optic flashes with sub-millisecond duration; (4) transient flashes with decisive predominance of UV range radiation in their optic spectrum; (5) inversely, the 'red' flashes with intensive IR signal and the absence of any noticeable ultraviolet radiation. In the time when the optic and radio emission detectors were operating together with a gamma ray detector the transient gamma radiation burst signal was seen from a thundery front in the energy range from ~100 keV and up to ~2 MeV. The duration of these bursts is about a few milliseconds or shorter, which complies well with duration of a typical TGF (terrestrial gamma flash events at extra-atmospheric satellites) but is much shorter than the TGE (terrestrial gamma radiation enhancements observed in the ground-based mountain experiments).

4. References

[1] A.V. Gurevicha et al, "Simultaneous observation of lightning emission in different wave ranges of electromagnetic spectrum in Tien Shan mountains", Atmospheric Research **211,** 73–84 (2018).

The interaction processes of the charged particles and light ions with the p- and sd-shell nuclei for astrophysical and thermonuclear applications

Burtebayev N.
Institute of Nuclear Physics, Almaty
e-mail: nburtebayev@yandex.ru

Abstract: Nuclear reactions with heavy ions are an intensively developing and productive direction of the modern nuclear research and also play an important role in field of applications such as nuclear astrophysics and nucleosynthesis, obtaining radioactive beams and superheavy elements, radiotherapy and surgery using heavy ions, etc. Can be used as a tool for analyzing the structure, properties of atomic nuclei and reaction mechanisms. In this case, the key point is the knowledge of the nucleus – nucleus potentials for the theoretical analysis of nuclear processes and the evaluation of the cross sections of the elastic and inelastic scattering and nuclear fusion. One interesting example of the scattering is the elastic transfer of the particles (a group of particles - a cluster) between two identical cores which allows describing the mechanism of the anomalous backscattering. In this approach, the study of the scattering provides information about single-particle and cluster states in nuclei.

In order to clarify the mechanism of the transfer cluster configurations in the scattering processes in light nuclear systems, a cycle of experiments was carried out to study the mechanisms of the formation of the elastic scattering cross sections at energies near the Coulomb barrier in systems $^{12}C(^{16}O,^{16}O)^{12}C$, $^{16}O(^{20}Ne,^{20}Ne)^{16}O$, $^{12}C(^{20}Ne,^{20}Ne)^{12}C$, $^{9}Be(^{13}C,^{13}C)\,^{9}Be$ etc., having a pronounced alpha-cluster structure. Such information can substantially clarify the formation dynamics of the elastic scattering cross sections of the charged particles and light ions on the p- and sd- shell nuclei in the future.

In order to clarify the mechanism of cluster configurations transfer in the scattering processes on light nuclear systems, a cycle of the experiments was carried out to study the mechanisms of formation of the elastic scattering cross sections at energies near the Coulomb barrier. The experiments were carried out at the K-160 cyclotron (University of Warsaw) and the DC-60 heavy ion accelerator (INP Branch, Astana).

Differential cross sections of the elastic scattering of heavy ions on light nuclei at energies near the Coulomb barrier were measured using multi-detector system and the reaction chamber ICARE (Warsaw) and ORTEC (Astana). Accelerated ^{12}C, ^{15}N and ^{20}Ne ions focused on target located in the center of the reaction chamber. The target thickness of the isotopes of the nuclei $^{10,11}B$, Al_2O_3 ranged from 0.05 mg/cm^2 to 0.25 mg/cm^2, depending on the energy of accelerated ions. Differential cross sections of the elastic scattering of ^{15}N, ^{12}C and ^{20}Ne ions on the studied nuclei were measured in the angular range of 5^0–40^0 in the laboratory system. The angular distributions of the elastic scattering have been obtained for the following nuclear systems $^{12}C(^{16}O,^{16}O)\,^{12}C$, $^{16}O(^{20}Ne,^{20}Ne)^{16}O$ and $^{11}B\,(^{15}N,\,^{15}N)^{11}B$ at energies of 1.75 -2.8 MeV/nucleon [1-4]. A characteristic feature of the studied angular distributions is a significant increase of the cross section at the backward scattering angle.

The description of the cross section rise at backward angles has been achieved, taking into account the contribution of the elastic transfer mechanism of the alpha cluster to the total cross section of the scattering process for nuclear systems $^{12}C(^{16}O,^{16}O)^{12}C$, $^{16}O(^{20}Ne,^{20}Ne)^{16}O$ and $^{11}B(^{15}N,\,^{15}N)\,^{11}B$. This made it possible to consider the ^{12}C, ^{15}N, ^{16}O and ^{20}Ne nuclei in the framework of the α-cluster model as nuclei consisting of 3, 4, 5, and α-particles, respectively. The obtained results are in good agreement with the results of other authors in this field of the research.

References

[1] N. Burtebayev, A. Duisebayev, B. A. Duisebayev et all "Elastic and inelastic scattering of α-particles by ^{20}Ne nuclei at energy of 48.8 MeV", International Journal of Modern Physics E Vol. **27**, No. 05, 1850042 (2018).

[2] N. Burtebayev, J.T. Burtebayeva, T. Zholdybayev et all, "Study of the elastic scattering of ^{20}Ne on ^{16}O nuclei at energy below the Coulomb barrier", Memorie della Societa Astronomica Italiana Vol. **88,** 424 (2017).

[3] N. Burtebayev, N. Amangeldi, D. Aalimov et all, "Scattering of ^{15}N ions by$^{10,11}B$ nuclei at the energy of 43 MeV", Acta Physica Polonica B, Proceedings Supplement V.**11,** 99 (2018).

[4] N. Burtebayev, A. Duisebayev, B. A. Duisebayev et all, "Scattering of α -particles and ^{3}He on ^{16}O nuclei and its excitation mechanism at energies near 50 MeV", International Journal of Modern Physics E Vol. **26,** (2017). id 1750018

Experimental researches to ensure nuclear power safety at the base of nnc rk facilities

E.G. Batyrbekov, V.V. Baklanov, D.A. Ganovichev, V.A. Gaydaychuk, A.N. Kotlyar, A.V. Pakhnits, A.D. Vurim

National Nuclear Center, Republic of Kazakhstan

e-mail: vurim@nnc.kz

The National Nuclear Center of the Republic of Kazakhstan operates a number of experimental facilities, including two nuclear research reactors and several electrophysical stands, designed for various studies of the serious problem of severe CDA (core damage accident) for nuclear reactors.

These studies are based on a long history that began in the early 80s of the last century. Those time the view on problem of the safety and operability of the nuclear fuel was radically changed comparing the previous period of nuclear energy development and that is why data base on the behavior of the fuel in the accidental conditions became extremely urgent.

The USSR had a lot of experimental installations appropriated for the life-time experiments with fuel, but it was necessary to collect a new information about behavior of the fuel in modes with destruction of the fuel including its melting. The IGR research reactor was chosen because of excellent operation parameters provided the possibility of the simulant CDA tests implementation.

Great experience and lessons were learned in frame of the single fuel pin experiments with simulation of the RIA (Reactivity Initiated Accident) and LOCA/LOFT (Loss of Coolant Accident / Loss-of-Flow Transient) conditions.

After the break-up of the USSR the NNC, been founded on the base of the so called Joint Expedition and former military organizations of the Semipalatinsk test site, continued expanding of the competences on experimental investigations of the nuclear fuel in accidental conditions.

All available forces have been directed on advertisement of the NNC's experience and capabilities around the all of world.

As a result in 1994 the foreign Customer, Japanese nuclear research company NUPEC (Nuclear Power Engineering Center) have signed a contract on experimental investigations of the behavior of the molten fuel inside the pressure vessel of LWR (Light Water Reactor), including studying of cool mode of fuel, fuel-coolant interaction, fuel-construction materials interaction, molten fuel in-vessel retention and etc.

In 1995 another Japanese nuclear energy research organization - PNC (The Power Reactor and Nuclear Fuel Development Corporation) specialized in special Breeder reactors have signed the first stage of the EAGLE contract on investigation of the controlled material relocation from the core of a sodium-cooled fast neutron reactor in order to eliminate an exceeding prompt criticality caused by compacting motion of molten fuel as well as to determine conditions that provide in-vessel retention of degraded core materials.

Currently NNC provides the EAGLE-3 stage of this biggest Project among all other been implemented at NNC. A several new installations have been designed and constructed especially for the purpose of the Japanese projects implementation.

It were carried out for the Japanese Customers more than hundred methodical and 8 full-scale in-pile tests in IGR reactor, as well as more than 65 tests were carried out in out-of-pile conditions using IGR research reactor, ANGARA and EAGLE experimental benchs.

In order of a results of these projects been presented in the science world, NNC got a reputation as scientific research center with capabilities to provide preparation and implementation the complicated and comprehensive R&D in the field of substantiation of the nuclear reactor safety.

It allows NNC have an optimistic view in a future regarding the market of experimental researches to ensure nuclear power safety at the base of NNC RK facilities.

Physical Properties of Epitaxial Silicon Carbide Films, Grown by Atomic Substitution on the High-resistance (111) Oriented Silicon

S.A. Kukushkin[1], K.Kh. Nussupov[2], A.V. Osipov[1], N.B. Beisenkhanov[2], D.I. Bakranova[2]

[1]Institute for Problems of Mechanical Engineering RAS, St. Petersburg, Russia

[2]Kazakh-British Technical University, 050000, Almaty, Kazakhstan

e-mail: beisen@mail.ru

The difference in the lattice parameters of silicon carbide (SiC) and single crystalline silicon (Si) is ~20%, and the difference in thermal expansion coefficients - 8%. Therefore, the growing of highly oriented epitaxial SiC layers on Si substrate is a complex task. In this paper, SiC films were synthesized by a new method of atom substitution directly inside the subsurface layer of the Si substrate at various temperatures and pressures of the CO working gas [1,2]. The method is based on the idea of replacing of some silicon atoms on carbon atoms within the silicon substrate. To implement this approach, a carbon atom is introduced in the interstitial position of silicon lattice and, neighboring silicon atom is removed, creating a silicon vacancy. An ensemble of dilatation dipoles is formed, which are stable complexes consisting of dilatation centers ($C\text{-}V_{Si}$) – carbon atom in the interstitial position and silicon vacancy. These two centers of dilatation elastically interact with each other in a crystal of cubic symmetry. If the carbon atoms are displaced from interstitial positions into positions occupied by vacancies, a layer of silicon carbide is formed in the upper part of the silicon. Since the lattice parameters (0.43596 nm) in SiC are much smaller than in Si (0.54307 nm), pores are formed below the SiC layer.

The composition and physical parameters of a multilayer silicon carbide (SiC) system on the surface of a high-resistance, low-dislocation single-crystal n-type silicon (Si) with (111) orientation were studied by X-ray reflectometry, ellipsometry, atomic force microscopy, profilometry and simulation. Samples with thickness of 1300 μm were subjected to plane-parallel double-sided grinding and polishing till gaining the thickness of 1100 μm. Then samples Nos. 1, 3 and 4 were etched in acid mixture HF: HNO_3 (in a ratio of 1:10) up to a thickness of 870 μm. Further, all samples Nos. 1-4 were etched in an alkaline KOH solution. The SiC films synthesis was carried out on the samples Nos. 1 and 2 for 15 min at the temperature of 1250°C and the pressure of the gas CO 264 Pa, and on the samples Nos. 3 and 4 – 7 min, 1330°C and 395 Pa.

The density of SiC_x layer on the sample No. 1 was 3.069 g/cm^3, on the sample No. 2 – 3.17 g/cm^3, on the sample No. 3 – 3.233 g/cm^3, on the sample No. 4 – 3.29 g/cm^3, respectively. The compositions of films No 1-4 were $Si_{0.46}C_{0.54}$, $Si_{0.49}C_{0.51}$, $Si_{0.480}C_{0.520}$, $Si_{0.423}C_{0.577}$, respectively. It was revealed that SiC films consist of a series of layers, differing in composition and thickness. The concentration of carbon decreases from the surface layer into the depth of Si substrate.

It has been experimentally proved that in all samples there is a carbon in the superstoichiometric state whose structure depends on the synthesis temperature. At 1250 ° C, the surface of the films is saturated with silicon vacancies and carbon in a structurally "friable" form resembling carbon in HOPG state. The formation of dense carbon nanostructures approaching in density to diamond, in SiC films grown at a temperature of 1330°C, preventing the formation of crystals with a clear fragmentation of the faces on the surface, has been revealed experimentally.

[1] Kukushkin S.A., Nussupov K.Kh., Osipov A.V., Beisenkhanov N.B., Bakranova D.I. Structural properties and parameters of epitaxial silicon carbide films, grown by atomic substitution on the high-resistance (111) oriented silicon. Superlattices and Microstructures. 111. 2017. 899-911.

[2] Kukushkin S.A., Nussupov K.Kh., Osipov A.V., Beisenkhanov N.B., Bakranova D.I. X-Ray Reflectometry and Simulation of the Parameters of SiC Epitaxial Films on Si(111), Grown by the Atomic Substitution Method. Physics of the Solid State. 59(5). 2017. 1014–1026.

Semitransparent Back-Contact Perovskite Solar Cells

Askhat N. Jumabekov
Department of Physics, Nazarbayev University, Nur-Sultan 010000, Kazakhstan
Author e-mail address: askhat.jumabekov@nu.edu.kz

Abstract: Transparent quasi-interdigitated electrodes (t-QIDEs) were produced by replacing the opaque components of existing QIDEs with indium tin oxide (ITO). We demonstrate their application in the first semitransparent back-contact perovskite solar cell. The use of ITO allows for illumination of the device from front and rear sides, resembling a bifacial solar cell, both of which yield comparable efficiencies. Coupled optoelectronic simulations reveal this architecture may achieve power conversion efficiencies of up to 11.5% and 13.3% when illuminated from the front and rear side, respectively, using a realistic quality of perovskite material.

Recently, back-contact electrodes have been used to make perovskite-based optoelectronic devices such as photodetectors and solar cells [1-3]. A typical back-contact electrode is an array of anode and cathode fingers arranged in an interdigitate fashion on a substrate. In perovskite solar cells (PSCs) with back-contact electrodes, the best device performances have been obtained using so-called quasi-interdigitated electrodes (QIDEs) [4]. The architectural difference of these electrodes from the typical interdigitated electrodes is that, one-half of the interdigitated electrode fingers (e.g. anode) is deposited over the continuous layer of the other electrode (e.g. cathode) and separated by a thin layer of insulator. The top contacts of the-state-of-the-art QIDEs are currently composed of opaque Al|NiCo fingers, which are strong absorbers/reflectors of incident light, preventing their use in semitransparent PSCs or as the top electrode in tandem perovskite-silicon solar cells [3,4]. Therefore, for QIDEs to reach their full potential, the top electrode must be replaced with a transparent conductor.

In this work we report the first transparent quasi-interdigitated electrodes (t-QIDEs) based on indium tin oxide (ITO), which has a high carrier concentration, low sheet resistance, and most importantly, higher optical transmittance (>85% in visible wavelengths) than Al|NiCo. t-QIDEs were produced by replacing the opaque components of existing QIDEs with ITO (**Figure 1a**). Furthermore, we demonstrate the first operational semitransparent bifacial back-contact PSCs (**Figure 1b**). The *J*−*V* characteristics of the devices were recorded with both front (perovskite) and rear (glass) side illumination. **Figure 1c** shows *J*−*V* curves under 1 sun AM1.5G illumination and in the dark. With front side illumination, values of 5.5 mA cm−2, 0.84 V, and 30% were recorded for short-circuit current density (*JSC*), open-circuit voltage (*VOC*), and fill factor (*FF*), respectively, yielding a PCE value of 1.4% for a reverse scan. For rear side illumination and reverse scan, a slightly higher PCE value of 1.7% was obtained, with *JSC*, *VOC*, and fill factor being 5.6 mA cm−2, 0.88 V, and 34%, respectively.

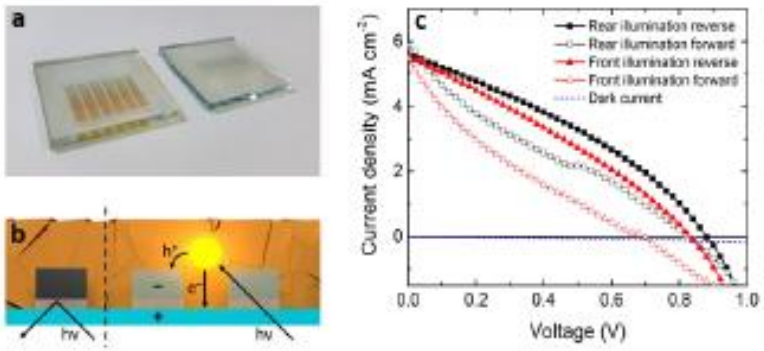

Figure 1. (a) Photograph of t-QIDEs before (left) and after annealing at 300 °C (right). (b) Cartoon of back-contact PSC with QIDEs *vs.* t-QIDEs. (c) *J*−*V* characteristics of a BC-PSC based on the Cs0.05FA0.79MA0.16PbI2.49Br0.51 photoabsorber and a t-QIDE measured under 1 sun illumination from the front (perovskite) side and rear (glass) side and in the dark.

References

[1] M.I. Saidaminov, V. Adinolfi, R. Comin, A.L. Abdelhady, W. Peng, I. Dursun, M. Yuan, S. Hoogland, E.H. Sargent, O.M. Bakr, "Planar-integrated single-crystalline perovskite photodetectors," Nat. Commun. **6**, 8724 (2015).

[2] L.M. Pazos-Outón, M. Szumilo, R. Lamboll, J.M. Richter, M. Crespo-Quesada, M. Abdi-Jalebi, H.J. Beeson, M. Vrućinić, M. Alsari, H.J. Snaith, B. Ehrler, R.H. Friend, F. Deschler, "Photon recycling in lead iodide perovskite solar cells," Science **351**, 1430-1433 (2016).

[3] A. Jumabekov, E. Della Gaspera, Z.-Q. Xu, A. Chesman, J. Van Embden, S. Bonke, Q. Bao, D. Vak, U. Bach, "Back-Contacted Hybrid Organic−Inorganic Perovskite Solar Cells," J. Mater. Chem. C **4**, 3125-3130 (2016).

[4] Q. Hou, D. Bacal, A.N. Jumabekov, W. Li, Z. Wang, X. Lin, S.H. Ng, B. Tan, Q. Bao, A.S.R. Chesman, Y.-B. Cheng, U. Bach, "Back-contact perovskite solar cells with honeycomb-like charge collecting electrodes," Nano Energy **50**, 710–-16 (2018).

Special Regimes under Diffusion in Gaseous Mixtures

[1]Kossov V.N., [2]Fedorenko O.V., [2]Mukamedenkyzy V.

[1]Abai Kazakh National Pedagogical University, 13 Dostyk Ave., Almaty, Republic of Kazakhstan

[2]Al-Farabi Kazakh National University, 71 al-Farabi Ave., Almaty, Republic of Kazakhstan

e-mail: kosov_vlad_nik@list.ru

Abstract: The features of the occurrence of convective flows during diffusion in multicomponent gas mixtures are considered. Experimental data and results of a numerical analysis of the emergence of convective motions during diffusion in three-component gas mixtures are presented. It is shown that the analysis of the stability of three-component gas mixtures can be carried out both in the framework of the linear stability theory and modern methods of numerical simulation.

1. Introduction

Molecular diffusion can lead to instability of the mechanical equilibrium of the mixture with the subsequent occurrence of natural convection, which noticeably intensifies the total mass transfer. In experiments on the study of mixing in multicomponent systems at different pressures and compositions [1], and diffusion of a mixture of solution vapors into an inert gas [2], convective flows were observed leading to a synergistic effect associated with a significant increase in the rate of mixing of the system components.

The solution of issues related to the determination of the mechanism of change of the regimes “diffusion – convection” in multicomponent gas mixtures and the parameters determining the occurrence of the convective mode are important for fundamental and applied problems of convective mass transfer.

2. Experimental data

In the ternary gas mixtures (for example 0.5538 H_2 + 0.4462 N_2 – CH_4 and 0.8846 H_2 + 0.1154 CH_4 – He [3], 0.5504 CH_4 (1) + 0.4496 Ar (2) – N_2 (3), 0.5143 He (1) + 0.4857 Ar (2) – 0.5148 CH_4 (3) + 0.4852 Ar (2) and 0.8366 CH_4 (1) + 0.1634 R12 (2) – n-C_4H_{10} (3) [4]) a regime change can occur, due to the difference in diffusion coefficients. The parameters defining such a transition are the pressure and the initial composition of the mixture [3, 4]. In this case, it is possible to realize the conditions when the transfer of the component with the highest molecular weight will be prior to the others. This situation that is not typical for the diffusion can be explained by the occurrence of convective structured formations.

3. Numerical analysis

Diffusion mixing near the boundary of the change of kinetic regimes can be described by the general system of hydrodynamic equations, which includes the Navier-Stokes equations written in the Boussinesq approximation, preserving the number of particles of a mixture and components [1, 3, 4]. This system of equations can be solved analytically using the linear stability theory [3] or by means of the splitting scheme for physical parameters [4].

First approach allows in terms of diffusion Rayleigh numbers to obtain the maps of stability for the ternary gas mixtures determining regime change “diffusion – concentration gravitational convection” for the vertical channels. Thus, in order to evaluate the theoretical effect of pressure (or other influencing parameter) on the occurrence of convection under the isothermal mixing of ternary gas mixture is necessary to consider the location of the partial Rayleigh numbers (as points) relative to the boundary line on the plane (Ra_1, Ra_2). If the partial Rayleigh numbers lie below the boundary line, then the diffusion process is observed in the system. If the partial Rayleigh numbers are in the area between the boundary line and zero density gradient line, then the stability paradox occurs in the system, i.e. there is an unstable diffusion mixing. If the partial Rayleigh numbers are situated above the boundary line, then the convective mixing is observed in the mixture.

The numerical model for the study of isothermal transfer in three-component gas mixtures permits to determine and analyse the behaviour of isoconcentration lines of the components. The main feature of the transition from the diffusion mode to the convective mode is the appearance of nonlinear isoconcentration lines due to a significant difference in the coefficients of mutual diffusion of the components. With increasing pressure or content in the mixture of the component with the highest molecular weight, the curvature of the isoconcentration lines increases which is the cause of the occurrence of convective instability. With unstable mixing, a pulsating transfer mode is possible, which is associated with the occurrence of structural convective formations.

4. Summary

Thus, the proposed mathematical models for the study of isothermal transfer in three-component gas mixtures allows for determining the conditions under which the change of regimes “diffusion – concentration gravitational convection” occurs.

[1] V. N. Kossov, D. U. Kul’zhanov, Y. I. Zhavrin, O. V. Fedorenko, “Emergence of convective flows during diffusional mass transfer in ternary gas systems: The effect of component concentration”, Russ. J. Phys. Chem. A 91 (6), 984 (2017).

[2] V.V. Dil’man, V.A. Lotkhov, “Molecular turbulent evaporation in a gravitational field”, Theor. Found. Chem. Eng. 49 (1), 102 (2015).

[3] V. Kossov, S. Krasikov, O. Fedorenko, “Diffusion and convective instability in multicomponent gas mixtures at different pressures”, Eur. Phys. J. Spec. Top. 226 (6), 1177 (2017).

[4] V. Kossov, O. Fedorenko, D. Zhakebayev, “Features of multicomponent mass transfer in gas mixtures containing hydrocarbon components”, Chem. Eng. Technol. 42 (4), 896 (2019).

Roton structure of dust-acoustic wave spectrum of complex plasmas with finite-size particles

A.E. Davletov, L.T. Yerimbetova

Al-Farabi Kazakh National University, 71 Al-Farabi av., 050040 Almaty, Kazakhstan

e-mail: Askar.Davletov@kaznu.kz

Abstract: The aim of the present report is to demonstrate the impact the finite size of dust particles has on the static and dynamic characteristics of the dust component of a plasma. Taking into account both the finite dimensions of dust grains and the plasma screening, a model expression is chosen for the interdust interaction potential. The static structure factor of dust particles is evaluated by iteratively solving the reference hypernetted-chain approximation, which inherently contains the hard sphere model handled within the Percus–Yevick closure. The self-consistent method of moments is then engaged to relate the static and dynamic structure factors by assuming that the second derivative of the latter with respect to the frequency vanishes at the origin. Thus, an analytical expression for the dynamic structure factor is validated over a broad domain of dusty plasma non-ideality and grains packing fraction. The calculated spectrum of dust-acoustic waves reveals the appearance of the roton minimum, which becomes less pronounced when the packing fraction of dust particles rises. It is also predicted that the wavenumber position of the roton minimum is *de facto* independent of the size of dust particles. New analytical expressions for the dust-acoustic wave spectrum and decrement of damping are proposed and thoroughly checked.

1. Interaction model

The density-response formalism provides the following interaction model of dust particles in a complex plasma [1]:

$$\varphi(r) = \frac{Z_d^2 e^2}{r+2R} - \frac{Z_d^2 e^2}{r}\left(1 - \exp(-k_D r) - k_D R\, B(r)\right),$$

where Z_d and R are the grain charge number and radius, respectively, e denotes the elementary charge, r stands for the distance between surfaces of interacting particles, and

$$B(r) = \exp\big(k_D(r+2R)\big)\mathrm{Ei}\big(k_D(r+2R)\big) - \exp\big(k_D(2R-r)\big)\mathrm{Ei}(2k_D R) + \exp\big(-k_D(2R+r)\big)\big[\mathrm{Ei}(-2k_D R) - \mathrm{Ei}\big(-k_D(r+2R)\big)\big]$$

with $\mathrm{Ei}(x)$ being the integral exponential function and k_D signifying the inverse screening length.

2. Dynamic properties of complex plasmas

Using the above stated model the reference hypernetted-chain approximation is utilized for evaluating the static structure factor, which incorporates the hard sphere model as a system of reference to take into account the finiteness of dust particles. With growth of the coupling parameter, non-monotonicity is found in the curves of the static structure factor, which turns sharper while the packing fraction and/or the screening parameter diminish. The static structure factor is then engaged within the self-consistent method of moments and the dynamic structure factor is analytically restored, corresponding to the strongly coupled regime of the dust component. At rather low values of the packing fraction, the dynamic structure factor is demonstrated to be in a very good agreement with the results of the molecular dynamics simulations for point-like dust particles, which has allowed us to predict its behavior with an increase in the packing fraction.

Furthermore, the spectrum of dust-acoustic waves is calculated and influence of the size of dust particles on their structure is estimated. The phonon structure at small wavenumbers remains unaltered when the size of dust particles grows. Moreover, it is shown that the position of the roton minimum with respect to the wavenumber, as well as the position of the maximum in the spectrum of dust-acoustic waves, is barely sensitive to the size of dust particles. Therefore, it is well grounded that the spectrum of dust-acoustic waves has several invariants that retain their characteristics regardless of the size of dust particles involved into the collective processes. In addition, the position of the roton minimum is proved to roughly coincide with the position of the first maximum in the curve of the static structure factor. This finding is, of course, not accidental and is thoroughly explained by a classical analog of the Feynman and Cohen hypothesis on the mutually inversed relationship between the square root of the static structure factor and the spectrum of collective oscillations. The latter insight is firmly supported by the present consideration, but in contrast to the Feynman and Cohen theory the self-consistent method of moments is shown to provide far more accurate description of the roton minimum in particular and the spectrum of dust-acoustic waves as a whole as it incorporates two characteristic frequencies both being determined by the static structure factor.

3. References

[1] A.E. Davletov, Yu.V. Arkhipov, I.M. Tkachenko, “Electric charge of dust particles in a plasma”, Contrib. Plasma Phys. 56, 308 (2016).
[2] Yu. V. Arkhipov, A. Askaruly, A. E. Davletov, D. Yu. Dubovtsev, Z. Donko, P. Hartmann, I. Korolov, L. Conde, I. M. Tkachenko, “Direct Determination of Dynamic Properties of Coulomb and Yukawa Classical One-Component Plasmas”, Phys. Rev. Lett. 119, 045001 (2017).
[3] L.T. Yerimbetova, A.E. Davletov, Yu.V. Arkhipov, I.M. Tkachenko, “Dynamic properties of strongly coupled dusty plasmas with particles of finite dimensions”, Contrib. Plasma Phys. 2019; e201800160, https://doi.org/10.1002/ctpp.201800160.

Non-Abelian Proca-Dirac-Higgs theory: particle-like solutions and a mass gap

V. Dzhunushaliev, V. Folomeev, T. Kozhamkulov, and A. Makhmudov
Department of Theoretical and Nuclear Physics, Al-Farabi Kazakh National University, Almaty
Institute of Experimental and Theoretical Physics,Al-Farabi Kazakh National University, Almaty
e-mail: v.dzhunushaliev@gmail.com

Abstract: We study a system consisting of a non-Abelian SU(2) Proca field interacting with nonlinear scalar (Higgs) and spinor fields. For such a system, it is shown that particle-like solutions with finite energy do exist. It is demonstrated that the solutions depend on three free parameters of the system, including the central value of the scalar field ξ_0. For some fixed values of ξ_0, we find energy spectra of the solutions. It is shown that for each of the cases under consideration there is a minimum value of the energy $\Delta = \Delta(\xi_0)$ (the mass gap $\Delta(\xi_0)$ for a fixed value of ξ_0). The behavior of the function $\Delta(\xi_0)$ is studied for some range of ξ_0.

We study a non-Abelian SU(2) Proca field interacting with nonlinear scalar and spinor fields. The scalar field is described by the Klein-Gordon equation with the Higgs potential. The spinor field ψ is described by the Dirac equation with a potential term of the form $\left|\bar{\psi}\psi\right|^2$. Our purpose here is to obtain particle-like spherically symmetric solutions and to study their energy spectra. We will show below that the energy spectrum depends on the parameters f_2, E, and ϕ_0. The parameter f_2 describes a behaviour of the SU(2) Proca field at the center of the system; $E/\hbar$ is a frequency of the stationary spinor field entering the factor $e^{-iEt/\hbar}$; the parameter ϕ_0 is a central value of the Higgs field ϕ. We show that the energy spectrum has a minimum, at least for some values of ϕ_0, and we argue that this will also take place for any value of ϕ_0 lying in the range $0 < \phi_0 < \infty$. The behaviour of this minimum as $\phi_0 \to \infty$ is of great interest: if in this limit the minimum is nonzero, one can say that there is a mass gap $\Delta \neq 0$ in non-Abelian Proca-Dirac-Higgs theory.

If such a mass gap does exist, this would be of great significance. The reason is that in quantum field theory there is a problem to prove the existence of a mass gap in quantum chromodynamics Since this problem is highly nontrivial, one of possible ways for solving it could be a consideration of simpler problems where *quantum systems* are replaced by *approximate classical systems*. In this case, if one could show that in such classical systems a mass gap can occur, this could be regarded as an indication of the possibility of existence of the mass gap in quantum systems. From this point of view, the classical system studied in the present paper and regarded as some approximation to realistic quantum systems can be of some interest.

Thus, our purpose is to (i) obtain particle-like solutions within a theory with a non-Abelian SU(2) Proca field plus a Higgs scalar field plus a nonlinear Dirac field; (ii) study energy spectra of these solutions; (iii) search for a minimum of the spectrum (a mass gap); and (iv) understand the mechanism of the occurrence of a mass gap within the theory under investigation and, on this basis, to suggest a similar mechanism for QCD.

The following results have been obtained:

- Particle-like solutions of the type Proca-monopole-plus-spinball have been found in some range of values of the system parameters $f_2, \tilde{E}$, and $\tilde{\xi}_0$.
- For such solutions, the energy spectra for some values of the parameter $\tilde{\xi}_0$ have been constructed. It was shown that they possess a minimum $\Delta(\tilde{\xi}_0)$.
- The behaviour of $\Delta(\tilde{\xi}_0)$ as a function of the parameter $\tilde{\xi}_0$ has been studied.
- It was shown that the solutions obtained give rise to a Meissner-like effect, which consists in the fact that a maximum value of the SU(2) gauge Proca field is located there where the Higgs field has a minimum.
- For the Proca monopole, it was shown that the Proca color "magnetic" field decreases asymptotically according to an exponential law.
- The non-Abelian Proca monopole obtained differs in principle from the 't Hooft-Polyakov monopole in the sense that the Proca monopole is topologically trivial.
- The main reason for the existence of the mass gap $\Delta(\tilde{\xi}_0)$ is due to the presence of the nonlinear Dirac field.
- The mechanism of the occurrence of a mass gap in QCD has been suggested.

This report is based on Ref. [1].

[1] V. Dzhunushaliev, V. Folomeev and A. Makhmudov, "Non-Abelian Proca-Dirac-Higgs theory: Particlelike solutions and their energy spectrum," Phys. Rev. D 99:076009, (2019); [arXiv:1903.00338 [hep-th]].

Plasma Technology for Biomedical Waste Processing

V.E. Messerle[1,2], A.L. Mosse[1], A.B. Ustimenko[1*]

[1] *Plasmatechnics R&D LLP, Institute of Experimental and Theoretical Physics of al-Farabi Kazakh National University, Almaty, Kazakhstan*

[2] *Combustion Problems Institute of Ministry of Education and Science of Kazakhstan, Almaty, Kazakhstan*

e-mail address: ust@physics.kz

Abstract: This report presents the results of thermodynamic analysis and experiments on gasification of the waste of various origins in the plasma reactor [1].

Biomedical waste (BMW) occupies a special place among hazardous carbon-containing wastes. The BMW includes food waste, paper, wood, textiles, leather, rubber, various types of plastics, glass, metal, ceramics, used therapeutic medicines, including radioactive elements, as well as various medical and chemical preparations. Any kind of waste containing infectious (or potentially infectious) materials is referred to BMW. A more promising technology for BMW processing is plasma gasification [1–3].

The BMWs used in this research were bony tissues (bones of animal origin) and averaged waste of healthcare facilities. To carry out the thermodynamic calculations, the TERRA code was used. The calculations were performed for temperatures up to 3,000 K and pressure of 0.1 MPa. The following processes were calculated: a dry bone tissue (BT) pyrolysis, wet BT pyrolysis, air processing of household waste (HW), and steam processing of HW. The thermodynamic calculations have shown that the maximum synthesis gas yield in the BMW plasma gasification in air and steam medium was achieved at a temperature not higher than 1,600 K. The calculations revealed that in the air-plasma and steam-plasma BT gasification, synthesis gas with concentrations 53.4 vol.% and 84.9 vol.%, respectively, can be obtained. Heat of combustion of the synthesis gas obtained in the air gasification amounts to 3,510 kJ/kg, and in the steam gasification it is 5,664 kJ/kg. At the temperature 1,600 K the power input into the air and steam BT gasification amounts, respectively, to 0.78 and 1.02 kW h/kg. The calculations showed that in the air-plasma and steam-plasma HW gasification, a high-calorific synthesis gas with concentrations 82.4 vol.% and 94.5 vol.% , respectively, can be obtained. Heat of combustion of the synthesis gas obtained in the air gasification of HW amounts to 13,620 kJ/kg, and in the steam gasification it is 18,497 kJ/kg. At the temperature 1,600 K the power input into the air and steam gasification of HW amounts, respectively, to 1.64 and 2.08 kW·h/kg.

The experimental study of BMW gasification was carried out on an experimental setup (Fig. 1), the primary components of which were a DC plasma torch 3 with rated power of 70 kW and a plasma reactor 2 whose output in terms of BMW was up to 30 kg/h. The BMW plasma gasification process included the following stages. After ignition of the plasma torch 3 and heating of the reactor 2 to the brick-lining inner surface temperature of 1,100 K as measured at a distance of 0.2 m from the reactor head, briquetted BMW was loaded into the gasification zone 4 of the reactor through the loading inlet 1. The mass of each briquette was 0.4 kg. The BMW underwent gasification in the air plasma jet providing a mass-mean temperature up to 1,700 K in the reactor volume.

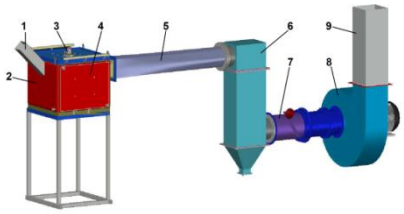

Fig. 1. Scheme of the experimental facility for BMW plasma gasification: 1 – an inlet for loading briquetted BMW into the reactor, 2 – a plasma reactor, 3 – an electric-arc direct current plasmatron, 4 – a BMW gasification zone, 5 – an off-gas cooling unit, 6 – a gas-cleaning unit with a bag filter, 7 – an exhaust gas tube with a system for gas sampling and temperature measurement, 8 – an exhaust fan, 9 – an exhaust tube.

Experiments on plasma-air gasification of BT and HW showed that total concentration of the synthesis gas was 69.6 and 71.1 vol.%, respectively. Carbon gasification degree reached 79.3 and 91.8 % and the specific power inputs range within 3.5 - 4.6 and 2.25 - 4.5 kW·h/kg, respectively for BT and HW processing.

Based on the results of thermodynamic calculations and gas and X-ray analyses, no harmful impurities were found in the gaseous and condensed products of the plasma gasification process of BMW. From the organic and mineral mass of BMW, respectively, high-calorific synthesis gas and a neutral slag were obtained. Energy balance and comparison of plasma gasification and conventional incineration of BMW showed a higher energy efficiency of plasma technology. The obtained characteristics of the BMW plasma gasification process in various gasifying agents can be used in developing and constructing a plasma facility.

The scientific work was supported by Ministry of Education and Science of the Republic of Kazakhstan in the form of grants (BR05236507, BR05236498, AP05130731 and AP05130031).

[1] Messerle V.E., Mosse A.L., Ustimenko A.B., “Processing of biomedical waste in plasma gasifier”, Waste Management, 79, 791–799 (2018).

[2] Messerle V.E., Mosse A.L., Ustimenko A.B., “Municipal Solid Waste Plasma Processing: Thermodynamic Computation and Experiment”, IEEE Transactions on Plasma Science, 44 (12), 3017-3022 (2016).

[3] Messerle V.E., Mosse A.L., Ustimenko A.B., “Plasma gasification of carbonaceous wastes: thermodynamic analysis and experiment”, Thermophysics and Aeromechanics, 23 (4), 637-644 (2016).

Induced Processes and Reactions in Neutron Star Crusts

N.Zh. Takibayev, A.N. Yermilov, V.O. Kurmangaliyeva
al-Farabi Kazakh National University, Almaty, Kazakhstan
e-mail: takibayev@gmail.com

Abstract. The presentation discusses the investigation of the induced reactions and processes at various depths in the envelopes of neutron stars and the development of structural transformations of nuclear matter with arising new forms of matter. The induced and coherent oscillations of degenerate Fermi electrons in an overdense crystal lattice in the envelopes of neutron stars are considered. The analysis of the pulsed periodic emission of neutrino-antineutrino pairs is given along with the calculations of the periodic emission of electromagnetic waves by surface layers of the outer crust. There are also investigated the stimulated nuclear reactions in deep layers of the neutron star envelopes and neutron resonances of a strictly periodic nature and specific forms in the few-body nuclear subsystems. A description of various nuclear matter transformations is considered as a function of the layer depth in the neutron star envelope.

Synthesis of nanocrystals in SiO_2/Si track template by electrochemical deposition of Zn

Alma Dauletbekova[1], Liudmila Vlasukova,[2] Zein Baimukhanov[1], Abdirash Akilbekov[1], Artem Kozlovskyi[3], Sholpan Giniyatova[1], Aibek Seitbayev[1], Abai Usseinov$_1$, Aiman Akylbekova[1]

[1]*L.N. Gumilyov Eurasian National University, 2 Satpayev str., 010008 Nur-Sultan, Kazakhstan*
[2]*Scientific Research Laboratory of Materials and Device Structures, Belarus State University, Kurchatov Str. 1, 22006 4, Minsk, Belarus*
[3]*Institute of Nuclear Physics, 1/ 2 Ablaikhan ave., 010008, Nur-Sultan, Kazakhstan*
e-mail: alma_dauletbek@mail.ru

This work represents the study of nanoclusters obtained by electrochemical deposition (ECD) of zinc in the a-SiO_2/Si-n track template. The nanoporous SiO_2 layer on Si substrate (track template) has been created by irradiation with swift Xe ions and further etching in HF solution. The morphology of SiO_2/Si-n track templates and precipitated Zn-based clusters was examined using SEM JSM 7500F. The crystallographic structure of the Zn-based precipitates was investigated by means of X-ray diffraction. X-ray analysis was carried out on a D8 ADVANCE ECO X-ray diffractometer. The BrukerAXSDIFFRAC.EVAv.4.2 software and the international ICDD PDF-2 database were used to identify the phases and study the crystal structure.
It has been shown that ECD in the voltage range of (1.5 – 1.85 V) during 10 minutes is not enough for complete and uniform filling all the pores. There are empty pores (nearly 25 – 30 % from the whole amount of pores) as well as the entirely filled pores with the "caps" at the SiO_2 surface (Fig. 1). As the voltage increases, protrusion of the deposited substance from the nanopores is observed as well as the formation of Zn-based precipitates on the non-irradiated regions of SiO_2 surface.

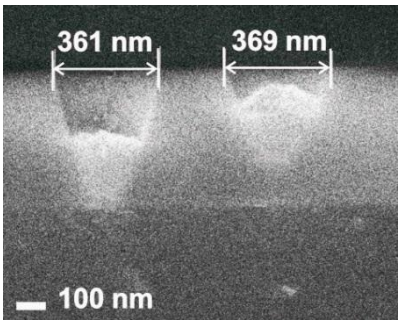

Figure 1 Cross section of SiO_2/Si samples after ECD of Zn for 10 minutes at electrode voltage U= 1.75 V

Nanoprecipitates deposited into SiO_2/Si templates were identified as ZnO according to XRD data. XRD revealed a formation of whole set of ZnO phases in dependence of applied voltage.
In the first time, nanocrystals of zinc oxide were obtained in three crystalline phases: wurtzite, sphalerite and rock salt structure during the electrochemical deposition of zinc in the track template *a*-SiO_2/Si. We assume that the formation of cubic structures of zinc oxide (sphalerite and rock salt) in the nanopores is related with the phase stabilization by a cubic face-centered Si substrate. The wurtzite structure is formed on the surface of amorphous SiO_2.

[1] A.Dauletbekova, L. Vlasukova, Z. Baimukhanov, A. Akilbekov, A. kozloskii, Sh. Gimiyatova, A. Seitbayev, A. Usseinov, A. Akylbekova "Synthesis of nanocrystals in SiO_2/Si track template by electrochemical deposition of Zn" Phys. Stat. Sol. B , 256, 1800408 (1 of 6) (2019)

On the theory of light propagation in the non-stationary gravitational lens. Problem formulation

L.M. Chechin[1,2], E.B. Kurmanov[2] and T.K. Konysbaev[1]

[1]*Fesenkov Astrophysical Institute, Almaty, Kazakhstan*

[2]*Al-Farabi Kazakh National University, Almaty, Kazakhstan*

e-mail: chechin-lm@mail.ru, ergaly_90@mail.ru

An important stage in the study of gravitational lenses was associated with new ideas about the substrate structure of the Universe. The most important for us are the new substances in the Universe, relates with dark energy (DE). Dark energy in cosmology is a hypothetical form of energy having negative pressure and uniformly filling the entire space of the Universe. It does not gather into bunches. According to general relativity, gravity depends not only on masses, but also on pressure, and negative pressure should generate repulsion, anti-gravity.

Another actual problem of modern cosmology, as it well known is the is dark matter (DM). Astronomical observations show that DM mainly concentrates around large-scale space objects such as galaxies and their clusters. In the beginning of the last century, astronomers found that some stars Cygnus X, HR 5171 A and galaxies behave differently than predicted by the theory. The revolving of the more remote parts of galaxies was not amenable to the laws of celestial mechanics. This marked the beginning of the search for a new, hidden mass, which as it was pointed out was called DM.

The main manifestations of DM unusually large mass ratios — luminosity in groups and clusters of galaxies, flat rotation curves on the periphery of disk galaxies, and excessive gravitational lensing of background objects on clusters of galaxies. There are several ways to measure the gravitational field in clusters of galaxies, one of which is gravitational lensing.

DM forms a halo which mass enriches about 90% of the galaxy total mass. (Note, that DM may form a different types of clumps without existence of any baryonic objects). It should be noted that distribution of DM in the halo of galaxies is not uniform - it concentrates in their centers and decreases to peripheries. The corresponding distribution function of DM (profile) is usually founded on numerical methods that are modeling the dynamics of stars in galaxies. Today a number of profiles are known, which include the unknown DM density in the centers of galaxies ρ_0, as well as a number of free parameters.

Finding numerical values of these quantities is one of unsolved cosmological problems that from our viewpoint, can be partially solved by examining the dynamics of dwarf galaxies. Note, that influence of DM on galaxies' dynamics successfully described even in the framework of Newtonian approach. Therefore we'll be used it in our searching for estimation the magnitudes of the DM halo's parameters. In our article [1] we found the magnitude of the DM central part. It is necessary to underline that our estimations are in good correlation with many previous articles.

Very important aspect of the DM searching is the considering it as the cosmological gravitational lens. In fact, baryonic matter, at the most basic level, serves as the construction material of the galaxies and their smaller-scale components (star clusters, stars, and planets). Questions of the influence of DM on the formation of galaxies have attracted the significant attention. Thus, observational data have been used to construct rotation curves of various galaxies; the question has been posed of the origin of the DM halo; a theoretical basis has been constructed for the distribution of DM and the magnitude of the central density of the DM halo and also its mass have been discussed. The question of whether perturbations of dark matter can become the centers of galaxy formation, i.e., actively accumulating baryonic matter into themselves, has been discussed. It has been shown that during the formation of galaxies, dark matter halos were the first objects that have been formed. Only after this their clumps attract ordinary matter into the own potential wells that later led to form the different types of galaxies [2].

At the same time, it must be noted that such work was based on the idea about the static nature of such halos. However, more recently the idea about non-stationary parameter of state for DM begun to take formed. In another words that density of DM in a halo can be depended on time. If it's so the effect on the movement of the image of the lensing object might be fixing. This effect will, by its nature, be analogous to the famous Pachinsky's effect. The essence of it is that the microlensing of galaxies must take into account the movement of an observer [3]. The motion of the image of lensing object in the non-stationary fields of DM and the movement of the observer will give the most complete picture of galaxies microlensing.

References

1. L. M. Chechin, D. Kairatkyzy and T. K. Konysbayev, "Toward a theory of the evolution of perturbations of the dark matter density in the very early universe"J. Rus. Phys., 61, 5 (2018)

2. L. M. Chechin and E.B. Kurmanov "On the new direction in the theory of gravitational lensing", Rec.contr. to phys., **1,** 68 (2019)

3. A. Udalski, M. Szymanski, J. Kałuzny, M. Kubiak, M. Mateo, W. Krzeminski and B. Paczynski " The Optical Gravitational Lensing Experiment. The Early Warning System: Real Time Microlensing", Acta Astronomica **44** (1994) pp. 227–234

Plasma Application for Uranium-Containing Solid Fuels Processing

V.E. Messerle[1,2], A.B. Ustimenko[1*]

[1] *Plasmatechnics R&D LLP, Institute of Experimental and Theoretical Physics of al-Farabi Kazakh National University, Almaty*

[2] *Combustion Problems Institute of Ministry of Education and Science of Kazakhstan, Almaty, e-mail address: ust@physics.kz*

Abstract: This report presents the results of thermodynamic and experimental investigation of plasma processing of uranium-containing Nizhneilli brown coal (NBC) of 12% ash content and Estonian dictyonema shale (EDS) of 88% ash content [1].

Because of the uranium content in the coals, huge coal reserves, for example Nizhneilli basin (10 billion tons), are not included in the State Fuel Balance of Kazakhstan. Currently, there are no known technologies for processing uranium-containing solid fuels (SF). The main technological difficulty in using such fuels is the impossibility of separating uranium-containing compounds from ash and slag waste generated during the combustion or gasification of SF. A promising solution to the problem of the use of uranium-containing SF is the use of technologies for their plasma gasification. Plasma technologies for SF processing have proved efficiency in obtaining synthesis gas from the organic mass of coal and valuable components from the mineral mass of coal [2, 3].

The essence of plasma processing of the uranium-containing SF is shown in Fig.1. It is in the conversion of the organic mass of SF into synthesis gas ($CO+H_2$), with the simultaneous release of uranium-containing compounds (U, UO, UO_2, UO_3) into the gas phase, followed by the production of uranium-free ash [1]. Endothermic effect of the carbon gasification reaction by water steam is completely compensated by the electric arc plasma power. Oxides of the mineral mass of SF are reduced to metals and metalloids.

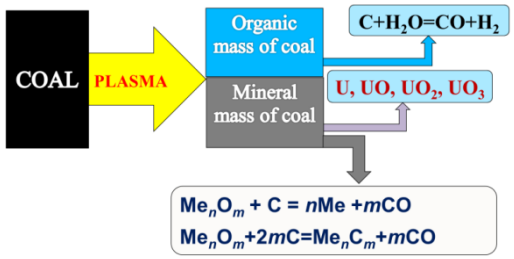

Fig. 1. Plasma processing of uranium-containing SF: Me is the metal or metalloid in the mineral mass of SF, *n* and *m* are the stoichiometric coefficients of the reactions.

Thermodynamic analysis showed that the gas phase products of plasma processing of highly different SFs consists of synthesis gas with a yield of more than 95%. Uranium, regardless of the type of SF, enters the gas phase in the form of oxides at temperatures above 1,750 K (pyrolysis of EDS and gasification of both SFs) and at temperatures above 3,200 K during pyrolysis of NBC. Complete gasification of carbon is achieved at 1,250 K with steam gasification of both types of SFs, 1,800 K for the case of pyrolysis of EDS, and 3,500 K during pyrolysis of NBC. Specific energy consumption for the plasma processing of fuels is relatively low and does not exceed 2 kWh/kg, with complete extraction of uranium into the gas phase.

In plasma pyrolysis of EDS, the degree of conversion into the gas phase of uranium reached 48% at a mean mass temperature in the reactor of 2,900 K, and the degree of gasification of shale carbon was 56.2%. With plasma-steam gasification of EDS, the degree of conversion to the gas phase of uranium reached 83.6% at a mean mass temperature in the reactor of 3,150 K. Also, the degree of gasification of the shale carbon was 70.4%. The experimental data obtained agrees satisfactorily with the thermodynamic calculations. Integral indices of plasma processing of uranium-containing SF can be improved by increasing the residence time of reagents in a plasma reactor and reducing its heat loss. To increase the conversion rate of uranium-containing solid fuels the SF, the oxidant ratio has to be varied.

The results obtained testify to the insensitivity of the plasma technology of SF gasification to the quality of the initial fuels. The investigation has shown that integral indices of plasma processing of uranium-containing fuels are higher when gasified than with pyrolysis.

The scientific work was supported by Ministry of Education and Science of the Republic of Kazakhstan in the form of grants (BR05236507, BR05236498, AP05130731 and AP05130031).

[1] Messerle V.E., Ustimenko A.B., “Plasma processing of uranium-containing solid fuels”, Fuel, 242, 447–454 (2019).
[2] Messerle V.E., Ustimenko A.B., Lavrichshev O.A.. “Comparative study of coal plasma gasification: Simulation and experiment”, Fuel, 164, 172-179 (2016).
[3] Messerle V.E., Ustimenko A.B., Lavrichshev O.A., “Plasma coal conversion including mineral mass utilization”, Fuel, 203, 877–883 (2017).

Optical reflectivity and dynamical conductivity of the dense semiclassical plasma on the basis of the effective potentials

K.N. Dzhumagulova[1*], E.O. Shalenov[1], T.S. Ramazanov[1], G. Röpke[2], and H. Reinholz[2]
[1]IETP, Department of Physics, al–Farabi KazNU, al–Farabi 71, 050040 Almaty, Kazakhstan
[2]Institute of Physics, University of Rostock, A.-Einstein-Str. 23-24, 18059 Rostock, Germany
e-mail: dzhumagulova.karlygash@gmail.com

Properties such as electrical conductivity and reflectivity are of great interest as the fundamental properties of any substances and are very important for technical applications of dense plasma. The theoretical study of such quantities of dense plasma is especially important for astrophysical problems and thermonuclear fusion (ICF). Interaction potentials should take into account the specific effects existing in the considered area of densities and temperatures. It is well known that the quantum mechanical diffraction effect plays an important role in calculating the properties of the dense, non-ideal plasma. So, we use the effective interaction potentials that take into account the quantum diffraction effect as well as the static and dynamic screening [1-4].

The measurements of reflectivity and theoretical analysis of the results are the common methods of investigation of the phase diagrams of substances, in particular, in shock wave experiments where the number of measured parameters is limited. Reflectivity coefficient was estimated by using the effective interaction potentials and the Drude–Lorentz formula that accounts for the electron–ion and electron–atom collisions in a partially ionized plasma, at the parameters corresponding to the experimental data [5].

We also investigated the dynamical conductivity of dense hydrogen plasmas on the basis of the effective interaction potential (taking into account static or dynamic screening and diffraction effects). Generalized Drude formula related the dynamical conductivity with collision frequency was applied. The influence of electron–ion collisions as well as influence of both electron-ion and electron-electron collisions were taken into account via a renormalization factor [6,7].

Our calculations showed that the systematic treatment of collisions of the different types of particles is essential for explaining the experimental results.

References

[1] K. N. Dzhumagulova, E. O. Shalenov, and G. L. Gabdullina Dynamic interaction potential and the scattering cross sections of the semiclassical plasma particles // Phys. Plasmas, **20**, 042702 (2013).

[2] K.N. Dzhumagulova, E.O. Shalenov, T.S. Ramazanov. Elastic scattering of low energy electrons in partially ionized dense semiclassical plasma // Phys. Plasmas, **22**, 082120 (2015).

[3] E.O. Shalenov, K.N. Dzhumagulova, T.S. Ramazanov. Scattering cross sections of the particles in the partially ionized dense nonideal plasmas // Phys. Plasmas, **24**, 012101 (2017).

[4] Dzhumagulova K. N., Shalenov E.O., Ramazanov T. S., Gabdullina G.L. Phase shifts and scattering cross sections of the particles of nonideal semiclassical plasmas based on the dynamic interaction potential // Contr. Plasma Phys. **55**, N2-3, 230-235 (2015).

[5] Shalenov E.O. , Dzhumagulova K.N., Ramazanov T.S. Rosmej S., Reinholz H. , Roepke G. Optical reflectivity based on the effective interaction potentials of xenon plasma // Contr. Plasma Phys. **57**, 486-492 (2017)

[6] Shalenov E.O., Dzhumagulova K.N., Ramazanov T.S., Roepke G., and Reinholz H. Dynamical conductivity of the dense semiclassical plasmas on the basis of the effective potential // Phys. Plasmas, **25**, 082706 (2018).

[7] Shalenov E.O. , Dzhumagulova K.N., Ramazanov T.S., Reinholz H. , Roepke G. Influence of dynamic screening on the conductivity of hydrogen plasma including electron–electron collisions // Contr. Plasma Phys. (2019) https://doi.org/10.1002/ctpp.201900024

Irreversibility and determinism in physics

V.M. Somsikov[1,2]
[1]Institute of Ionosphere, Almaty, 050020,
[2]Al-Farabi Kazakh National University, Almaty, 050040, Kazakhstan.
E-mail: vmsoms@rambler.ru

Annotation. The role of the deterministic mechanism of irreversibility in the development of the physical picture of the world is analyzed. It is demonstrated how it is connected with the principle of causality in physics, which opens up possibilities for the realization of the ideas of universal evolutionism and the construction of the physics of evolution. Using the example of the relationship between the laws of the evolution of systems and the laws of the dynamics of their elements, we study the question of how the law of transition of quantity into quality is implemented. It is shown how, according to the deterministic mechanism of irreversibility, statistical laws follow from the laws of nature. The possibility of constructing physics from simple to complex is analyzed.

Keywords: determinism, evolution, transition of quantity to quality, irreversibility.

Dynamical structure factor of strongly coupled ions in warm dense matter

Zh.A. Moldabekov[1;2], H. Kählert[2], T. Dornheim[2], S. Groth[2], M. Bonitz[2], T.S. Ramazanov[1]

[1] *Institute for Experimental and Theoretical Physics, Al-Farabi Kazakh National University, 71 Al-Farabi ave., 050040 Almaty, Kazakhstan*

[2] *Institut für Theoretische Physik und Astrophysik, Christian-Albrechts-Universität zu Kiel, Kiel, Germany*

e-mail: zhandos@physics.kz

Advance on dense plasmas diagnostics using X-ray scattering technique [1] has allowed to gain insight on ionic dynamics at extreme conditions. As the result, such properties as an ion acoustic dispersion and corresponding sound velocity in dense plasmas and warm dense matter can be probed experimentally. This development of experimental diagnostics capabilities has motivated the theoretical investigation of the ionic dynamical structure factor (DSF) [2, 3, 4]. For the understanding of the DSF of strongly coupled ions in dense plasmas and in warm dense matter, an accurate analysis of the effects related to quantum degeneracy and electronic correlations is needed. Therefore, in this work we present the results of the investigation of the impact of the electronic correlations on the DSF of non-ideal ions. The DSF of ions was computed using a screened ion potential in molecular dynamics simulation, where the screening by electrons was calculated on the basis of liner response theory. In order to take into account the electronic correlations, we used the Singwi-Tosi-Land-Sjölander ansatz (STLS) [5, 6]. The range of plasma parameters at which the STLS approximation is applicable for the description of the screening was defined in our recent work [7]. The analysis of the impact of the electronic correlations on the ionic DSF has been done by comparing the STLS potential based results to the MD data obtained using the screened ion potential in random phase approximation (i.e., neglecting electronic correlations) [e.g., see Fig. 1 from Ref. [8]]. Additionally, the applicability of the Yukawa model for the description of the ionic DSF in dense quantum plasmas is discussed [8].

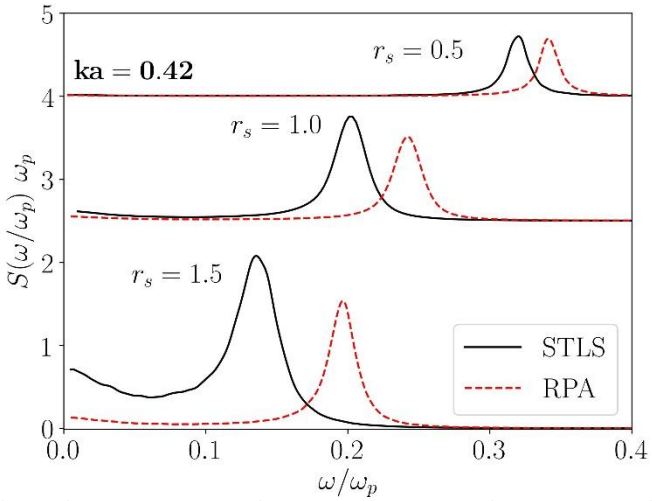

Fig. 1. Dynamical structure factor of ions at three values of the *density parameter* [defined as the ratio of the mean inter-ionic distance to the Bohr radius]. The data obtained including and neglecting electronic correlations are denoted as STLS and RPA, respectively. The DSF curves for different density are shifted vertically for clarity. The data presented for the quantum regime with the thermal energy of electrons ten times smaller than the Fermi energy.

3. References

1. E. E. McBride et.al., Rev. Sci. Instrum. 89, 10F104 (2018).
2. T. G. White et.al., Phys. Rev. Lett. 111, 175002 (2013)
3. H. R. Rüter and R. Redmer, Phys. Rev. Lett. 112,145007(2014).
4. J. Vorberger et.al., Phys. Rev. Lett. 109, 225001 (2012).
5. K.S. Singwi, M.P. Tosi, R.H. Land, and A. Sjölandar, Phys. Rev. 176, 589 (1968).
6. S. Tanaka and S. Ichimaru, J. Phys. Soc. Jpn. 55, 2278 (1986).
7. Zh. Moldabekov, S. Groth, T. Dornheim, H. Kählert, M. Bonitz, and T. S. Ramazanov, Phys. Rev. E 98, 023207 (2018).
8. Zh. Moldabekov, H. Kählert, S. Groth, T. Dornheim, M. Bonitz, and T. S. Ramazanov, Phys. Rev. E 99, 053203 (2019).

New high-current pulsed ion INURA accelerator facility at Nazarbayev University: new opportunities for advanced materials, nano science, plasma and charged beams physics.

M. Kaikanov[1], A. Kemelbay[1], D. Imanaly[1], B. Amanzhulov[1], A. Abduvalov[1], G. Remnev[2], M. Zhuravlev[2], R. Sazonov[2], W. Waldron[3], J. Kwan[3], E. Henestroza[3], A. Kozlovskiy[1,4], K. Baigarin[1], A. Tikhonov[1]

[1]Nazarbayev University, Astana, Kazakhstan
[2]Tomsk Polytechnic University, Tomsk, Russia
[3]Lawrence Berkeley National Laboratory, Berkeley, USA
[4]Astana Branch of Institute of Nuclear Physics, Astana, Kazakhstan
e-mail: atikhonov@nu.edu.kz

The Nazarbayev University is currently developing a new research activity in the field of pulsed-beam technologies based on the recently launched INURA high current pulsed ion accelerator (INURA - Innovative Nazarbayev University Research Accelerator), which was commissioned in NU in November 2018. INURA pulsed ion accelerator was developed in collaboration with Lawrence Berkeley National Lab (Berkeley, USA) and Tomsk Polytechnic University (Tomsk, Russia). INURA currently accelerates high current ~10 kA short pulsed ~80 nsec beam of protons with energies up to 500 keV [1].

INURA is a new facility, and currently we focus at both further development of the INURA hardware and new pulsed- ion/electron beams technologies, and to establish the scientific agenda, suitable for unique capabilities of INURA accelerator. Hardware development incudes development of INURA electron beam capability and establishing plasma-chemistry synthesis of metal-oxide nanoparticles. Also, we develop the nano-fabrication facilities at NU, including clean-rooms based nano-fabrication and characterization. Based in these capabilities, we will be fabricating materials, modifying them with INURA ion/electron beam and will be using them in various devices.

Here we describe several examples of our work in the field of radiation material science. Irradiating Ni.nanotubes with the electron and ion beam, we observe structural modifications, improving conductivity and resistance to corrosion in acid environment [2,3]. The established mechanisms of these effects include controlled annealing of nanotube defects and modification of the grain sizes.

In one of our first examples of device fabrication work we used pulsed ion beam to irradiate HfO2 thin film samples, converting them into the ferroelectric state, and currently we work to utilize this ferroelectric HfO2 to produce carbon nanotube based transistor with negative capacitance properties. The nano-fabrication work and some of the characterization is done at Bekeley Lab, USA, while we work to establish similar nano-fabrication capabilities and NU.

We also work to establish synthesis of 2D-materials like structures. In our current development, we established the growth of WS_2 structures synthesized by lateral conversion of metal-oxide layers encapsulated between SiO2 layers [4]. The approach enables the formation of precisely patterned WS_2 structures using standard lithographic techniques and tools widely used in industry and academia, such as ALD and dry etching. The converted materials were analyzed using WLRM, Raman spectroscopy, XPS, and TEM.

Fig. 1. INURA accelerator (left). Work at Molecular Foundry, LBL (right)

References

[1] 1. M. Kaikanov, K Baigarin, A Tikhonov, A Urazbayev, J W Kwan, E Henestroza, G Remnev, B Shubin, A Stepanov, V Shamanin and W L Waldron. “An accelerator facility for WDM, HEDP, and HIF investigations in Nazarbayev University”/ Journal of Physics: Conference Series 717 012099 (2016).

[2] A. Kozlovskiy, M. Kaikanov, A. Tikhonov, I. Kenzhina, D. Ponomarev and M. Zdorovets “Radiation modification of Ni nanotubes by electrons"/ Materials Research Express, 4, 105042 (2017).

[3] G. Kalkabay, A. Kozlovskiy, M.A. Ibragimova, D.I. Shlimas, M.Zdorovets, D. Borgekov, A.Tikhonov, “Ni nanotubes reaction activity in media with different pH” / Crystallography Reports, Vol. 63, No. 1, pp. 90–95 (2018).

[4] Aidar Kemelbay, Aldiyar Kuntubek Nicholas Chang, Christopher T. Chen, Christoph Kastl, Vassilis J. Inglezakis, Alexander Tikhonov, Adam M. Schwartzberg, Shaul Aloni, Tevye R. Kuykendall “Lateral chemical conversion of encapsulated thin-films as a synthetic route to lithographically-patterned transition metal dichalcogenides” / submitted to the NanoLetters.

F(R,T,X,ϕ) cosmology solution involving one arbitrary function

Nurkasimova Saule, Meruert Zhassybayeva, Meirbekov Bekdaulet, Yerzhanov Koblandy, Bauyrzhan Gulnur

e-mais: SauleNurkasim@mail.ru, yerzhanovkk@gmail.com

Abstract: We consider exact cosmological solutions for F(R, T, X, ϕ) - model of gravity. Founded the general solution for F(R, T, X, ϕ) - function involving one arbitrary function.

To describe modern observational data, we investigate one of the forms of modified gravity F(R, T, X, ϕ) — gravity model. On the one hand, this model generalizes the k-essence, that is the scalar field model ϕ with a kinetic term X. On the other hand, this model generalized F(R) -gravity, where the Ricci R scalar and the teleparallel gravity F(T), where T is the torsion scalar [1-3].

The action of F(R, T, X, ϕ) gravity has the following form [4-7]:

$$S_{43}=\int d^4x\sqrt{-g}[F(R,T,X,\varphi)+L_m], \tag{1}$$

where

$$\mathrm{R}=\varepsilon_1 g^{\mu\nu}\mathrm{R}_{\mu\nu}+u(a,\dot{a}), \tag{2}$$

$$\mathrm{T}=\varepsilon_2 \mathrm{S}_{\rho}^{\mu\nu}\mathrm{T}_{\mu\nu}^{\rho}+v(a,\dot{a}). \tag{3}$$

$$X=\frac{1}{2}\dot{\varphi}^2 \tag{4}$$

Here L_m is the matter Lagrangian. The action of F(R,T,X, ϕ) gravity for the FRW metric has the following form [8-11]:

$$S=2\pi^2\int dt\, a^3\left\{F(\mathrm{R},\mathrm{T},\mathrm{X},\phi)-\lambda_1\left[R-u+6\left(\frac{\ddot{a}}{a}+\frac{\dot{a}^2}{a^2}\right)\right]-\lambda_2\left[T-v+6\left(\frac{\dot{a}^2}{a^2}\right)\right]-\lambda_3\left[X-\frac{1}{2}\dot{\varphi}^2\right]\right\}. \tag{5}$$

From the symmetry properties we have:

$$F(\mathrm{R},\mathrm{T},\mathrm{X},\phi)=e^{C_1(R+T)}+C_2(R+T)+C_3X+C_4\varphi^2+C_5 \tag{6}$$

were $C_1 \ldots C_5$- constants.

We considered the F(R,T,X,ϕ) gravity model and found an expression for an action with one arbitrary function..

4. References

[1] R. Myrzakulov, K. Yerzhanov, K. Yesmakhanova et al. g-Essence as the cosmic speed-up. Astrophysics and Space Science. V.341, I.2 , 681-688

[2] E. Gudekli, N. Myrzakulov, K. Yerzhanov, R. Myrzakulov Trace-anomaly driven inflation in f(T) gravity with a cosmological constant. Astrophysics and Space Science, (2015) 357: 45

[3] R. Myrzakulov. Accelerating universe from F(T) gravity Eur.Phys.J. C71 (2011) 1752

[4] R. Myrzakulov. Dark Energy in F(R,T) Gravity. [arXiv:1205.5266]

[5] R. Myrzakulov. FRW Cosmology in F(R,T) gravity. The European Physical Journal C, 72, N11, 2203 (2012). [arXiv:1207.1039]

[6] M. Sharif, S. Rani, R. Myrzakulov. Analysis of F(R,T) Gravity Models Through Energy Conditions. Eur. Phys. J. Plus, 128, N11, 123 (2013). [arXiv:1210.2714]

[7] A. Pasqua, S. Chattopadhyay, R. Myrzakulov. A dark energy with higher order derivatives of H in the modified gravity f(R,T). ISRN High Energy Phys. 2014 (2014) 535010. [arXiv:1306.0991]

[8] S. Capozziello, M. De Laurentis, R. Myrzakulov. Noether Symmetry Approach for teleparallel - curvature cosmology. International Journal of Geometric Methods in Modern Physics, v12, N9, 1550095 (2015) [arXiv:1412.1471]

[9] R. Myrzakulov. F(T) gravity and k-essence. General Relativity and Gravitation, v.44, N12, 3059-3080 (2012)

[10] K. Bamba, R. Myrzakulov, O. Razina, K. Yerzhanov. Cosmological evolution of equation of state for dark energy in G-essence models. International journal of modern physics D, V. 22 (6), 1350023, 2013

[11] Yi-Fu Cai, Salvatore Capozziello, Mariafelicia De Laurentis, Emmanuel N. Saridakis. f(T) teleparallel gravity and cosmology. Reports on Progress in Physics. Vol. 79 (2016) no.4, 106901. [arXiv: 1511.07586]

Investigation of structures in the distribution of particles from the central area of extensive air showers on Hadron-55 installation

Y. M. Tautaev*, T. Kh. Sadykov and etc
Satbayev University, Institute of Physics and Technology, Almaty, Kazakhstan
e-mais: tautaev@mail.ru

Abstract. The ionization calorimeter “Adron-55”, located at an altitude of 3340 meters above sea level, is part of the unified registration system for the shower installation of the Tian-Shan high-mountain station. The “Hadron-55” installation is a 2-tier ionization calorimeter consisting of a shower system, a gamma block and a hadron block located under it with a vertical air gap of 2.2 meters. The calorimeter consists of 6 layers of ionization chambers with 144 chambers in each layer and a spatial resolution of the WAS structure equal to 11 cm. The total area of the calorimeter is 55 square meters with an absorber thickness of 1150 g / cm^2. The calorimeter also contains helium counters for recording the neutron component. The central shower calorimeter system contains 30 scintillation detectors with an area of 400 m^2 and 8 peripheral Sc-detectors at a distance of up to 100 m. The total area of the entire recording system is ~ 30000 m^2. Over 4 years of operation, more than 120,000 events with energies above 10^{15} eV have been recorded. Currently, the processing and analysis of the data being obtained are performed.

Observation of CTA 102 Blazar on Tien-Shan Astronomical Observatory

Kuratova A.K.
Al-Farabi Kazakh National University, Reva I.V., FAI, Almaty city
e-mais: aizhik03@gmail.com

In December 2016 rare phenomenon was observed, namely CTA 102 blazar started sharply increase its brightness [1]. A lot of astronomers became interested in this phenomenon. Scientists from 15 countries in 28 observatories on 39 telescopes took part in the research of blazar brightness sharp increase. Observations were carried out as in radio so in spectrum optical range. In Kazakhstan observations were conducted in spectrum visible range in Tien-Shan Astronomical Observatory of Fessenkov Astrophysical Institute.

Specification of conducted astronomical observations depended on clear nights in that period. Our observations were carried out in blazar maximum activeness [2]. It was found that CTA 102 blazar increased its brightness from 16 to 10 magnitudes (i.e. nearly in 300-500 times). Preliminary results of one of such episodes in CTA 102 blazar history which in December 28, 2016 became the brightest one among thousands of today's well-known blazars, were published in "Blazar spectral variability as explained by a twisting inhomogeneous jet" article in Nature journal from December 4, 2017 (doi:10.1038/nature24623) [3].

Fig.1 demonstrates the change of CTA 102 observed values in R band as Julian date function (JD). Different colors and symbols are related to different telescopes of WEBT international company. Outburst peak in 2016-2017 was observed in December 28, 2016 and points out the brightness increase about 6 magnitudes relatively to faint state.

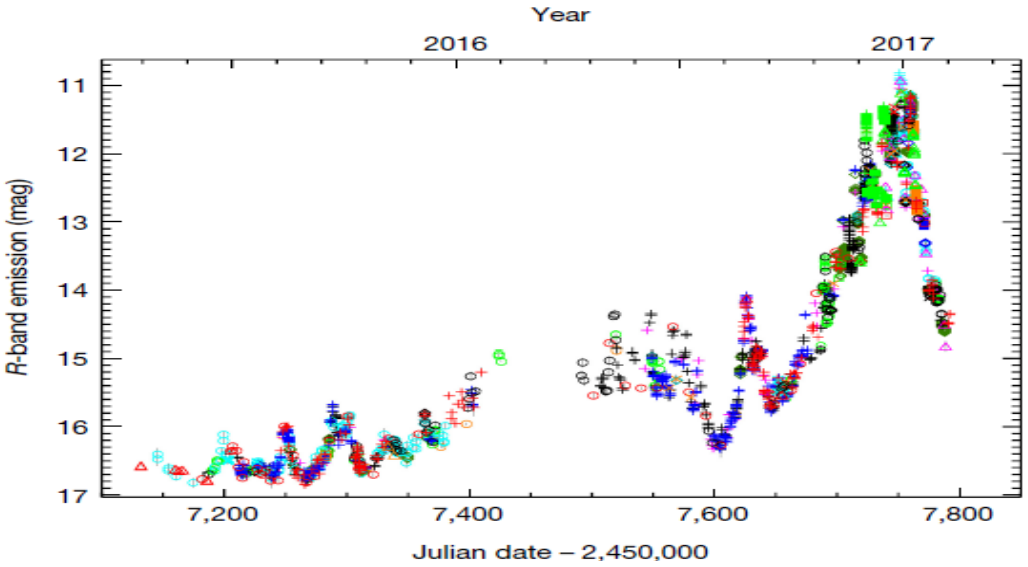

Fig.1. The change of CTA 102 blazar brightness in magnitudes in R band as Julian date function (JD)

References:

1. Ajit K. Kembhavi and Jayant V. Narlikar, Quasars and Active Galactic Nuclei, Cambridge University Press, 1999.
2. Gregory A. Shields, A Brief History of Active Galactic Nuclei. // The Publications of the Astronomical Society of the Pacific. 1999. Vol. 111. P. 661.
3. C.M. Raiteri, M. Villata, K.S. Kuratov et al, Nature, Blazar spectral variability as explained by a twisting inhomogeneous jet, Dec.4, 2017

Conversion of the ivg.1m research reactor

E.G. Batyrbekov, V.S. Gnyrya, A.D. Vurim, R.A. Irkimbekov
NNC RK, Kurchatov, Kazakhstan
e-mais:Irkimbekov@nnc.kz

The IVG1 reactor is operated since 1972. NIKIET JSC is a designer of the reactor, scientific leader of the project is IAE named after I.V. Kurchatov, Russian Company LUCH developed the fuel for the reactor. Initially, the main line of the reactor operation was to test components of the nuclear rocket engine (NRE) with gas working medium. The fuel elements of the reactor were manufactured based on solutions of zirconium and niobium uranium carbides without protective coating. It was achieved a record temperature of hydrogen heating – 3100 K.

In 1990, the reactor was modernized – its core was transferred to water cooling one (new title – IVG.1M). The loop channel of the reactor retained the ability to test gas-cooling channels. The fuel elements were made of uranium and zirconium alloy with a protective coating from zirconium-niobium alloy. Maximum reactor power was determined equal to 60 MW. Operation of the reactor was carried out, as a rule, at a power of 6 MW within 6 hours.

Since 2010, RSE NNC RK under the auspices of the Argonne National Laboratory (ANL) carry out the activities to converse the reactor to the low-enriched uranium fuel. Russian Institute PNITI is a designer of all kinds of the fuel for the reactor. Since November 2016, the testing of new fuel assemblies have been started, it will last until 2020. After that, in case of successful results, a new fuel will be fully loaded into the reactor.

In the course of works, the existing reactor performances were analyzed, as well as ability to improve them, a lot of thermophysical and neutronic calculations and systems of its cooling and shutdown cooling were carried out.

It was designed type of the core composition with low-enriched uranium fuel, modernization of the reactor cooling system is required that will provide the ability to work with different devices under test at increasing the reactivity reserve and duration of the reactor operation at the power. The change of the fuel enrichment from 90% to 19.75% leaded to the increasing of ^{235}U mass inside of it and to the deterioration of thermal neutron flux per unit of the reactor power.

Currently, two assemblies with LEU fuel are loaded and tests of the fuel in real conditions are being conducted.

Dynamical and structural properties of dense plasmas

M.T. Gabdullin[1], T.S. Ramazanov[2], T.N. Ismagambetova[2], Zh.A. Moldabekov[2]
[1]KBTU, Kazakh British Technical University, Almaty, 050000, Kazakhstan
[2]IETP, al-Farabi Kazakh National University, Almaty, 050040, Kazakhstan
e-mais:gabdullin@physics.kz

Abstract: In this work dense non-ideal plasma was considered. To study how the oscillations of electrons induced by an external field change the inter-particle interaction, the impact of the single particle oscillations on the screening of the test charge has been analyzed using the polarization function in the long wavelength limit [1]. Analysis has been done by considering and neglecting the contribution of ions on the screening. It was shown that single particle oscillations lead to the creation of an oscillatory pattern of the test charge's potential at large distances. Impact of the quantum diffraction (non-locality) and of the collisional damping on the test charge's potential was considered. It was shown that electrons are unable to provide screening of the test charge if the frequency of the induced single particle oscillations larger than the electron-plasma frequency.

Moreover, the structural properties of a dense non-ideal plasma were calculated on the basis of ion-ion interaction micropotential, taking into account quantum-mechanical effects of diffraction. Dense non-ideal plasmas are plasmas where interactions between particles play a dominant role when the potential energy at the average distance exceeds their thermal energy. The state of plasma is described by the dimensionless parameters such as the coupling parameter, relation between Coulomb energy of interaction and thermal energy, and the degeneracy parameter of ions, which is the relation between thermal energy and Fermi energy. Plasma parameters were the following: temperature – $T=10^3 - 10^8$ K, number density – $n=10^{24} - 10^{33}$ cm^{-3}. Screening effect was taken into account by solving the Ornstein-Zernike equation [2] in the HNC approximation. The results for the pair correlation functions were compared with results for Yukawa potential. The difference appearing at denser plasma and larger values of coupling parameter can be explained by the more pronounced influence of quantum mechanical effect.

References

[1] T.S. Ramazanov, Zh.A. Moldabekov, and M.T. Gabdullin, Eur. Phys. J. D. 72, 106 (2018).
[2] C. Kittel, Introduction to Solid State Physics Nauka, p. 789 (1978).

Propagation of gravitational and electromagnetic waves through the magnetic field of the magnetar

Abishev M.E., Denisov V.I., Khassanov M.K., Toktarbay S.
Al-Farabi Kazakh National University, IETP, Almaty, Republic of Kazakhstan,
Moscow State University, Moscow, Russia
e-mails: abishevme@gmail.com

Abstract: The calculations of electromagnetic radiation, caused by a plane gravitational wave propagating in a magnetic dipole fields, have been performed. It is shown that a radiated electromagnetic wave has the frequency of the gravitational wave, and its amplitude is proportional to the square of that frequency. Polarization of the arising electromagnetic wave coincides with the polarization of the gravitational wave. Based on an example of how a gravitational wave propagates in a magnetar's magnetic dipole field, an evaluation of a conversion coefficient of gravitational waves into electromagnetic waves has been made: the required amplitude of a gravitational wave for on-Earth detection of electromagnetic radiation has been calculated as well. The difference Δt in propagation times of normal waves from the common source of electromagnetic radiation to the receiver is calculated. It is shown that the forward part and the "tail" by length $c\Delta t$ of any hard radiation pulse due to the nonlinear electromagnetic influence of the magnetic dipole and quadrupole fields turn out to be linearly polarized in mutually perpendicular planes, and the remaining part of the pulse must have elliptical polarization.

At the present time it is necessary to pay attention to gravitational waves of high frequencies. The processes of gravitational waves conversion into electromagnetic waves can most effectively occur in strong magnetic fields of astrophysical objects such as white dwarfs, pulsars and magnetars. The interaction region between the gravitational waves and the magnetars magnetic field formally spreads to infinity and the interaction intensity decreases inversely to the third power of the distance from the center. To obtain an upper bound for the efficiency of the process of gravitational waves conversion into electromagnetic waves in the strong magnetars magnetic field, we make the calculations, ignoring the plasma existence in magnetosphere as well as the other disturbances, which reduce the efficiency of the process considered.

Analysis of the obtained expressions shows that in the plane in which the neutron star, the source and receiver of hard radiation are located, the field of the magnetic dipole acts on the rays as a collecting lens. The deviation of the rays caused by the magnetic quadrupole field and its superposition with dipole field is not sign-definite and depends on the orientation of the vector m, relative to the principal axes of the magnetic quadrupole, so can serve both as a collecting lens and a scattering lens. Further, in the magnetic dipole field the second normal mode propagates slower than the first normal mode for any orientation of the vector m. The joint action of the dipole field and the magnetic quadrupole field can lead to a decrease in the value of Δt, compared with the value Δt, created only by magnetic dipole field. The calculation showed that, according to the equations of nonlinear electrodynamics of vacuum, the magnetic dipole and quadrupole fields bends the rays of electromagnetic waves and the magnitude of the angle of this curvature depends on the orientation of the dipole and quadrupole moments with respect to the direction of propagation of the electromagnetic wave. The propagation velocities of electromagnetic pulses at $\eta 2 <> \eta 1$ depend on the polarization of the electromagnetic wave. If a short pulse is emitted from the electromagnetic radiation source, then in the general case it will propagate in the magnetic dipole and quadrupole fields in the form of two normal waves having mutually perpendicular polarization. In the receiver these pulses will arrive along different rays and at different instants, as a result of which the recorded total pulse will have an unusual polarization: the front and back parts of each pulse of length $c\Delta t$ will be linearly polarized in mutually perpendicular planes, and the rest part of pulse will be elliptically polarized. A simple analysis shows that at $xs \sim Rs \sim 10$ km and $|B| \sim 1013$ G the value of (23), with a favorable orientation of the dipole and quadrupole relative to the z axis of the Cartesian coordinate system chosen by us, can reach several tens of nanoseconds. This effect can be detected after the creation of spacebased polarimeters, such as wide-field gamma ray (0.023.0 MeV) telescope GAMMASCOPE (Denisov et al. 2017b), which is elaborated now at Moscow State University as a part of Russian space program, such as the XIPE (X-ray Imaging Polarimetry Explorer) project (Soffitta 2013) being developed by ESA and the Imaging X-ray Polarimetry Explorer (IXPE) (Weisskopf 2016) being developed by the NASA / Italian Space Agency.

[1] M. Abishev et al., "The evaluation of electromagnetic forward radiations during the propagation of gravitational waves through the
dipole field of the magnetar" Astroparticle Physics. Volume 103, 2018, p. 94-97
[2] M. Abishev et al., "Effects of non-linear electrodynamics of vacuum in the magnetic quadrupole field of a pulsar" Monthly Notices
of the Royal Astronomical Society, Volume 481, Issue 1, 2018, p.36-43.

Heterojunction Silicon Solar Cells

Nurlan Tokmoldin[1,2], Nikolay Chuchvaga[1,2], Eugene Terukov[3] and Serekbol Tokmoldin[2]

[1] *Institute of Physics and Technology, Satbayev University, 11 Ibgaimov Street, Almaty, 050032,*

[2] *Scientific Production Center of Agricultural Engineering, 312 Raiymbek Avenue, 050005,*

[3] *R&D Center TFTE, Polytechnicheskaya 28, Saint Petersburg, 194064, Russia*

e-mail: ntokmoldin@gmail.com

Abstract: Heterojunction silicon solar cells are offering a number of advantages over conventional silicon photovoltaic devices, including higher efficiency, facile processing and better real-life operating performance. As any cell based on monocrystalline silicon, they demonstrate similar output characteristics for front-side and back-side illumination, which results in significant improvement in their electricity generation, as well as enhanced utilization versatility. At the same time, the impressive trend of rising efficiency of the past several years reveals a high potential of further growth in performance of this type of photovoltaic devices. This paper reports on our effort of optimizing the structure of heterojunction silicon solar cells by means of computer simulation and experimental studies with reasonable correlation observed between the two approaches.

1. Introduction

Silicon photovoltaics currently represents the largest sector of the photovoltaic industry with its dominance unlikely to falter in the near future. At the same time, the silicon industry itself is experiencing rapid modernization due to the gradual reduction in the cost of monocrystalline silicon and market penetration of high efficiency technologies, such as bifacial heterojunction silicon solar cells.

The silicon heterojunction cells have a rather complex structure representing a p-i-n-i-n+ junction, where an n-type monocrystalline silicon wafer is "sandwiched" between nanoscale intrinsic and doped layers of amorphous silicon (a-Si). The multilayered structure of the cell brings significant complications to optimization of its performance in laboratory due to the requirement to simultaneously consider several parameters. Herein we report an approach to optimization of silicon heterojunction cells, as well as the recent progress in their fabrication and study.

2. Results and Discussion

Analysis of operational characteristics of bifacial silicon solar cells based on the “monocrystalline silicon – amorphous silicon” heterojunction (Fig. 1) was performed using the AFORS-HET photovoltaic simulation tool using front-side and rear-side illumination with intensity of 1000 W/m^2 corresponding to the AM1.5 conditions. Device fabrication was performed using commercial 170 μm-thick n-type onocrystalline silicon wafers subjected to proprietary processes of texturing and oxidation. Oxide layer removal was performed immediately prior to the amorphous layer deposition in a dilute aqueous solution of hydrogen fluoride. This was followed by plasma-enhanced chemical vapour deposition (PECVD) of intrinsic (i) and doped (p/n) a-Si layers on both sides of the wafer to obtain a p-i-n-i-n+ structure, which was capped with indium-tin oxide (ITO) by means of magnetron sputtering. Finally, the contact grid was printed using a commercial Ag-based metallization paste.

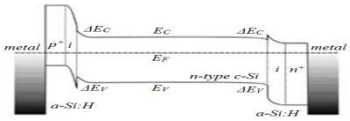

Fig. 1. Band diagram of a heterojunction silicon solar cell structure

Optimization of the device structure included variation of a number of parameters, namely thicknesses and doping levels of the functional layers. Three of those were used to compare computer simulation with experimental results: thickness of the front intrinsic a-Si layer, thickness of the p-type front emitter layer and thickness of the n$^+$-type rear layer. Based on laboratory optimization of the heterojunction silicon solar cell structure, optimal device parameters were elucidated for the given wafer quality and an optimized solar cell was fabricated with efficiency of 20.64%. In addition, simulation of output performance for front- and back-illuminated cells showed that the difference in short-circuit current for the two cases was around 10%.

3. Conclusion

Improved performance and versatility of bifacial solar cells based on the “monocrystalline silicon – amorphous silicon” heterojunction attracts considerable interest to this technology. The reported work on simulation and fabrication of these cells elucidates optimal parameters of the device structure for the given wafer quality to achieve the efficiency exceeding 20%. Further work is expected to focus on improvement of the cell fabrication processes on a photovoltaic fabrication line based at Almaty Institute of Physics and Technology.

4. References

[1] N.S. Tokmoldin, N.A. Chuchvaga, V.N. Verbitskii, A.S. Titov, K.S. Zholdybayev, E.I. Terukov, S.Zh. Tokmoldin, “The use of solar cells with a bifacial contact grid under the condition of Kazakhstan”, Tech. Phys. **62**, 1877 (2017).

[2] N.A. Chuchvaga, D.V. Zhilina, S.R. Zhantuarov, S.Zh. Tokmoldin, E.I. Terukov, N.S. Tokmoldin, “Study and optimization of heterojunction silicon solar cells”, J. Phys.: Conf. Ser. **993**, 012039 (2018).

Elastic property assessment of nanoscale-thick refractory metal films by nanosecond laser acoustics

Zhandos N. Utegulov[1], Talgat A. Yakupov[1], Taha Demirkan[2], Tansel Karabacak[3]

[1]*Department of Physics, School of Science and Technology, Nazarbayev University, Nur-Sultan, Kazakhstan*

[2]*Department of Materials Science and Engineering, Gebze Technical University, Kocaeli, Turkey*

[3]*Department of Physics and Astronomy, University of Arkansas at Little Rock, USA*

e-mail: zhutegulov@nu.edu.kz

Abstract. We have investigated thickness-dependent elastic and structural properties of refractory W, Ta and Mo thin films fabricated by RF magnetron sputtering on silicon substrates [1]. Elastic properties are measured by non-destructive nanosecond laser pulse induced surface acoustic wave technique, while their structural and dimensional properties are analyzed using XRD and SEM, respectively. Young's modulus of these films increases with their nanoscale thickness and for W and Mo films it was consistently higher than those of their bulk values. However, the modulus of Ta films was higher than that of the corresponding bulk metal except for the film with the lowest thickness (22 nm). XRD analysis revealed that all films are under compressive stress, but this stress is diminished in thicker films.

1. Introduction

Refractory metals possess extraordinary properties of resistance to extreme temperatures and wear which have been found in numerous industrial applications ranging from protective coatings in tools, lighting, nuclear reaction control rods, catalysts, tribological applications including, but not limited to, metal cutting and forming [2].

2. Experimental

Ta, Mo and W thin films of thicknesses ranging from 20 to 450 nm were fabricated on Si substrates using RF magnetron sputtering technique. Films crystal structure and orientation were studied by θ-2θ scan Bruker D8 XRD diffractometer. Young's modulus was obtained nondestructively by the frequency dispersion of phase velocity of acoustic waves generated by nanosecond laser pulses, and by independent measurement of film thicknesses and mass densities of film and the substrate. This technique enables measuring elastic properties of thin films with thickness down to few nanometers [3].

3. Conclusion

Nanosecond laser-induced surface acoustic waves were employed to evaluate elastic properties of studied films, while XRD was used to deduce crystallographic composition of the films. Young's moduli of refractory films increase with the corresponding film thicknesses due to nanoscale effect. Lower Young's modulus and density values of the films with smaller thicknesses can be explained by the Zone-1 columnar microstructure of structure-zone model (SZM) [4] of these films in which there are more voids present. It can also explain that these modulus values do not reach corresponding bulk modulus values for these materials. However, for refractory films made from softer metals the film-to-bulk modulus ratio typically is higher than that of the films made of harder metals. This ratio for Ta films even exceeds 1, i.e. Young's modulus of Ta thin films gets higher than that of the bulk metal, which is believed to be due to finer grain size of the tetragonal β-Ta thin films structure comparing to bulk α-Ta [5]. For soft refractory metals, thin films might be more mechanically robust than their corresponding bulk metals. Further grain size analysis of fabricated films will be needed to get deeper insight into this nano-mechanical property.

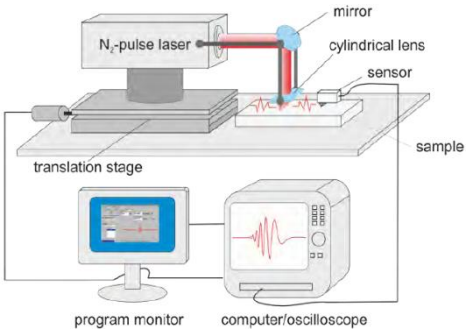

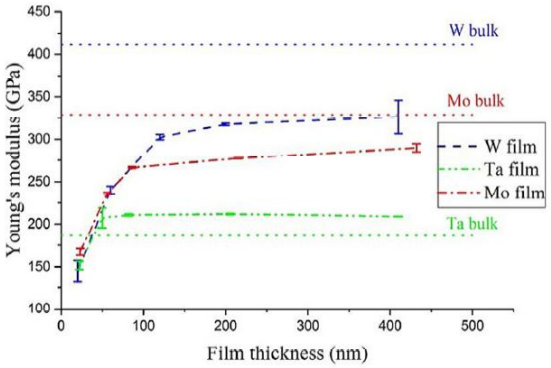

3. References

[1] Talgat Yakupov, Zhandos N. Utegulov, Taha Demirkan, Tansel Karabacak "Elastic and structural properties of nanometer scale-thick refractory metal films", Materials Today: Proceedings, 4(3), Part A, 4469–4476 (2017)

[2] S. Hogmark, P. Hedenqvist, S. Jacobson, Surface and Coatings Technology, 90 (3), 247-257 (1997).

[3] D. Schneider, P. Siemroth, T. Schülke, J. Berthold, B. Schultrich, H.-H. Schneider, R. Ohr, B. Petereit, and H. Hillgers, Surface & Coatings Technology, 153, 252-260 (2002).

[4] J. A. Thornton, J. Vac. Sci. Technol. 11, 666 (1974).

[5] M. Zhang, Y.F. Zhang, P.D. Rack, M.K. Miller and T.G. Nieh, Scripta Materialia, 57, 1032–1035 (2007).

Grain Surface Heating in Cryogenic Environment

M. M. Muratov[1,2] , T. S. Ramazanov[2], and Zh. A. Moldabekov [2,3]

[1] *National Nanotechnological Laboratory of Open Type , Al-Farabi Kazakh National University, 71 Al-Farabi ave., 050040 Almaty, KAZAKHSTAN*

[2] *Institute for Experimental and Theoretical Physics, Al-Farabi Kazakh National University, 71 Al-Farabi ave., 050040 Almaty, KAZAKHSTAN*

[3] *Institute of Applied Sciences and IT, 40-48 Shashkin str., 050038 Almaty, KAZAKHSTAN*

e-mail: mukhit.muratov@gmail.com

Surface temperature of the dust particle in cryogenic complex plasmas at low gas pressure is considered. A relation that represents the temperature ratio of the dust particle surface to that of the surrounding gas, in low-pressure weakly ionized complex plasmas, was used to study a dust particle heating at cryogenic conditions [1]. Orbit motion limited theory was used to compute the electron as well as ion flux to the dust particle surface in a weakly collisional case [2]. It is shown that comparing with background gas, the dust particle surface temperature at low pressure is significantly higher (up to ten times). The gas temperature near the grain surface is a slowly decreasing function of distance with asymptotic ~ 1/r behavior. Therefore, the dust particle surface heating is important for near space around dust particle. At distances comparable with average inter-dust distance, the neutral shadowing interaction appearing due to large temperature difference between the grain surface and surrounding gas can lead to a significant changes in the structural properties of a cluster of dust particles [3]

1. Introduction

Dusty plasma has been the subject of intensive research since the beginning of the nineties. There is a large scope of experimental data on static and dynamic properties of dusty plasmas, which were successfully explained in the framework of theoretical models and computer simulation.

2. Theory

In this work, we consider the dust particle surface temperature in the low pressure plasma *p=0.6–10* Pa in cryogenic conditions. It was discovered that the dust particle surface temperature can be significantly higher than that of the background gas.

To calculate the electron flux to the grain surface, the collisionless orbit motion limited (OML) expression can be used:

$$J_e = \sqrt{8\pi} a^2 n_e \upsilon_{T_e} exp(-z), \qquad (1)$$

where a is the grain radius, n_e is the electron density, $\upsilon_{T_e} = \sqrt{k_B T_e / m_e}$ is the electron thermal velocity, $z = e|Q_d|/(ak_B T_e)$ is the normalized charge of the dust particle and k_B is the Boltzmann constant.

An approximate expression for the ion flux in a weakly collisional regime was taken in the following form:

$$J_i = \sqrt{8\pi} a^2 n_i \upsilon_{T_i} \left(1 + z\tau + 0.1\,(z\tau)^2 \frac{\lambda}{l_i}\right), \qquad (2)$$

here, $\tau = T_e/T_n$ is the ratio of the electron temperature to the neutral atom temperature, λ is the screening length, and $l_i \sim 1/n_n \sigma_{in}$ with the cross section $\sigma_{in} \sim 10^{-15}$ cm^{-2} of the resonant charge exchange of the helium ion with a stationary atom. In our model, $\lambda \approx \lambda_i = (k_B T_i / 4\pi n_i e^2)^{1/2}$ and $T_i \approx T_n$.

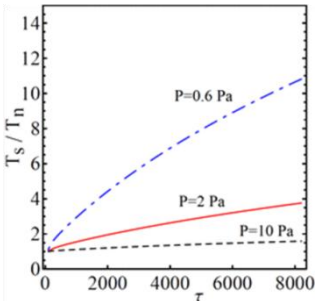

Fig. 1. Relative temperature of the dust particle surface T_s/T_n vs. temperature ratio $\tau = {}^{T_e}/_{T_n}$ at $T_e \approx 3eV$ for neutral gas pressures.

3. References

1. S.A. Khrapak, G.E. Morfill, Grain surface temperature in noble gas discharges: Refined analytical model, Phys.Plasmas 13, 104506 (2006)

2. S.A. Khrapak, S.V. Ratynskaia, A.V. Zobnin, A.D. Usachev, V.V. Yaroshenko, M.H. Thoma, M. Kretschmer, H. Hofner, G.E. Morfill, O.F. Petrov, and V.E. Fortov, Particle charge in the bulk of gas discharges, Phys.Rev. E 72, 016406 (2005).

3. Ramazanov, Moldabekov, and Muratov, Grain Surface Heating in Cryogenic Environment, Phys. Plasmas 24, 050701 (2017)

Fission fragments' and electrons' coupled Boltzmann equations and degradation energy spectra formation in a weakly ionized plasma irradiated by fission fragments

Sandybek Kunakov[1, a)] and Aigerim Shapiyeva[2, b)]

[1)] *Al Farabi National University, Almaty, Kazakhstan*

[2)] *Moscow Institute of Physics and Technology, Dolgoprudny, Moscow region, Russia*

[1)] *email: sandybeck.kunakov@gmail.com, [2)] shapieva.ae@phystech.edu*

Abstract: Coupled self-consistent Boltzmann equations for fission fragments and created primary electrons are defined for weakly ionized dense plasma irradiated by fission fragments. On the base of these equations, fast particles' energy formation kinetics in plasma studied. Steady-state analytical solutions for fission fragments and the primary electrons' functions of energy distribution are found and analyzed for the helium-3 plasma irradiated by thermal neutron flux. Results are validated by Monte Carlo energy spectra calculations.

1. Introduction

Any gas irradiated by high energy particles demonstrates its modified chemical properties which might be applied in a variety of technologies like direct nuclear energy transformation to coherent optical radiation. If test gas contains fissionable component (FC) interacting with neutrons like helium-3 [^3He] or uranium hexafluoride [UF_6], and set into the thermal neutron flux, then the created plasma turns to be a unique physical object. Within this physical condition it is possible to realize the direct transformation of the nuclear energy[3] into electro- magnetic radiation of excited atoms. This challenging technology has some internal unsolved problems waiting its solution and the major is the energy distribution of fission fragments and primary electrons.

2. Electrons' energy distribution

Electrons energy distribution entirely depends on fission fragments energy distribution and time and space formation kinetics described by self-consistent system of Boltzmann equations.

Energy distribution functions of fission fragments and electrons consist of two parts. The first one is their formation due to degradation processes in the medium and the second is an external source which may be of different nature, mostly defined by component and neutral flux time and space distribution.

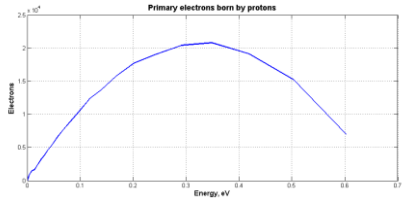

Figure1.Electrons energy distribution in helium-3 fissioning plasma set into the thermal neutron flux

We come to the conclusion that any particle released as a result of process will acquire the amount of energy around MeV and antineutrino as an immanent satellite will demonstrate its existence due to weak and strong interactions within nuclei. process for helium-3 isotope might be exposed in the following way

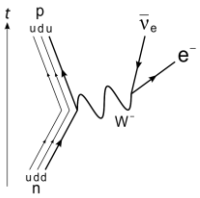

Fig. 2.Fission and weak interactions lead to the neutrino flux: immanent satellite of any fissioning process

$$^3He + n \rightarrow \left|\begin{matrix} u & u & u & u \\ d & d & d & g \\ u & d & d\bar{d} & d \\ d & d & u & W^+ \end{matrix}\right| \forall 578\ keV + \\ + \left|\begin{matrix} u & & u & \\ d & d\bar{d} & g & e^+ \\ & g & W^- & \end{matrix}\right| \forall 198\ keV + e + \bar{\nu} + e^+$$

3. Coupled Boltzmann equations

In nuclear induced plasma, three functions of energy distribution, namely, for protons, tritium nucleuses and electrons are defined. Let's denote three fast particles (protons, tritium nuclei, primary electrons) energy distribution functions as $f_p(t, r, v)$, $f_T(t, r, v)$, $f_{pe}(t, r, v)$:

$$\frac{\partial f_p}{\partial t} + \mathbf{v_p} \cdot \frac{\partial f_p}{\partial \mathbf{r}} + \frac{\mathbf{F}}{m_p} \cdot \frac{\partial f_p}{\partial \mathbf{v}} = I_{sp} + I_{pi} + \sum_{i=1}^{N} I_{pexc,i} + I_{pelastic} + I_{prec}$$

$$\frac{\partial f_T}{\partial t} + \mathbf{v_T} \cdot \frac{\partial f_T}{\partial \mathbf{r}} + \frac{\mathbf{F}}{m_T} \cdot \frac{\partial f_T}{\partial \mathbf{v}} = I_{sT} + I_{Ti} + \sum_{i=1}^{N} I_{Texc,i} + I_{Telastic} + I_{Trec}$$

$$\frac{\partial f_{pe}}{\partial t} + \mathbf{v_{pe}} \cdot \frac{\partial f_{pe}}{\partial \mathbf{r}} + \frac{\mathbf{F}}{m_{pe}} \cdot \frac{\partial f_{pe}}{\partial \mathbf{v}} = I_{pi} + I_{Ti} + I_{pei} + \\ + \sum_{i=1}^{N} I_{peexc,i} + I_{peelastic} + I_{perec} + I_{peaff},$$

The primary electrons might be found from the following equation:

$$\mathfrak{J}_{pe}(v_e) = [BG] \sum_k^N Z_{j,k}^2 \int_I^{E_e} dv_{j,k} \delta(v_{j,k} - \frac{1}{2} v_{j,k}^0)$$
$$\int_I^{E_{j,k}} \Sigma_{j,k}^{ion}(v_j, \triangle E_{j,k} = E_{j,k} - I - E_{pe,k}) v_{j,k} d\triangle E_j,$$

4. Conclusions

1. Electrons energy distribution entirely depends on fission fragments energy distribution and time and space formation kinetics described by self-consistent system of Boltzmann equations.
2. Energy distribution functions of fission fragments and electrons consist of two parts. The first one is their formation due to degradation processes in the medium and the second is an external source which may be of different nature, mostly defined by component and neutral flux time and space distribution.

5. References

[1] J. C. Guyot, G. H. Miley, and J.T.Verdeyen, Nuclear Science and Engineering **48**, 373 (1972).

[2] Kunakov S., Son E, Bolatov Zh., Kaster. N Optical spectra in helium plasma generated by nuclear fission fragments International Journal of Mathematics and Physics , 6, N0.1,75-81 (2015)

[3] Kunakov S., Shapiyeva A. Probe diagnostics of $^3He+UF_6$ plasma, generated in the core of nuclear reactor WWW- International Journal of Mathematics and Physics, 6, N0.1, 75 (2015), 69-74 pp.

The Hypothesis about Mechanism of Heat Transfer and The Nature of Its Carrier

B.T. Utelbaev[1], E.N. Suleimenov[1], A.B. Utelbaeva[2]

[1,2]Kazakh-British Technical University (Almaty), Kazakhstan

b.utelbayev@mail.ru,

[2]South Kazakhstan State University. M. Auezov (Shymkent), Kazakhstan

e-mail: mako_01-777@mail.ru

In the scientific literature there are three types of heat transfer: thermal conductivity, or conduction; convection, or the transfer of heat by moving particles of a substance; radiation, or radiation. At first glance, the temperature seems to be a very simple quantity characterizing warmth, but in reality it is a complex parameter that ensures the physicochemical transformations of the mate-real world. Recently, the view has been expressed that the heat in solids is transferred due to the motion of phonons. Phonon - quantum of oscillations of atoms of the crystal lattice, introduced by Tamm I.E. by analogy with the quantum of the electromagnetic field photon.

heat carriers. By analogy with the elementary carrier of light energy - a photon we have put forward a hypothesis which states that the carrier of heat is an elementary particle, which we conditionally call “thermal meter”.

The transfer of heat energy to the system by “heat-collectors” from the outside primarily changes the structure of the substance and its energy state. Similarly, during the activation of reagents, heat energy is absorbed by thermal energy, changing the shape of the electron clouds of the “chemical individuals” of the original substances.

Based on the Gibbs equations and molecular-kinetic theory, the mass of the proposed elementary particle and its velocity in various media are calculated.

[1] Utelbayev B.T, Suleimenov E.N, Utelbayeva A.B. The hypothesis about mechanism of heat transfer and the nature of its carrier. International Scientific Researches Journal “Ponte, Florence, Italy”, 2016, Vol. 72, Feb.

Investigation of carbon nanowalls synthesis by pecvd method

D.G. Batryshev[1], Ye. Yerlanuly[1], M.T. Gabdullin[2], T.S. Ramazanov[1]
[1]*Al-Farabi Kazakh National university, Almaty, 050040, Kazakhstan*
[2]*Kazakh-British Technical University, Almaty, 050000, Kazakhstan*
e-mail: batryshev@physics.kz

In this work, we present the results of study of carbon nanowalls synthesis in the plasma of radio-frequency discharge by plasma enhanced chemical vapor deposition method. So-called carbon nanowalls (CNWs) are one of the allotropes of carbon with vertically oriented graphene sheets and high-aspect ratio with large surface area. Due to this, they have a potential for application in astronomy as an absolutely black-bode material for bolometers, in electronics and energy as electrodes for supercapacitor and solar cells, etc.

The morphologies of obtained samples were investigated by scanning electron and probe microscopy, and also Raman spectroscopy is used for identification of their structure. It was found that an increase in the discharge power caused a decrease in the height of carbon nanowalls and an increase in their thickness. It is seen that argon ion irradiation enhances surface reaction in the growth phase, whereas the increasing of ion irradiation inhibits the growth process of carbon nanowalls due to the etching effects. Also, some explanation is given for understanding the formation of agglomerated nanoclusters on the surface of carbon nanowalls with increasing the power of radio-frequency discharge [1-3]. The obtained results can be useful for the scientists and engineers, who are interested in understanding the synthesis process of CNWs.

[1] D. Batryshev, Ye. Yerlanuly, T. Ramazanov, and M. Gabdullin, Investigation of Synthesis of Carbon Nanowalls by the Chemical Vapor Deposition Method in the Plasma of a Radio Frequency Capacitive Discharge // IEEE TRANSACTIONS ON PLASMA SCIENCE (2019). DOI 10.1109/TPS.2019.2903145
[2] D.G. Batryshev, Ye. Yerlanuly, T.S. Ramazanov, M.K. Dosbolayev, M.T. Gabdullin, Elaboration of carbon nanowalls using radio frequency plasma enhanced chemical vapor deposition // Materials Today: Proceedings. 2018. Vol. 5, No. 11. Pp. 22764-22769.
[3] Ye. Yerlanuly, D. Batryshev, T. Ramazanov, M. Gabdullin, Synthesis of carbon nanowalls by the PECVD method for creating supercapacitors // Book of Abstaracts of International conference on Advanced Energy Materials AEM2019, 10-12 September 2018, Surrey, England. P. 77.

Observational properties of a black hole mimicker

Daniele Malafarina

Department of Physics, Nazarbayev University Kabanbay batyr 53, 010000, Nur-Sultan (Kazakhstan)

e-mail: Daniele.malafarina@nu.edu.kz

Abstract: Recently, the Event Horizon Telescope collaboration released the image of the 'shadow' of the black hole candidate in the galaxy M87 [1]. While the data allows to rule out some alternative models to black holes, it is still possible that a black hole mimicker could produce a qualitatively similar image. We consider here one such mimicker, described by a known static axially symmetric space-time and investigate which observational features would allow to distinguish it from a black hole.

1. The γ -metric

The γ –metric is a well-known static exact solution of Einstein's equations in vacuum that can be written a

$$ds2=-F(r)\gamma dt2+F(r)\gamma 2-\gamma G(r,\vartheta)1-\gamma 2(dr2F(r)+r2d\vartheta 2)+F(r)1-\gamma r2\sin\vartheta 2d\varphi 2 \ , (1)$$

with

$$F(r)=1-2mr \ , (2)$$

$$G(r, \theta)=1-2mr+m2r2\sin\vartheta \ . (3)$$

The metric reduces to the Schwarzschild space-time for $\boldsymbol{\gamma - 1}$ and it describes the field outside a prolate (oblate) object for $\boldsymbol{\gamma < 1}$ ($\boldsymbol{\gamma > 1}$, respectively) [2]. The surface r=2m is singular for all values of γ except, therefore besides the spherically symmetric case, it cannot be considered as a black hole. In the following we will describe some observational properties of the γ -metric that may allow to distinguish it from a black hole.

2. Orbits in the γ -metric

The study of orbits for test particles and photons in the equatorial plane of the γ -metric provides several quantities that may correspond to observable features of the space-time[3-5]. These are:

- The innermost stable circular orbit (ISCO) for massive test particles, risco.
- The photon capture orbits, rps.
- The boundary for marginally bound orbits, rmb.

The values of the radii for such orbits depends on the value of the deformation parameter γ (see Figure 1) and corresponds to optical properties of particles in the accretion disk or light rays deflected by the gravitating source.

Fig. 1. The dependence of the values of characteristic orbits in the γ –metric as a function of γ.

From these quantities we may study the motion of neutral and charged particles in the accretion disk surrounding the compact object [3], the 'shadow' of the compact object as seen by distant observers [4] and the frequencies of oscillations of particles in the accretion disk [5]. Such observables depend on the value of γ and therefore, if measured in astrophysical black hole candidates, may allow to determine whether the geometry is well described by the Schwarzschild or Kerr solutions or if the source has a non-vanishing quadrupole moment.

3. References

[1] K. Akiyama et al. (Event Horizon Telescope), "First M87 Event Horizon Telescope Results. I. The Shadow of the Supermassive Black Hole", Astrophys. J. 875, L1 (2019).

[2] W. B. Bonnor, "Physical interpretation of vacuum solutions of Einstein's equations. Part I. Time-independent solutions", General Relativity and Gravitation 24, 551 (1992).

[3] Carlos A. Benavides-Gallego, Ahmadjon Abdujabbarov, Daniele Malafarina, Bobomurat Ahmedov, Cosimo Bambi, "Charged particle motion and electromagnetic field in γ spacetime", Phys. Rev. D 99, 044012 (2019).

[4] Askar B. Abdikamalov, Ahmadjon A. Abdujabbarov, Dimitry Ayzenberg, Daniele Malafarina, Cosimo Bambi, Bobomurat Ahmedov, "A black hole mimicker hiding in the shadow: Optical properties of the γ metric", arXiv:1904.06207.

[5] Bobir Toshmatov, Daniele Malafarina, Naresh Dadhich, "Harmonic oscillations of neutral particles in the γ-metric", arXiv:1905.01088.

Effect of Non-Stationary Electric Current on The Oxide Meline System - Gas Phase

S.A. Krasikov[1], B.T. Utelbayev[2], E.N. Suleimenov[2],
[1]*Institute of Metallurgy UB RAS, Ekaterinburg, Russia*
[1]*sankr@mail.ru,*
[2]*Kazakh-British Technical University (Almaty), Kazakhstan*
e-mail: metallaim@mail.ru

We have published materials containing experimental results on the influence of physical factors on chemical reactions between the components of the gas phase and the oxide melt. In particular, the influence of non-stationary electric current (square wave) with a frequency of 50 pulses per minute. A melt of synthetic slag of the following composition was used, %: 41.44 SiO_2, 10.48 Al_2O_3, 13.62 FeO, 3.42 Fe_2O_3, 32.37 CaO .; melting point 1200^oC. The value of the "working" current in the system for this type of slag was 180 mA. After stabilization of the set temperature at 1250 ° C, the circulation pump was turned on and the gas was pumped over the melt for 30 minutes. Then the pump was turned off and a potential difference of 75, 110 or more volts was applied to the electrodes. Fixed starting current and current after 5, 10, 15 and 20 seconds. In almost all experiments, a decrease in pressure was observed in the system circulation, the compensation rubber chamber was strongly compressed, and it was not possible to measure the composition of the gas components. For several experiments, the amount of gas absorbed by the melt was determined, which ranged from 800 to 1200 cm^3. Visually, an unusual variety of chemical reactions occurring in the gas-oxide melt system under the influence of a non-stationary electric current was observed. In particular, a change in current intensity can cause triboelectric effects when solid inclusions move along the surface of the melt. A complete analogy is revealed in the behavior of the macrosystem and the microsystem during the melt processing by the components of the gas phase. The use of electric current can promote such chemical reactions that are considered unlikely. and directly a chemical reaction can generate an electric current during the process, which in some cases will change the course of the process.

[1] S. A. Krasikov, B. T. Utelbaev, E. N. Suleimenov. Effect of a Nonstationary Electric Current on the Oxide Melt–Gas Phase System. Russian Metallurgy (Metally), Vol. 2018, No. 2, pp. 197–200.

Note. The authors thank the leadership of the Indian Institute of Science (Bangalore, Republic of India), the leadership of the Materials Technology Department and personally Professor K. Chattohadhyay for the opportunity to conduct research on the products of the reaction of the gas phase and the melt at research.

Properties of the Complex Plasma in the Radiofrequency Discharge With Imposed DC Field

A.U. Utegenov, M.K. Dosbolayev, T.S. Ramazanov
IETP, Al-Farabi KazNU, 050040, 71a Al-Farabi ave., Almaty
e-mail: almasbek@physics.kz

Abstract: In this paper the results of an experimental investigation of the effect of a electrostatic field on the structural characteristics of plasma-dust formations in radio-frequency discharge are presented. The pair correlation function of the distribution of dust particles was calculated. The results of experimental investigation reveal that the effect of the electrostatic field on the dusty structure leads to the changes in the spatial and structural characteristics of plasma-dust formation.

1. Introduction

Complex or dusty plasma is an ionized gas composed of electrons, slow-moving ions and neutral gas molecules as well as externally added solid particles with nano- and micron-sizes. The presence of dust in the plasma in many technological industries shows negative effect, e.g. during processing, etching and sputtering of material surfaces by plasma [1], in fusion devices with magnetic confinement [2]. Therefore, the study of plasma-dust is an actual problem, and this problem has been studied for the past three decades.

In regards to this subject several methods to study the dusty plasma have been demonstrated, for instance, investigation of the growth of dust particles in the plasma of a mixture of chemically active and inert gases [3-4], investigation of the behavior of dust particles in several types of gas discharges [5-6], investigation of the behavior of dust particles near the Langmuir probe [7]. Also, applications of the dusty plasma should be noted: separation of dust particles in the plasma environment in order to obtain monodisperse powders [8], technology of deposition of aerosol particles in combustion products or thermal stations.

2. Results and discussions

In the experiments, we used monodisperse particles, so that they formed a single layer structure over the lower electrode. The shifting of dust structure in vertical direction was obtained by applying a DC voltage to the inter-electrode space. Also, the dust shifting to up or down was dependent on the polarity of the applied DC voltage. From the intensity of the plasma emission it was also observed that with increase of the negative signed constant field the plasma compressed in vertical direction, which reveals the increasing of plasma-sheath. The most part of the discharge glow was distributed uniformly (except for the near-electrode region), which means that in this area the process of excitation of atoms occurs approximately uniformly. It follows, that under these conditions, electrons have time to acquire enough energy to excite the atoms.

The external constant field affects the structure of the plasma buffer, compressing it in the center of the inter-electrode space, being that the dusty structure formed at the boundary of plasma-sheath a negative voltage also influences its spatial position. For more detailed study of the structural characteristics of dust formation pair correlation functions (PCF) were calculated. From the obtained data, one can note that with increase of the constant field the average inter-particle distance decreases.This behavior can be explained by the fact that with increase of negative field an additional ion flow appears which is directed to the lower electrode. This process reduces the fluctuations of the charge of the dust particles, whereupon the structure becomes strongly coupled system [9].

3. References

[1] Lieberman, M. A. and Lichtenberg, A. J., Principles of Plasma Discharges and Materials Processing, Second Ed.(Wiley Interscience, 2000)
[2] Fortov, V.E. Encyclopedia of low-temperature plasma. Nauka Press. (Moscow, 2000)
[3] S. A. Orazbayev, Y. A. Ussenov, T. S. Ramazanov, M. K. Dosbolayev, A.U. Utegenov. A calculation of the electron temperature of complex plasma of noble gases mixture in CCRF discharge. Contrib. Plasma Phys. **55** (5). 428-433. (2015).
[4] A.A. Fridman, L. Boufendi, T. Hbid, B.V. Potapkin, A. Bouchoule. Dusty plasma formation: Physics and critical phenomena. Theoretical approach. Journal of Applied Physics. **79**. 1303-1314. (1996).
[5] T.S. Ramazanov, K.N. Dzhumagulova, A.N. Jumabekov, M.K. Dosbolayev. Structural properties of dusty plasma in direct current and radio frequency gas discharges. Physics of Plasmas. **15**. 053704. (2008).
[6] S. Iwashita, E. Schungel, J. Schulze, P. Hartmann, Z. Donko, G. Uchida, K. Koga, M. Shiratani, U. Czarnetzki. Transport control of dust particles via the electrical asymmetry effect: experiment, simulation and modelling. J. Phys. D: Appl. Phys. **46**. 245202. (2013).
[7] T.S. Ramazanov, N.Kh. Bastykova, Y.A. Ussenov, S.K. Kodanova, K.N. Dzhumagulova, M.K. Dosbolayev. The behavior of dust particles near Langmuir probe. Contrib. Plasma Phys. **52** (2). 110-113. (2012).
[8] D.G. Batryshev, T.S. Ramazanov, M.K. Dosbolayev, M.T. Gabdullin. A method of separation of polydisperse particles in the plasma of radio-frequency discharge. Contrib. Plasma Phys. **55** (5). 407-412. (2014).
[9] Dosbolayev M.K., Utegenov A.U. Ramazanov T.S., Structural Properties of Buffer and Complex Plasmas in RF Gas Discharge-Imposed Electrostatic Field. IEEE Transactions on Plasma Science. **44** (4), 469-472. (2016).

Experimental investigation of the properties of plasma-dust formations on pulsed plasma accelerator

M.K. Dosbolayev, Zh. Raiymkhanov, A.B. Tazhen, T.S. Ramazanov
Institute of Experimental and Theoretical Physics, Al-Farabi Kazakh National University, Almaty 050040, Kazakhstan
e-mail: merlan@physics.kz

Abstract: In this work, the process of interaction of a pulsed plasma with the surface of graphite plates is studied. Trajectories of the scattered dust particles at plasma erosion of plate surface are obtained. The high-speed «Phantom VEO710S» camera with the capture rate of 78,000 frames/sec were used to capture the interaction of a pulsed plasma flow with the surface of the graphite plates and the evolution of the particles The size of deposited carbon nanoparticles varies within the range of 20-180 nm. In addition, nanoparticles of the electrode material were obtained.

Introduction

Currently, one of the main challenges in successful devise and operation of the ITER is erosion of the internal walls of the reactor's vacuum chamber. The product of this erosion process is the particles of micron to submicron size found in the reactor chamber. The presence of dust in the plasma pinch negatively affects the thermonuclear processes in ITER. Plasma-thermal (radiation) effects on the walls of the chamber is one of the key challenges in constructing safe and durable chambers, it is the adverse effects of pulsed plasma flow to the walls of the reactor chambers is the key issue in understanding and tackling the plasma dust formation issue in ITER [1, 2].

The experiments were carried out on the installation of a pulsed plasma accelerator IPU-30 [3]. The schematic diagram of the experiment is shown in Figure 1 (top view). There are two graphite plates (Figure 1), placed in the plasma flow path at a 45-degree angle to the axis of chamber, at a distance 60 mm from the end of the electrodes. The length of the plates extends to the diameter of the outer electrode, so the plasma flow appeared in interelectrode space pass through the any sector of the graphite plates. These plates are the source of carbon dust particles. The particles are emitted when the plasma flow is interacting with the surface of the plate and moves along the plasma flow direction in sufficient value of the discharge voltage. The copper substrates are placed at a distance of 30 mm from the graphite plate. These substrates are used to collect the dust particles that are formed during the erosion of the plates.

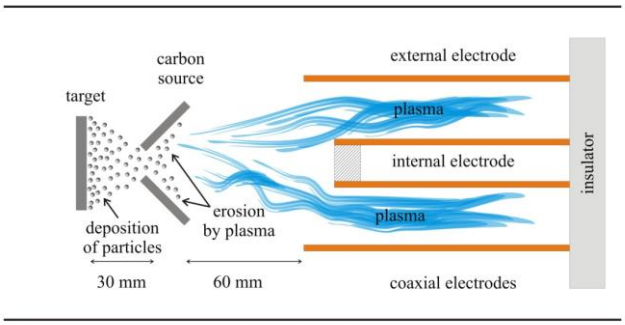

Fig. 1. Schematic diagram of the experimental setup and plasma processes in it. Top view.

The interaction of a pulsed plasma flow with the surface of the graphite plates and the evolution of the particles were captured by the high-speed "Phantom VEO710S" camera. The capture rate of 78,000 frames/sec. Thus, the distance between neighboring frames is 12.82 μsec. The size of collected carbon dust particles varies within the range of 20-180 nm [4, 5].

References

J.C. Flanagan et al., "Characterising dust in JET with the new ITER-like wall" Plasma Phys. Control. Fusion **57**, 014037 (2015).
A. Yu. Pigarov, S. I. Krasheninnikov, T.K. Soboleva, T.D. Rognlien, "Dust–particle transport in tokamak edge plasmas" Phys. Plasmas 12, 122508 (2005).
M.K. Dosbolayev, A.U. Utegenov, A.B. Tazhen, T.S. Ramazanov, "Investigation of dust formation in fusion reactors by pulsed plasma accelerator" Laser and Particle Beams **35**, 741-749 (2017).
M.K. Dosbolayev, Zh. Raiymkhanov, A.B. Tazhen, T.S. Ramazanov, "Experimental investigation of the properties of plasma-dust formations on pulsed plasma accelerator" IEEE Transactions on Plasma Science, in press (2019).
M.K. Dosbolayev, Zh. Raiymkhanov, A.B. Tazhen, T.S. Ramazanov, "Impulse Plasma Deposition of Carbon Nanoparticles" Acta Physica Polonica A, in press (2019).

Synthesis of carbon nanoparticles in plasma medium and their application

S.A. Orazbayev[1,2], T. S. Ramazanov[1], R.E. Zhumadylov[2], M.T. Gabdullin[1,2], M.Henault[3], L. Boufendi[3]

[1] IETP, Al Farabi Kazakh National University - Al Farabi av., 71, Almaty, Kazakhstan
[2] NNLOT, Al Farabi Kazakh National University - Al Farabi av., 71, Almaty, Kazakhstan
[3]GREMI, UMR7344 CNRS/Université d'Orléans, F-45067 Orléans, France
e-mail: rakimzhan@gmail.com

Abstract: In this paper, methods for the synthesis of carbon nanoparticles and the dependence of their growth rate on plasma parameters were developed and studied. To obtain carbon nanoparticles, an RF discharge plasma was used in a mixture of methane (2%) and argon (98%) gases at different pressures, powers, and synthesis times. Graphs of the time of nanoparticle nucleation as a function of gas temperature for different plasma parameters and the distribution of the diameter and concentration of nanoparticles on the synthesis time in Ar / CH_4 plasma were also obtained. Experimental results on the synthesis of carbon nanoparticles in plasma of combined RF+DC discharge were presented. Experimental results on the production of hydrophobic surfaces based on carbon nanoparticles in an RF discharge plasma were also given.

1. Introduction

The study of nanomaterials attracts considerable attention because of their unique properties. Nanoparticles and nanostructured materials are used in many spheres of human activity - in electronics, computer science, materials science, energy, engineering, biology, medicine. Carbon nanomaterials are considered the most widely discussed and used nanomaterials over the past decades. Carbon nanoparticles due to strong photoluminescence, depending on the size and wavelength of excitation, are the subject of close study. Due to the presence of numerous carboxyl groups on the surface, carbon nanoparticles have outstanding solubility in water and the ability to form polymeric, organic, inorganic and biological molecules.

2. Results and conclusions

Synthesis of carbon nanoparticles was carried out in a plasma of RF discharge in a mixture of methane (2%) and argon (98 %) gases at different pressure, power and duration. Graphs of the time of nanoparticle nucleation as a function of gas temperature for different plasma parameters and the distribution of the diameter and concentration of nanoparticles on the synthesis time in Ar / CH_4 plasma were also obtained [1,2]. Experimental results on the synthesis of carbon nanoparticles in the plasma of a combined RF + DC discharge were presented [3,4]. The RF discharge power was varied within 1 ÷ 50 W, the voltage of the constant power source was 0 ÷ 100 V, the gas pressure was 0.1 ÷ 1 Torr. As a result of the experimental work carried out at various negative stresses, the corresponding samples were obtained, which were studied on the basis of SEM. This analysis of the samples indicates the presence of carbon nanoparticles and surface roughness, regardless of the negative voltage. SEM images show that the distribution of particles is uniform, the average diameter of the synthesized particles is about 60-70 nm, the film thickness is about 300 nm. That is, the surface roughness is sufficient for the manifestation of hydrophobic properties.

Experimental results on the obtaining of hydrophobic surfaces based on carbon nanoparticles in an RF discharge plasma were also given. An experimental setup for obtaining hydrophobic surfaces in low-temperature atmospheric pressure plasma was developed. The optimal plasma parameters for the synthesis of hydrophobic surfaces whose contact angle with water is above 150^0 were determined. A series of experiments was carried out for silicon and aluminum substrates, the deposition duration was 15, 20 seconds, the RF discharge power varied from 10 to 40 W in 10 watts steps. The deposition was carried out in the flow of the working gas Ar and Ar + CH_4 at atmospheric pressure, the gas flow rate was 5 l / min [5].

3. References

[1] J. Lin, S. Orazbayev, M. Hénault, Th. Lecas, K.Takahashi, L.Boufendi., Effects of gas temperature, pressure, and discharge power on nucleation time of nano-particles in low pressure C_2H_2/Ar RF plasmas // J. App. Phys., – 2017. – Vol. 122. – P. 163302.

[2] S. A. Orazbayev M. Henault, T. S. Ramazanov, L. Boufendi, D. G. Batryshev M. T. Gabdullin, Influence of gas temperature on nucleation and growth of dust nanoparticles in RF plasma, IEEE Transactions On Plasma Science. – 2019. doi: 10.1109/TPS.2019.2912805.

[3] S. A. Orazbayev, A.U. Utegenov, A.T. Zhunisbekov, M. Slamyiya, M.K. Dosbolayev , S. Ramazanov, Synthesis of carbon and copper nanoparticles in radio frequency plasma with additional electrostatic field // Contrib. Plasma Phys. – 2018. – Vol. 58, No. 10. – P. 961.

[4] S. Orazbayev, A.T. Zhunisbekov, T.S. Ramazanov, D.B. Omirbekov, M.K. Dosbolayev, M.T. Gabdullin, R.E. Zhumadylov, Synthesis of carbon nanoparticles in combined RF-DC plasma // Materials Today: Proceedings, – 2018. – Vol. 5. – P. 22819.

[5] S.A. Orazbayev, M.T. Gabdullin T.S. Ramazanov M.K. Dosbolayev D.B. Omirbekov Y. Yerlanuly, Obtaining of superhydrophobic surface in RF capacitively coupled discharge in Ar/CH4 medium, Applied Surface Science, – 2019. – 472 – P. 127-134.

Particle-solid surface interactions

F.F. Umarov[1] and A.A. Dzhurakhalov[2]

[1]Kazakh-British Technical University, Tole bi Str. 59, 050000 Almaty, Kazakhstan

[2]University of Antwerp, Middelheimlaan 1, 2020 Antwerp, Belgium

e-mail: farid1945@yahoo.com

The peculiarities of the some processes (ion scattering, sputtering and implantation as well as nanoclusters deposition and thin film growth) accompanying the particle-solid surface interactions has been investigated by different computer simulation methods (binary collision approximation, molecular dynamics) [1-3].The **scattering** and **sputtering** processes at 0.5-5 keV Ne grazing ion bombardment of Si(001), SiC(001), $Cu_3Au(001)$, Ni(100) and Cu(100) surfaces and their possible application for the surface modification have been studied by computer simulation in binary collision approximation. The energy, angular distributions and trajectories of particles **scattered** on surfaces with both ideal and damaged, and semi-infinite and isolated atomic steps, have been calculated. It has been shown that from the correlation between the experimental and calculated energy distributions of the scattered particles, one may determine the spatial extension of the isolated atomic steps and the distance between them on the single crystal surface damaged by ion bombardment. **Sputtering** yields in the primary knock-on recoil atoms regime versus the initial energy of incident ions (E_0 = 0.5-5 keV) and angle of incidence (ψ = 0-30°) counted from a target surface have been calculated. It was shown that in the case of grazing ion bombardment the layer-by-layer sputtering is possible and its optimum are observed within the small angle range of the glancing angles near the threshold sputtering angle. Ion **implantation** of 1 keV Be^+ and Se^+ into GaAs(001) surface under grazing ion bombardment has been investigated. It was shown that in this case the main peak of the implanted depth distributions is considerably shallow, the range for Se is shallower and the half-width of the profile for Se is narrow than that for Be. The obtained results allow to select the optimum conditions for obtaining the implanted depth distributions with demanded shape in narrow near-surface area (5-10 atom layers) of crystals. The **deposition** of bi-metallic Ag_nCo_m nanoclusters on Ag(100) surface and **thin film growth** have been studied at the atomic scale by means of classical molecular dynamics simulation [4]. It was shown that the embedded atom model potential may be used successfully for studying of Ag_nCo_m nanocluster deposition on Ag(100) surface at the slowing down energies (0.25 eV – 1.5 eV per/atom). When slowing down on an Ag crystalline surface, only the smallest ones undergo profound reorganization and, in all cases, **the core-shell structure is preserved** to a large extent. The Co core and Ag shell deformations subsequent to impact are **different**. Deformation of the Co cores is less pronounced because Ag is loosely bound to cores and flows to the substrate surface during the impact. In the energy range considered, the penetration of the clusters into the substrate is limited to a few atomic layers and is found energy dependent. The fraction of cluster atoms penetrating the substrate surface is not significantly size dependent. It is limited to a few percent. As a result of the accumulation of clusters on the surface, the interface formed is crystalline and Ag originating from the clusters is epitaxial.

References

1. Mukashev K.M., Umarov F.F., Shokanov A.K. Radiation-stimulated Bulk and Surface Effects in Materials. **Monograph**. USA, Middletown, DE, 2018, ISBN 9781973567622, 233P.

2. Andrianova N.N., Borisov A.M., Makunin A.V., Mashkova E.S., Ovchinnikov M.A., Umarov F.F. Surface corrugation of carbon fiber via high-fluence nitrogen ion irradiation. **Journal of Physics.** Conference series. Vol. 1121, Issue 1, 26 November 2018, Paper N 012002.

3. Shokanov A.K., Umarov F.F., Mukashev K.M. Radiation-thermal Effects in the single-and multi-component Materials. **Monograph**. Almaty, KazNPU named after Abai, 2019, 303pp. ISBN 978-601-298-803-1.

4. Dzhurakhalov A.A., Rasulov A.M., Van Hoof T., and Hou M. Ag-Co clusters deposition on Ag(100): an atomic scale study. **Eur.Phys.J.**, 53-61, 2004.

Nanostructured Potassium Sulfate Crystals

Marat Myrzakhmet*, Gulzipa Sataeva, Seitzhan Yessengali
Eurasian National University, 5 Munaitpasov Street, Astana 010008, Kazakhstan
e-mail: myrzakh@gmail.com

Abstract: The implementation technique of potassium sulfate was developed in a three-dimensional opal lattice by sedimentation method from solution. Samples of potassium sulfate–thallium-opal composites were obtained. Degree of pore filling of opal matrix controlled in two ways: (1) increase in mass of the sample and (2) the shift of the maximum in the optical absorption spectrum filled with potassium sulfate–thallium samples relative to the initial opal matrices. The results obtained by the two methods were similar. The luminescence of the composites was studied. Optimal conditions for the synthesis of opals filled with nanocrystals were identified in terms of getting the maximum luminescence intensity.

1. Introduction

Nanocomposites using the precious opal host were created by filling its regular nanocavities by precious metals, nanocrystals of semiconductors and nanocrystals of crystalline phosphors on the basis of rare-earth ions [1]. So far the ionic nanocrystals with tetrahedrally-coordinated anions or cations have not been used for such a purpose. Tl-doped K_2SO_4 could be suitable for such a purpose. The first line of the first paragraph of a section or subsection should start flush left. The first line of subsequent paragraphs within the section or subsection should be indented 0.2 in. (0.62 cm).

It is interesting to research the optical properties with decreasing size of crystals (size effects). To do this, we used the pores of opal matrices [2]. Such structures provide photonic material properties and formed an entire branch of research in the field of opal photonic crystals. Previously, we have not seen in the literature to use as a second component of the nanocomposite the ion nanocrystals with tetrahedral anions.

2. Experiment

We worked on technological methods of synthesis of opal matrices with the necessary physical and chemical characteristics and predetermined optical properties.

The process of obtaining opal matrices can be divided into several stages. At the first stage we performed the hydrolysis of tetraethoxysilane (TEOS) in a hydroalcoholic solution, in one case with an acidic catalyst (nitric acid), and the other catalyst we used an aqueous solution of ammonia, i.e. an alkaline catalyst. It should be noted that the mechanisms of the processes of hydrolysis and condensation in these cases are different.

With the introduction of potassium sulfate and potassium chloride, thallium and thallium ratio was 1000:1. Potassium sulfate is not subjected to hydrolysis, as formed by a strong base and strong acid. Therefore, potassium sulfate is highly soluble in water. In the initial stage of the process the mixture of potassium sulfate with thallium chloride is dissolved in water at a ratio of 15:1.

We used as an acid catalyst (nitric acid), and alkaline catalyst (ammonia water). Each catalyst differently reacted with potassium sulfate and chloride of thallium. When we used as an acid catalyst, after 24 h of stirring the suspension with magnetic stir bar was divided into two phases and, after drying, we observed that the upper phase appears as crystals, whereas the lower is as white powder. In the alkaline catalyst after 24 h on a magnetic stirrer was formed gel which after drying formed a white powder.

We measured the emission spectra and excitation spectra of the synthesized samples in the form of powders. Wavelengths on the horizontal axis shows in nanometers, the vertical axis shows relative intensity. The measurements were performed on a standard spectrofluorimeter at room temperature. Sharp changes in the area of 424 nm in the emission spectrum associated with the change of the diffraction gratings in the spectrofluorimeter. The emission spectra were measured in the excitation region of 215 and 225 nm. The excitation spectra were measured with radiation of 292, 350, 370 and 417 nm. Two bands of 295 and 380 nm are clearly visible in the emission spectra. In the excitation spectra we can distinguish a narrow band in 210 nm and two broad bands in 215 and 235 nm.

3. Discussion

Pure potassium sulfate single crystals are transparent in a wide spectral range up to 155 nm and do not show fluorescence and absorption over a wide spectral range of 200–800 nm before and after X-ray irradiation of the samples. The centers of luminescence in thallium doped potassium sulfate crystals

showed a maximum absorption of 216 nm and emission of 285 nm at room temperature. These centers are singly charged thallium ions. Two different positions of substitution of the ions have little effect on fluorescent characteristics of these crystals.

The luminescence centers in the composites in which the potassium sulfate is in the form of nanocrystals with a size equal to the pore size of the opal matrix. If maximums of the excitation bands in the crystal and the composite is almost the same (216 and 215 nm), maximums of the emission band in the composite is shifted to longer wavelengths by 10 nm (285 and 295 nm). In addition, a new group of bands appeared in the luminescence spectra of the composite (narrow band 210 nm and the band at 235 nm in the excitation spectra and the long-wave-length band of 380 nm in the emission spectrum). These bands seem to be related to the influence of the surface on luminescence of the nanoclusters thallium centers.

4. Conclusions

We worked on technological methods of synthesis of opal matrices with the necessary physical and chemical characteristics and predetermined optical properties. The implementation technique of potassium sulfate was developed in a three-dimensional opal lattice by sedimentation method from solution. Samples of composites K_2SO_4:Tl-opal were obtained. The luminescence of the composites was studied. We measured the emission and excitation spectra of the synthesized samples in the form of powders. Optimal conditions for the synthesis of opals filled with nanocrystals were identified in terms of getting themaximum luminescence intensity. The luminescence centers in the composites in which the potassium sulfate is in the form of nanocrystals with a size equal to the pore size of the opal matrix. A new group of bands appeared in the luminescence spectra of the composite. These bands seem to be related to the influence of the surface on luminescence of the nanoclusters thallium centers.

Reference

[1] A.N. Gruzintsev, G.A. Emel'chenko, Yu.V. Yermolayeva, et al., Materials for Nanophotonics: The Formation and Properties of Nanoparticles and Nanostructures, ISMA, Kharkiv, 2010, (in Russian).
[2] M. Myrzakhmet, G. Sataeva, S. Yessengali, G. Kuralbayeva. Luminescence of nanostructured potassium sulfate crystals. Journal of Luminescence 169 (2016) 804–806

Investigation of the stability of orbits by using the adiabatic theory of motion in General Relativity

S. Toktarbay*, M.E. Abishev[1], A.Z. Talkhat and A. Muratkhan 1

[1]*Department of Theoretical and Nuclear Physics,*
Al-Farabi Kazakh National University, Almaty, Kazakhstan
E-mail: saken.yan@yandex.com

Abstract: We investigate the problem of the orbital stability of the motion of a test body in the restricted three-body problem, where all bodies have their own rotation. The stability of the orbits is investigated by using vector elements of orbits such as orbital moment and its time derivative. We show that it is possible to get some insight into the stability properties of the motion of test bodies.

The problem of the orbital stability of circular motion of a test body in the restricted three-body problem has been investigated in[1]. The resting position of the central body coincides with the reference point of coordinates, the second body moves along the circle around the central body and is not subject to the disturbance. The test body moves in a perturbed circular orbit and the relativistic corrections are:

$$U_2 << U_1; U_1/U_2 \approx v^2/c^2 \tag{1}$$

The relativistic Lagrange function can be represented as:

$$L = L^{(0)} + L^{(rot)} \tag{2}$$

Where $L^{(0)}$ is the relativistic Lagrange function for three point masses, and the second term $L^{(rot)}$ is responsible for corrections containing rotational terms. Regarding the $L^{(0)}$ term, in [1] it is shown that the motion of the test body in the plane of the orbit of the two body is stable when all bodies have no proper rotation. In this work, we consider the case when all bodies have their own rotation. Our aim to find the evolution equation of motion for the test (third) body, which describes the average change of its orbital momentum. To do that, we will study the evolution equations of motion by using the asymptotic methods of adiabatic theory, through the process of averaging of the corresponding equations using the vector elements **M** (the orbital moment) and **A** (the Laplace vector). M.M.Abdildin[2,3] and Burmberg[4] devoted an entire book to the motion of extended body with the internal structure and rotation in GR, where the Lagrange derived for N body using the Fok's approach. We derived the second term of Eq.(2) for the three masses without consideration of internal structure. The details of this derivation will be presented elsewhere. According to the adiabatic theory, the evolutionary motion of the test(third)body describes the average change of its orbital momentum. Therefore, we write down the orbital angular momentum of the test body:

$$M = [\vec{r}, \vec{p}] \tag{3}$$

where the square bracket means the vector cross product. The evolutionary motion of the test(third)body is:

$$\dot{M} = \left[\dot{\vec{r}}, \vec{p}\right] + \left[\vec{r}, \dot{\vec{p}}\right] \tag{4}$$

where the dot represents time derivative.

According to the Eqs.(2) the time derivative of orbital angular momentum reduce to $\mathrm{M}^{(rot)}$

$$\dot{M} = \dot{M}^{(0)} + \dot{M}^{(rot)} \tag{5}$$

Our approach consists in finding the evolutionary equation of motion the test body (third), which describes the average change of its orbital momentum.

In order to obtain the equations of motion one needs to integrate the Eq.(5) for the repetition period of the system configurations T (synodic period of the test body). In general, it is a complicated task to integrate the above differential equation. Suppose that the test body is moving along a circular orbit, and integrating the relativistic rotational component we can find that[5]

$$\dot{\bar{M}}^{(rot)} = \frac{1}{T}\int_0^T \dot{M}^{(rot)} dt = 0. \tag{6}$$

The orbital stability of the test body by definition means the equality to zero of the average change of the angular momentum. As we can see from this expression, in GR, in the first approximation, the circular motion of a test body in the plane of the orbit of the second body in the restricted circular three-body problem is stable.

References

[1] M.E. Abishev, S. Toktarbay, B. A. Zhami, Gravit. Cosmol. 20 252-254(2014).
[2] V. Fok. *The theory of space, time and gravitation* (2nd English edn.). (Pergamon,Oxford 1964)
[3] M. M. Abdil'din,*Mechanins of Einstein theory of gravity*, Alma-Ata: Nauka,(1988)
[4] V.A. Brumberg, *Relativistic Celestial Mechanics*, Moscow, Nauka (1972)
[5] M.E. Abishev, S. Toktarbay, A.Zh. Abylayeva, A.Z. Talkhat, EPJ Web of Conferences,. 168 04001 (2018).

Photoelectrochemical Application of Heterostructured Semiconductors

Bakranov N.[1], Kudaibergenov S.[1,2]

[1]*Kazakh National Research Technical University after Satpayev, Almaty, Kazakhstan*

[2] *Institute of Polymer Materials and Technology, Almaty, Kazakhstan*

e-mail: bakranov@gmail.com

Abstract: Hierarchically assembled photocatalysts based on nanoscale semiconductor materials can effectively be used for photoelectrochemical processes of water decomposition. This work demonstrates simple techniques for assembling photoelectrodes of an electrochemical cell based on nanolayers of wide-band and narrow-band semiconductors, such as ZnO/CdS and low-dimensional plasmonic silver particles in a hierarchical manner. Interlayer deposition of silver nanoparticles into the ZnO/CdS heterostructure semiconductor makes it possible to obtain a ZnO/Ag/CdS nanocomposite with high photocorrosive resistance.

Simulation of hydrogen isotopes absorption by metals under uncompensated pressure conditions

Timur Kulsartov, Zhanna Zaurbekova, Maratbek Gabdullin
Kazakhstan-Britain Technical University,59, Tole bi str., Almaty, Kazakhstan
e-mail: tima@physics.k

Abstract: This paper presents a model that allows to describe the absorption of hydrogen isotopes by a thin sample with known geometric dimensions. The sample was saturated with hydrogen isotopes from the gas phase at a given temperature in experimental chamber under uncompensated pressure. The initial pressure and gas composition of hydrogen isotopes mixture was fixed. The model was applied to describe the results of experiments on the saturation of V4Cr4Ti vanadium alloy sample with hydrogen isotopes.

1. Introduction

Studying of hydrogen isotopes interaction with materials determines the interest in a wide range of problems that arise in developing industry and energy areas such as: nuclear and fusion engineering, hydrogen power, petrochemical industry, hydrogen power sources for cars, drones, etc. Simulation of hydrogen interaction with materials is important for describing its absorption and further assessing the processes that occur in materials and are crucial because of safety concerns and prediction of equipment operational characteristics. Therefore, it is essential to assess the hydrogen amount in materials and to develop the methods to simulate the processes of hydrogen absorption by materials.

2. Results

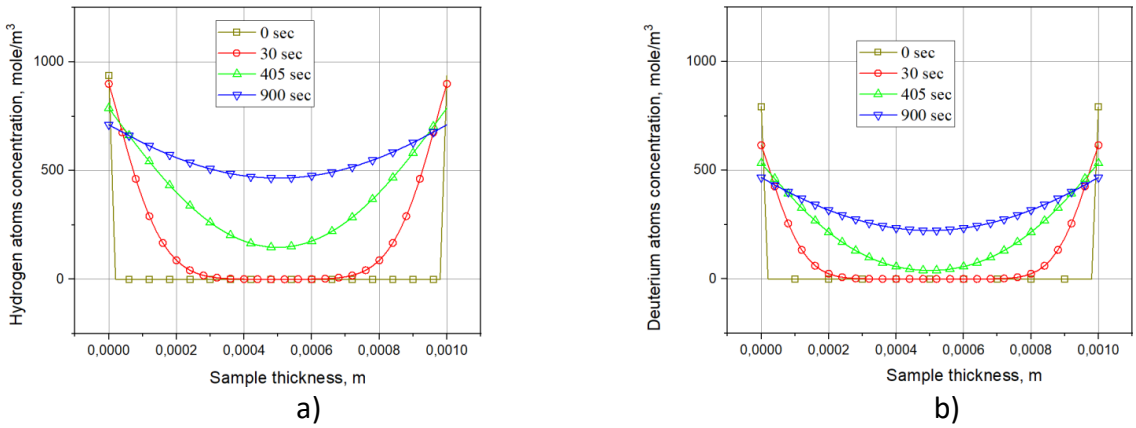

Fig. 1. Change of hydrogen (a) and deuterium (b) atoms concentration through the sample thickness during absorption process.

Thus, using the developed model for the absorption of hydrogen isotopes by thin samples, it was possible to describe the experimental results on the absorption of a three-component mixture of hydrogen isotopes and to determine the concentration profile of hydrogen and deuterium atoms in the sample during the absorption process. The main advantages of the model include the fact that having the experimental data on the absorption of hydrogen isotopes mixture by a thin sample and assuming that diffusion processes determine the absorption rate, it is possible to determine the concentration profiles of hydrogen isotopes of the sample without a detailed description of numerous processes on the surface. The proposed model can be used to simulate the absorption of one/multicomponent mixtures of hydrogen isotopes (or other gases) in materials. The model can be applied to estimate the profile of dissolved hydrogen and/or deuterium in the materials of the nuclear and fusion reactors, petrochemical industries, etc.

The work was carried out with the support of the Ministry of Education and Science of the Republic of Kazakhstan in the framework of the program # BR05236800.

4. References

[1] . Tritium: Fuel of Fusion Reactors. Monograph. Editors: Tetsuo Tanabe. 2017. ISBN 9784431564584. DOI: 10.1007/978-4-431-56460-7.

[2] Shmakov AA, Kalin VA, Ioltukhovsky AG. Theoretical study of the kinetics of hydride cracking in zirconium alloys. Metal Sci & Heat Treatment 2003;45(7-8):315–320.

[3] Robinson SM, Chattin MR, Giaquinto JM, Jubin RT. Evaluation of Tritium Content and Release from Pressurized Water Reactor Fuel Cladding, ORNL/SPR-2015/425, also FCRDMRWFD-2015-000617, UT-Battelle, LLC, Oak Ridge National Laboratory, September 2015. [1] A.V. Gurevicha et al, “Simultaneous observation of lightning emission in different wave ranges of electromagnetic spectrum in Tien Shan mountains”, Atmospheric Research **211,** 73–84 (2018).

[4] Topilnitskij P. Corrosion protection of oil production and refinery equipment. Chemistry & Chemical Technology 2007;1(1):45–54.

[5] 1 Schur DV, Gabdullin MT, Bogolepov VA, Veziroglu A, Zaginaichenko SYu, Savenko AF, et al. Selection of the hydrogen-sorbing material for hydrogen accumulators. Int J Hydrogen Energy 2016;41(3):1811–1818.

Diagnostics of dusty plasmas with nanoparticles

Y. A. Ussenov1,2, E. von Wahl3,4, Z. Marvi3,5, T. S. Ramazanov1, H. Kersten3

1 IETP, NNLOT, Al Farabi Kazakh National University - Al Farabi av., 71, Almaty, Kazakhstan
2 Institute of Applied Science and Information Technology - Shashkina str. 40, Almaty, Kazakhstan
3IEAP, University of Kiel, Leibnizstr. 11-19, 24098 Kiel, Germany
4GREMI, UMR7344 CNRS/Université d'Orléans, F-45067 Orléans, France
5Eindhoven University of Technology, P.O. Box 513, 5600 MB Eindhoven, Netherlands
e-mail: yerbolat@physics.kz

Abstract: This work presents the results of Langmuir probe measurements of the electron density and temperature and also the plasma potential in an asymmetric RF (radio frequency - 13.56 MHz) argon - acetylene plasma with growing nanoparticles. To avoid contamination of the probe surface by charged nanoparticles the so-called "complex probe voltage sweep" and a combination of ion bombardment and electron heating were used. The experimental results were obtained at different phases of the nanoparticle growth cycle and compared with the self-bias voltage signal of the driven electrode in the discharge. The probe position was compared to the dust cloud position by means of a laser light scattering system (LLS) and the simultaneously recorded plasma light emission used to check the validity of the electron temperature measurement [1].

1. Introduction

There are different methods used for the synthesis of nano-sized particles, and one of the most common and convenient methods is chemical vapor deposition from the gas phase in a low-temperature plasma. This method has a number of important features and advantages as compared with other methods of nanoparticle synthesis such as precipitation in fluids, mechanical fragmentation, etc. Basic principles of nanoparticle synthesis in plasmas are determined by physical and chemical processes occurring in the so-called "dusty" or "complex" plasma [2,3].

The common plasma diagnostic methods such as Langmuir probes, which has been quite successfully used in dusty plasmas of noble gases with micro particles, causes some problems in its application in chemically active gas discharge nanoparticles containing plasmas. The main difficulty is the contamination of the probe surface and deposition of thin dielectric films on the probe tip. In this contribution the new alternative method of obtaining of parameters of nanoparticle containing plasmas by means of Langmuir probe with "complex" voltage pattern is presented.

2. Results and conclusions

The problem of the probe surface contamination by charged nanoparticles was overcome by the application of a sufficiently fast "complex" sweep pattern of the probe voltage and a combination of ion bombardment and electron heating. The "complex" sampling of the probe voltage sweep, which has already been used in micron size dusty plasmas, was applied to a nanodust containing chemically active plasmas for the first time. The results were obtained at different times during nanoparticle growth and compared with voltage measurements of the discharge self-bias. It has been shown, that the electron density decreases due to the surface absorption by nanoparticles during charging, whereas the electron temperature and plasma potential increase. An exact upper limit for the dust plasma frequency was determined as well.

The data concerning the influence of nanoparticles on the plasma parameters obtained by the probe method and the applied method itself may be used in further detailed studying of the processes of nanoparticle synthesis in low-temperature plasmas. In addition, monitoring of temporal evolution of main plasma parameters like electron density, electron temperature and plasma potential with proposed electrical probe method might be useful for the prediction of nanoparticle size and density for large scale manufacturing of nanocomposite materials, where nanoparticles can be embedded for tailoring certain properties. Also in processes, where nanoparticles are not desired, the measured plasma parameters might be used as an indicator of particle occurrence.

3. References

[1] Y.A. Ussenov, E. von Wahl, Zahra Marvi, T.S. Ramazanov, H. Kersten, Langmuir probe measurements in nanodust containing argon-acetylene plasmas, Vacuum, 166, 15-25 (2019).

[2] S. A. Orazbayev, Y.A Ussenov, T. S. Ramazanov, M. K. Dosbolayev, and A.U. Utegenov, "A Calculation of the Electron Temperature of Complex Plasma of Noble Gases Mixture in CCRF Discharge", Contrib. Plasma Phys. 55(5), 428 – 433 (2015).

[3] Y. A. Ussenov, T. S. Ramazanov, K. N. Dzhumagulova and M. K. Dosbolayev, "Application of dust grains and Langmuir probe for plasma diagnostics ", Europhysics Letters, 105 15002 (2014) .

System of radiation monitoring of water and air environment on the Semipalatinsk Test Site

O.L. Lyakhova, A.O. Aidarkhanov, M.R. Aktayev, D.V. Turchenko, Yu.V. Svetacheva

Branch "Institute of Radiation Safety and Ecology" NNC RK, Kurchatov, Republic of Kazakhstan

e-mail: Lyahova@nnc.kz

Abstract:

One of the main activities of the National Nuclear Center of the Republic of Kazakhstan (NNC RK) is to ensure the radiation and nuclear safety of the former Semipalatinsk test site (STS), taking into account the specific features of its territory. In order to obtain up-to-date information on the radiation state of the water and air environment at the sites for conducting nuclear tests at adjacent territories, radiation monitoring works are regularly carried out in the STS site.

1. Introduction

Results of the radiological survey of the STS have been carrying out by the NNC RK since 2008 show that there are areas in which levels of radioactive contamination exceed guideline values by thousand times and more.

Radioactive contamination is mostly concentrated at nuclear testing places like "Opytnoe pole", "Degelen", "Balapan", "Sary-Uzen" and other technical sites where nuclear tests were conducted. Currently, the potential mechanisms of radionuclide migration from STS venues of nuclear tests are transfer of radionuclides by wind, ground, surface and underground water. In this context, the existing system of radiation monitoring at STS involves two major areas – air and water monitoring.

2. The results of research

Air environment monitoring. In order to monitor radiation situation at STS and the adjacent territory, there were 5 fixed air monitoring stations deployed. Observations are carried out in areas of such deposits as "Karazhyra", "Karadzhal", facilities like RRK "IGR" and RRK "Baikal-1", geographically associated with the main testing areas of the STS. The background-monitoring site is deployed in the in Kurchatov city located at a distance of 60 km from the STS. The content of the major man-made radionuclides in the air - $^{239+240}$Pu, ^{241}Am, ^{137}Cs, ^{90}Sr is monitored at each station as well as meteorological parameters are observed once a month. Outputs over 2015 – 2018 showed that concentration of radionuclides of interest in the air environment at each monitoring station was below the detection limit of the methodological instrumentation being used.

Water environment monitoring. As part of the water monitoring, the content of man-made radionuclides in ground water occurring in impact zones of venues of underground tests is overseen in "Degelen", "Balapan" and "Sary-Uzen". The content of ^{3}H used as an indicator of migration processes are monitored in each water body. Selectively, the content of $^{239+240}$Pu, ^{137}Cs and ^{90}Sr is determined in water depending on the level of radioactive contamination where a water body is located.

There have been some 50 operating water wells and wells identified, which cover all of the potential areas in which ground water moves and located in different parts of the test site for monitoring the status of ground water in the STS territory. The radiation situation in ground water is monitored selectively lasting from 1 to 3 years depending on radiation characteristics of a water body and its location. According to monitoring findings, radionuclide contamination of ground water flowing beyond STS testing areas is attributable to ^{3}H and ^{90}Sr present in water. ^{3}H activity concentration in ground water varies from a minimum of <12 to a maximum of 500,000 Bq/kg, that of ^{90}Sr was 5 Bq/kg.

Surface water was monitored in each major stream flow and water body of STS located in radioactively contaminated areas and adjacent territories. Monitoring frequency is 2 times per year (in spring and autumn). The main monitoring sites at STS are creeks of "Degelen" and the Shagan river that flows through "Balapan" area in water of which numerical values of ^{3}H are registered up to 350 kBq/kg.

Conclusions

The data analysis has demonstrated that over the STS monitoring period the transfer of radioactivity by air beyond the STS territory was not registered nor were any substantial changes observed in the content of man-made radionuclides in water environment.

Quantum concentration of the liquid

Askar Kassymov[1], Serik E. Kumekov[2]
[1]*Shakarim State University of Semey, festland2@yandex.kz*
[2]*Satbayev University, skumekov@mail.ru*

Abstract: The novel concept of quantum concentration for the liquid phase of elements was introduced which indicates the number of possible states of atoms per unit volume. Thermodynamic energy model for a solid-liquid phase transition is used to define the quantum concentration for the liquids. Values of quantum concentration for liquid phase of most of elements were calculated and analyzed. It was revealed that the metalloids such as boron, silicon, germanium, antimony, tellurium and bismuth exhibited a highest value of quantum concentrations compared with other elements. The size dependence of melting temperatures of Au, Pb and Sn spherically symmetric nanoparticles were calculated and compared well with experimental data and theoretical model based on generalized Gibbs-Thomson predictions.

In this work we introduce concept for a statistical interpretation of the entropy of melting using the quantum concentration for the liquid phase n_{QL}, which allows statistical calculation of the free energy in the liquid [1,2]. The quantum concentration of liquids can be determined using a geometrical relation derived from the thermodynamic energy model for a solid-liquid phase transition. The thermodynamic energy model to calculate the size dependence of the melting temperature of spherically symmetric nanoparticles is considered. The relation between the results and limited experimental observations is also discussed.

At the melting point T_m the free energies in solid and liquid phases are equal to each other:

$$f^{\,solid} = f^{\,liquid} \tag{1}$$

Thus from Equation (1) it follows:

$$W_{lat.heat} = -\frac{kT_m}{c_l}\{c_l \ln c_l + (1-c_l) ln(1-c_l)\} \tag{2}$$

Here $c_l = {}^{n}/_{n_{QL}}$, n – the number of atoms of the pure phase.

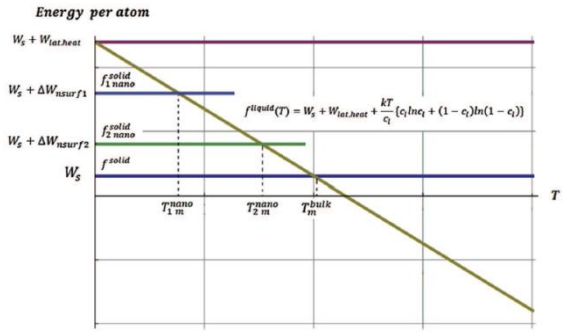

Fig. 1. Diagram of the thermodynamic model for a solid-liquid phase transition for nanoparticles

In the framework of classical thermodynamics, melting of a solid is defined as a first-order discontinuous phase transformation following at a critical temperature at which Gibbs free energies of the solid and the liquid states are equal. Numerous experimental observations verified that melting temperature of nanoparticles decreases with decreasing of the particle size. Melting point depression is a very important issue for materials and device applications containing nanostructured particles, as it decreases the functional range of the solid phase and increases the chemical reactivity. Novel concept of quantum concentration was used for the calculation of the melting point depression of elements.

The mathematical model for the estimation of melting temperature of spherical nanoparticles was established by using quantum concentration for the liquids. Size dependence of melting temperatures of Au, Pb and Sn nanoparticles were estimated and compared well with experimental data and theoretical predictions [3,4].

[1] Askar Kassymov, Hanno Schaumburg, Serik E. Kumekov, Karen S. Martirosyan, "Quantum concentration for the liquid phase of elements", Materials Chemistry and Physics **161** (2015), pp. 130-134.
[2] Askar Kassymov, Serik E. Kumekov, "Quantum concentration of real gas," in New Concepts in Condensed Matter Physics, (KazNITU, Almaty, 2014), pp.54-55.
[3] K.K. Nanda, "A simple classical approach for the melting temperature of nanoparticles," Chem. Phys. Lett. **419** (2006), pp. 195-200.
[4] W.H. Qi, "Size effect on melting temperature of nanosolids," Phys. B **368** (2005), pp. 46-50.

Regular effects of non-equilibrium atmospheric gas – solar radiation system in theory and experiment

***Nurgaliyeva K.E.*[1]*, Somsikov V.M.*[2]**

[1]*Al-Farabi KazNU, Almaty, Kazakhstan*

[2]*Institute of the Ionosphere, Almaty, Kazakhstan*

e-mail: vmsoms@rambler.ru

The non-equilibrium system of atmospheric gas and solar radiation with taking into account the atmospheric structures and a radiation flux interrelation was investigated in this work [1]. The dispersion equation of acoustic-gravity waves (AGW) on the base of dynamic equations set in the frames of non-equilibrium thermodynamics was found. The theoretical were done and experimental conformations of theoretical results were presented. The dispersion relation was numerically analyzed for different conditions: in the presence of solar radiation in the atmosphere and without this radiation, as well as for the equilibrium case at different atmospheric altitudes. It was found that for non-equilibrium atmosphere AGW spectra is shifted into high-frequency region. Also a numerical calculation shows that at the heights of ionosphere these effects become brighter at transition times, when the solar energy input changes abruptly. It was shown that the results of calculations demonstrating the increasing of the high-frequency component of the atmospheric oscillation spectrum with increasing solar radiation intensity correspond qualitatively to the experimental data when the spectra of waves in the ionosphere for different periods of solar activity.

1 A. B. Andreev, V. M. Somsikov, S. N. Mukasheva, V. I. Kapytin, and K. A. Nurgaliyeva. Nonequilibrium Effects in Atmospheric Perturbations Caused by Solar Radiation Flux// Geomagnetism and Aeronomy, 2018, Vol. 58, No. 1, pp. 106–112

Probing Uncertainty Relations in Non-Commutative Space

Pritam Chattopdhayay[1], Ayan Mitra[1;2]; Goutam Paul[1]
[1] *Cryptology and Security Research Unit, Indian Statistical Institute, Kolkata, India and*
[2] *Energetic Cosmos Laboratory, Nazarbayev University, Nur-Sultan, Kazakhstan*
e-mail: ayan.mitra@nu.edu.kz

In this talk we show, how we compute uncertainty relations for non-commutative space and obtain a better lower bound than the standard one obtained from Heisenberg's uncertainty relation. We also derive the reverse uncertainty relation for product and sum of uncertainties of two incompatible variables for one linear and another non-linear model of the harmonic oscillator. The non-linear model in non-commutating space yields two different expressions for Schrödinger and Heisenberg uncertainty relation. This distinction does not arise in commutative space, and even in the linear model of non-commutative space.

Improved pseudocapacitive performance of W@WO_3 structure

A A. Markhabaeva, Kh. A. Abdullin, Zh.K. Kallkozova
National Nanotechnology Laboratory of Open Type (NNLOT), Kazakh National University, Almaty, 050012 Kazakhstan
e-mail: Aiko_marx@mail.ru

Electrochemical energy storage electrodes have been intensively studied. Carbon materials like nanotubes, graphene, activated carbon and etc are good candidate for supercapacitor electrodes where charge storage mechanisms based on a double dielectric layer. Also several transition metal oxides such as RuO, MnO_2, V_2O_5 and WO3 have pseudocapacitive behaviors. Pseudocapacitors provide high capacitance, long cycle life, and metallic type conductivity due to reversible redox reactions. Tungsten oxide is the only n-type semiconductor material that can change the oxidation state to +6 [1]. In this work, W@WO3 electrode materials with a high conductivity and capacitance were developed. Metallic tungsten particles were obtained via further reducing tungsten oxides in hydrogen gas atmosphere. Our experimental results showed that the metallic tungsten and its oxide layers as electrode materials demonstrated better electrochemical performance than tungsten oxide electrodes [2].

A simple synthesis method like pyrolysis and template method was developed to synthesize tungsten oxide particles. Ammonium tungstate $NH_4W_{12}O_{40}$ was used as a precursor and the cotton fiber was applied as template for the synthesis WO_3 nanoparticles. 0.01 M ammonium metatungstate ($(NH_4)_6H_2W_{12}O_{40}\times H_2O$) aqueous solution was used for synthesis WO_3 aerosol particles. As a result, the hexagonal and monoclinic structure of WO_3 was obtained. Also metallic tungsten nanoparticles were obtained by the subsequent thermal reduction of tungsten oxide in hydrogen atmosphere. The metastable phase of tungsten beta-W was obtained after hydrogen reduction. Structural and morphological characterizations were performed using X-ray diffraction (XRD), Raman spectroscopy and scanning electron microscopy (SEM). The effect of annealing temperature on nanoparticle sizes was investigated. The electrochemical characteristics of synthesized tungsten oxide and reduced metallic tungsten electrodes was studied using cyclic voltammetry, impedance spectroscopy and galvanostatic charge-discharge methods. It is shown that the reduced metallic tungsten with natural oxide layer has significantly better characteristics than the initial WO_3.

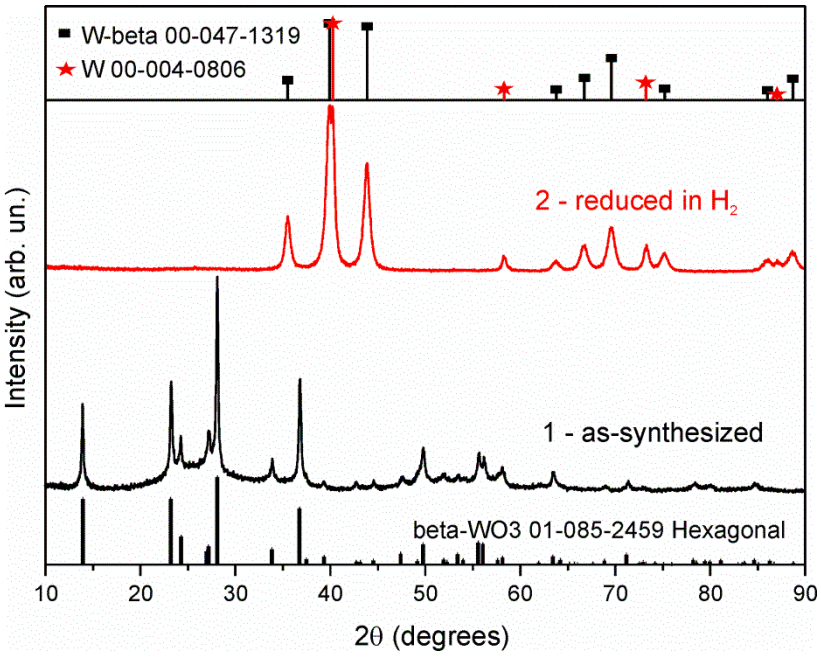

XRD patterns of the WO_3 sample synthesized at the temperatures 400°C (1) and reduced at 400°C in hydrogen flow (2)/

[1] Kou, T., et al., "Recent advances in chemical methods for activating carbon and metal oxide based electrodes for supercapacitors", Journal of Materials Chemistry A, **5**(33), 17151-17173 (2017).
[2] Kh. A. Abdullin, Zh.K. Kallkozova, A A. Markhabaeva, R. Dupre, Md. Moniruddin and N. Nuraje, "Core−Shell (W@WO3) Nanostructure to Improve Electrochemical Performance", ACS Appl. Energy Mater. 2, 797−803 (2019).

Impact of neutral shadowing force on dust particles' structural and dynamical properties in cryogenic environment

Ye. Aldakulov[1], Zh.A. Moldabekov[1,2], T.S. Ramazanov[1], M. Muratov[1,3]

[1] *Institute for Experimental and Theoretical Physics, Al-Farabi Kazakh National University, 71 Al-Farabi ave., 050040 Almaty, KAZAKHSTAN*

[2] *Institute of Applied Sciences and IT, 40-48 Shashkin str., 050038 Almaty, KAZAKHSTAN*

[3] *National Nanotechnological Laboratory of Open Type , Al-Farabi Kazakh National University, 71 Al-Farabi ave., 050040 Almaty, KAZAKHSTAN*

e-mail: yessenbek.aldakul@gmail.com

The difference in temperature of the dust particle's surface and that of the atoms results in an additional *neutral shadowing force* acting between dust particles [1]. While this force can be safely neglected in the case of atoms at room temperature, at cryogenic conditions (in cryogenic plasmas) neutral shadowing force is comparable with Coulomb repulsion between charged grains [2]. Therefore, the investigation of the neutral shadowing force impact on the structural and dynamic properties of dust particles is needed.

In this work, we present the results of 2D molecular dynamics simulation of charged particles taking into account screened Coulomb interaction as well as the neutral shadowing force. The screened Coulomb interaction is characterized by two parameters: coupling parameter $\Gamma = \frac{Q^2}{4\pi\varepsilon_0 a k_B T}$ and screening parameter $k = a/\lambda_D$, where λ_D – is Debye radius.

The force between dust particles taking into account the neutral shadowing force reads

$$\frac{\vec{\mathbf{F}}_{ij}}{(k_B\,T/a)} = -\boldsymbol{\nabla}\left[\frac{\Gamma}{R}exp(-kR)\right] + \frac{\alpha}{R^2}\hat{\mathbf{r}}_{ij},$$

where k_BT characterizes thermal energy, α - parameter describing the repulsion due to the neutral shadowing force

$$\alpha = \begin{cases} \dfrac{3\pi {a_d}^4 P(T_s - T_n)}{8 a k_B T_d T_n}, & \text{if } R < l/a = r_{cut}, \\ 0, & \text{otherwise} \end{cases}$$

where the cut-off radius r_{cut} is defined by the mean free path of neutrals l, a_d is dust particle radius, P is a gas pressure, T_s is the dust particle surface temperature and T_n is the temperature of atoms.

We have investigated the radial distribution function, velocity autocorrelation function (VACF), spectrum of VACF, and sound speed (Table 1) at different values of Γ and α.

It was revealed that at cryogenic conditions the neutral shadowing force does change structural and dynamical properties of the system if mean-free path of neutrals exceeds mean-interparticle distance [3, 4].

TABLE 1 The values of a sound speed, $c/(a\omega_p)$, at $k = 1$

		$\alpha = 0.1$		$\alpha = 0.2$	
Γ	**$\alpha = 0$, (Yukawa)**	**$r_{cut} = 1$**	**$r_{cut} = 2$**	**$r_{cut} = 1$**	**$r_{cut} = 2$**
50	0.84 ± 0.06	0.82 ± 0.06	0.87 ± 0.06	0.8 ± 0.05	0.9 ± 0.06
100	0.79 ± 0.05	0.78 ± 0.05	0.86 ± 0.06	0.77 ± 0.05	0.95 ± 0.06
150	0.8 ± 0.05	0.79 ± 0.05	0.88 ± 0.05	0.8 ± 0.05	0.97 ± 0.05

References:

1. V.N. Tsytovich, Ya. K. Khodataev, G.E. Morfill, R. Bingham, and J. Winter "Radiative dust cooling and dust agglomeration in plasmas", *Comments Plasma Phys. Controlled Fusion, vol. 18, p. 281, 1998.*
2. T.S. Ramazanov, Z. Moldabekov, M. Muratov, "Grain surface heating in cryogenic environment" *Phys. Plasmas, vol. 24, p. 050701, 2017.*
3. Muratov M.M., Aldakulov Ye, Ramazanov T, Moldabekov Zh "Impacts of neutral shadowing force on dust particle dynamics in cryogenic plasma", *Contributions to Plasma Physics 2019.* DOI: 10.1002/ctpp.201800175
4. Ye. Aldakulov, M. Muratov, T.S. Ramazanov, Zh.A. Moldabekov "Neutral shadowing force impact on structural properties of dust particles in cryogenic environment". Accepted to IEEE TPS (2019) [in production].

Structural Properties of Epitaxial Silicon Carbide Films, Grown by Atomic Substitution on the Silicon

S.A. Kukushkin[1], K.Kh. Nussupov[2], A.V. Osipov[1], N.B. Beisenkhanov[2], D.I. Bakranova[2,*]

[1]Institute for Problems of Mechanical Engineering RAS, St. Petersburg, Russia

[2]Kazakh-British Technical University, 050000, Almaty, Kazakhstan

e-mail: dinabakranova@gmail.com

In this paper, SiC films were synthesized by a new method of atom substitution directly inside the subsurface layer of the Si substrate at various temperatures and pressures of the CO working gas [1,2]. The method is based on the idea of replacing of some silicon atoms on carbon atoms within the silicon substrate.

The structure of a multilayer silicon carbide (SiC) system on the surface of a high-resistance 1987–3165 Ohm·cm, (111) oriented low-dislocation single-crystal n-type silicon (Si) with a diameter of 20 mm and 1300 μm thick were studied by Raman spectroscopy, IR spectroscopy, electron diffraction and X-ray diffraction analysis. The SiC films synthesis was carried out on the samples Nos. 1 and 2 for 15 min at the temperature of 1250°C and the pressure of the gas CO 264 Pa, and on the samples Nos. 3 and 4 – 7 min, 1330°C and 395 Pa. CO gas consumption during the synthesis of all films was 12 sccm, and SiH_4 – 0.25 sccm.

It was revealed that the upper layers (70-120 nm) have a complex layered structure with a single-crystal 3C-SiC (15 nm) layer on the surface, and lower layers lying in the depth of the substrate contain mainly 3C-SiC nanocrystals with a high degree of structure perfection and an average size of 3-7 nm capable of preferential orientation (311), as well as large crystals with sizes of 60-260 μm. The greatest content of crystalline phases of SiC has films with the composition closest to stoichiometric. Depending on the synthesis conditions, the upper layers (below 15 nm) can be a multilayer "sandwich" with alternating vertical interlayers of cubic and hexagonal SiC polytypes (IR absorption in the range 792.1 – 799.7 cm^{-1}). Among the hexagonal polytypes, unstable in the usual state, but stable in a multilayer structure, the polytype 2H-SiC prevails. The multilayered structure SiC on Si is most favorable from an energy point of view, because in this case there is an additional relaxation of the mechanical elastic stress, generated due to the great differences in the lattices parameters of Si and SiC.

A single crystalline SiC layer lies on the porous surface of Si, like a bridge on piles. The inner surface of Si pores is coated by textured SiC layer. The concentration of carbon decreases from the surface layer into the depth of Si substrate, which leads to the formation of small nanocrystals and disordered nanoclusters containing Si-C bonds of varying lengths (IR absorption in the range 818 - 957 cm^{-1}).

The peak of IR spectra with maximum in range 957.5 cm^{-1} – 959.0 cm^{-1} is presented in spectra of all samples, especially Nos. 3 (958.8 cm^{-1}) and 4 (959.0 cm^{-1}). This peak corresponds to the mechanical bond of the elastic dilatation dipole oscillation energy (C-V_{Si}).

[1] Kukushkin S.A., Nussupov K.Kh., Osipov A.V., Beisenkhanov N.B., Bakranova D.I. Structural properties and parameters of epitaxial silicon carbide films, grown by atomic substitution on the high-resistance (111) oriented silicon. Superlattices and Microstructures. 111. 2017. 899-911.

[2] Kukushkin S.A., Nussupov K.Kh., Osipov A.V., Beisenkhanov N.B., Bakranova D.I. X-Ray Reflectometry and Simulation of the Parameters of SiC Epitaxial Films on Si(111), Grown by the Atomic Substitution Method. Physics of the Solid State. 59(5). 2017. 1014–1026.

Study of the mechanisms of formation of modulation effects in the angular distributions of differential cross sections of elastically scattered alpha particles on light multi-cluster nuclei

Dyachkov V.V.[1], Dyussebayeva K.S.[2], Zaripova Yu.A. [1], Yushkov A.V. [1]

[1] National Nanotechnology Laboratory of Open Type, Almaty, Kazakhstan;

[2] Kazakh National University named al-Farabi, Almaty, Kazakhstan;

E-mail: slava_kpss@mail.ru

One of the methods of experimental detection of a multi-cluster structure is the decomposition of experimental angular distributions of differential cross sections for elastic diffraction scattering into multi-cluster components. Within the framework of the diffraction theory and under the assumption of total absorption inside the sphere of interaction, the authors obtained a decomposition of the total amplitude into several multi-cluster modes [1], and for the first time measurements of nuclear clustering by two direct methods on medium-energy alpha particle beams [2] were performed.

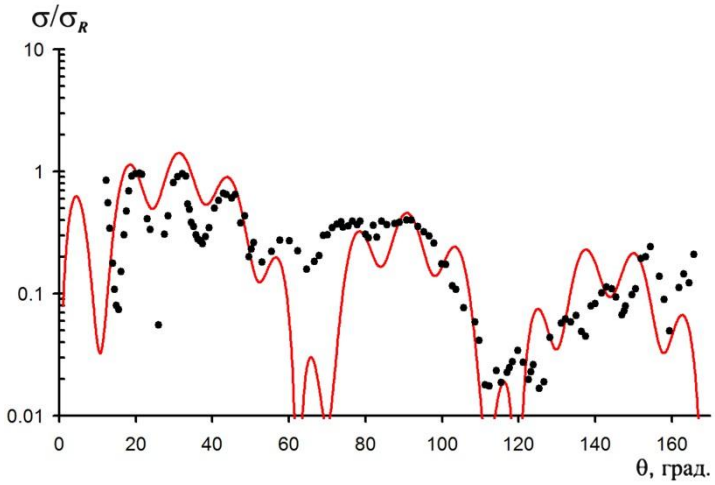

Points are global experimental data; curve - own calculation.

Fig – Angular distributions of elastic diffraction scattering $^{20}Ne(\alpha,\alpha)^{20}Ne$ E_α=54.1 MeV

The authors described experimental data on the angular distributions of light alpha-cluster nuclei. The analysis of the angular distributions of the elastic scattering of alpha particles was performed on the assumption of total absorption within the sphere of the cluster structure and the sphere of the interaction nucleus. These assumptions made it possible to expand the scattering amplitude into components-scattering on the nucleus itself, on the alpha cluster, and on a smaller cluster structure. As a result of the proposed model, the following was obtained. The authors proposed a model in which the amplitude for describing the diffraction elastic scattering of 4n±1 light nuclei in the framework of the theory of diffraction scattering as superpositions of wave functions in the approximation on an absolutely black core and on its absolutely black substructures. In the total scattering amplitude, an important contribution is made to the alpha-partial mode, as well as scattering modes on the correlated motion of nucleons and on isolated nucleons. This can be manifested as growth in angular distributions due to the interference of the alpha-cluster mode with the modes of smaller cluster structures and nucleons. Due to these effects, it is possible not only to unevenly raise the angular distributions of the differential cross sections over the Rutherford cross section, but also to rise at the rear angles.

1. Dyachkov V.V., Zaripova Yu.A., Yushkov A.V., Zholdybayev T.K., Kerimkulov Zh.K. Kinematic Method for Separating Dominant Types of Cluster Configurations in a Complex Nucleus // Bulletin of the Russian Academy of Sciences: Physics. 81 (10), 2017, pp. 1174 – 1178.

2. Yu.A. Zaripova, V.V. Dyachkov, A.V. Yushkov, T.K. Zholdybayev, D.K. Gridnev. Direct experimental detection of spatially localized clusters in nuclei on alpha-particle beams // International Journal of Modern Physics E. 27 (2). 2018. pp. 18500171 – 185001716

Structural and Phase Transformations in Wear Resistant Fe-Ni-Cr-Cu-Si-B-C Coatings

Kapsalamova F.
Kazakh-British Technical University
e-mail: faridakapsalamova@gmail.com

Abstract: At current stage of machinery development, technologies that provide the possibility of modifying building surfaces, or applying coatings with protective and other functions to those surfaces, are of intense interest. Thermal spraying and mechanochemistry in particular, are just the methods. Powdered hardfacing alloy synthesized mechanochemically from Fe-Ni-Cr-Cu-Si-B-C composition is used in flame-spray coating. The resulting Fe-Ni-Cr-Cu-Si-B-C composite surface coating was studied by metallography and a Vickers hardness test. Micro-identification results revealed higher hardness compared to PG-Zh40 hardfacing alloy obtained by metallurgy method. This was evidenced by an increase in weld metal hardness from 450 to 549 HV.

Influence of spin-orbit interaction on the process of formation and recombination of electron-hole pairs in dyed polymer semiconductor matrixes

Afanasyev D.A.[1,2], Ibrayev N.Kh.[1], Seliverstova E.V.[1]

[1]Institute of Molecular Nanophotonics, Buketov Karaganda State University, Universitetskaya str. 28, Karaganda 100028, Kazakhstan;

[2]Institute of Applied Mathematics, Universitetskaya 28A, 100028, Karaganda, Kazakhstan

Author e-mail address: niazibrayev@mail.ru

Abstract: The role of spin-orbit interaction in the process of formation and recombination of electron-hole pairs (EHP) in semiconductor composites based on new halogen-derived poly-N-epoxypropylcarbazole and organic dye was studied. Measurements of external magnetic field effect on the luminescence kinetics of dye in polymer matrix with a different number of "heavy" atoms in a wide time range allowed determining the characteristic times for recombination processes involving EHPs formed from singlet and triplet excited electronic states of dye molecules.

Polymer composite films based on semiconductor polymers and organic molecules attract the attention of researchers due to their using in electroluminescent and photovoltaic cells. Semiconductor polymers doped with organic molecules have properties that are not possessed by pure polymers. They are used as elements of organic electronics, and as a model system for the study of the formation and recombination of charge carriers in organic semiconductors [1,2].

The spin state of the initial components plays an important role in the generation and recombination of electron-hole pairs (EHP) in semiconductor polymer composites. The EHP generation in composites mainly occurs upon photoexcitation from the singlet state of acceptor's. Hovewer, in ref. [3, 4] it was shown, that along with the singlet state of the acceptor, the triplet electronic state of organic molecules and polymers can also be involved in the process of charge transfer.

In present work results of a study of the role of spin-orbit interaction in the processes of formation and decomposition of EHP in matrices of halogen derivatives of poly-N-epoxypropylcarbazole (PEPC) doped with cationic polymethine dye molecules are presented [3-5].

Spectroscopic and quantum-chemical studies of halogen-containing derivatives of poly-N-epoxypropylcarbazole were performed. It was shown that a heavy atom in the structure of a polymer molecule leads to bathochromic shifts in the absorption, fluorescence, and phosphorescence spectra. This is a consequence of a decrease in the energy of the electron levels due to a change in the electron density distribution over the π-electron system in the chromophores of 2IPEPC and 3BrPEPC. Quantum-chemical estimation of the intramolecular transition constants has shown that the probability of the singlet–triplet intercombination conversion in the halogen-containing PEPCs is higher in PEPC. This leads to a markedly stronger phosphorescence of the iodine and brominecontaining polymers and a shorter luminescence lifetime.

Singlet and triplet states of the cationic polymethine dye in polymers – derivatives of PEPC were studied. It was shown that the presence of heavy atoms in the structure of the polymer leads to the appearance and buildup of the dye phosphorescence due to the growth of the spin-orbit interaction in the dye molecule and an increase in the rate of singlet-triplet transitions. An additional channel of relaxation of excited states of the dye in polymer films with a hole type of conductivity is the formation and recombination of EHP, which is manifested in the appearance of recombination luminescence. Measuring the external magnetic field effect on the kinetics of dye luminescence in a wide time range from nanoseconds to milliseconds allowed to determine the characteristic times of the recombination processes with the participation of EHP formed from singlet and triplet excited electronic states of dye molecules. An increase of the spin-orbit interaction in polymers with different numbers of heavy atoms leads to an increase in a value of the magnetic effect (g (B)) in the nanosecond time range and to a decrease in g(B) in the microsecond time range. A comparison of the dependence of the magnetic effect *g* on the magnetic field induction *B* shows the competing influence of the external magnetic field and the spin-orbit interaction on the spin state of the EHP.

[1] N.Kh. Ibrayev, D.A. Afanasyev, K.A. Zhapabaev, "Effect of potassium iodide on luminescent and photovoltaic properties of organic solar cells P3HT-PCBM," IOP Conf. Series: Mat. Sci. Eng. **110**, 012067 (2016).

[2] N. Ibrayev, A. Nurmakhanova, D.Afanasyev. "Role of spin states in the process of electron en-ergy transformation in P3HT films, doped KI salt," IOP Conf. Series: Mat. Sci. Eng. **168**, 012060 (2017).

[3] N. Ibrayev, E. Seliverstova, D. Afanasyev, A. Nurmakhanova, I. Davydenko, N. Davydenko, "Features of deactivation of excited states of cationic polymethine dye in the matrices of halogen-containing derivatives of poly-N-epoxypropyl carbazole," J. Lum. **124,** 349 (2018).

[4] E.V. Seliverstova, N.Kh. Ibrayev, A.K. Nurmakhanova, D.A. Temirbayeva, "Spectroscopic and quantum-chemical studies of halogen-containing derivatives of poly-n-epoxypropylcarbazole," Opt. Spectr. **125**, 499 (2018).

[5] D.A. Afanasyev, N.Kh. Ibrayev, A.T. Yedrissov, "Time-resolved magnetic effects in luminescence of halogen-containing derivatives of poly–N–epoxypropyl carbazole doped with polymethine dye," J. Phys. Chem. C (*in Press*).

Influence of plasmon effects of metal nanoparticles on spontaneous and stimulated emission in condensed media

Ibrayev N.Kh., Aimukhanov A.K., Afanasyev D.A.

Institute of Molecular Nanophotonics, Buketov Karaganda State University, Universitetskaya 28, 100028, Karagandy, Kazakhstan

Author e-mail address: a_d_afanasyev@mail.ru

Abstract: The results of the study of influence of metal nanoparticles (NPs) on the spectral-luminescent and lasing properties of dye molecules in solutions and films of porous aluminum oxide (POA) are presented. The influence of gold and silver NPs on the spectral-luminescent properties of dye molecules in solutions has been studied. The fluorescence duration of dyes doesn't change after added NPs in solutions. The stimulated emission of the dye with an expressed mode composition was obtained in the region of the maximum of the fluorescence band. The presence of silver nanoparticles leaded to an increase in the intensity and lowering of the threshold for the generation of stimulated emission of dyes in solutions. The spectral-luminescent properties and the properties of stimulated emission of dyes in PAO with the addition of metals NPs have been studied. A number of dyes are determined for which molecular aggregation is observed. It is determined from the spectral-luminescent properties of dye molecules in films. An increase in the fluorescence intensity and a decrease in the generation threshold of stimulated emission of dye molecules is observed in the presence of NPs in the films.

Nanoplasmonics is currently an intensively developing field of nanotechnology because of its very promising use in various practical applications. The creation of plasmon lasers and nanolasers is one of the promising areas for the use of localized plasmon resonance. The addition of metals nanoparticles (NPs) to the active medium of dye lasers leads to an increase in the intensity of stimulated emission and a decrease in the generation threshold. However, the properties of plasmon-enhanced generation and the mechanism of action of the plasmon effect on electronic processes in molecules of organic dyes and materials based on them remain largely unexplored.

The results of the study of influence of metal nanoparticles on the spectral-luminescent and lasing properties of dye molecules in solutions and films of porous aluminum oxide (POA) are presented.

Primarily the influence of metal NPs on the spectral-luminescent properties of dye molecules in solutions has been studied. The addition of the silver NPs causes first growth and then a decrease in the intensity of absorption and fluorescence of the dye molecules. The quantum yields of the fluorescence of the dye with an increase in the concentration of NPs increases and doesn't change after reaching a maximum. Absorption spectra of dye doesn't change and the fluorescence intensity decreased after adding gold NPs in the solution. The fluorescence lifetime of the dye doesn't change when metal nanoparticles are added in the solution. The stimulated emission of the dye with an expressed mode composition was obtained in the region of the maximum of the fluorescence band. The threshold for the generation of stimulated emission is determined. The presence of Ag NPs leads to an increase in the intensity of stimulated emission and reduction of the threshold for laser emission [1,5].

The spectral-luminescent properties and properties of stimulated emission of dyes in PAO with the addition of plasmonic NPs have been studied. A number of dyes are determined for which molecular aggregation is observed. It is determined from the spectral-luminescent properties of dye molecules in films. The stimulated emission of dyes in films is obtained at the maximum of the fluorescence band. Low-Q generation of stimulated emission of dyes in the POA is observed. An increase in the fluorescence intensity and a decrease in the generation threshold of stimulated emission of dye molecules are observed in the presence of NPs in the films. A reduction in the duration of the stimulated emission pulse is observed. The degree of change in the full width at half maximum of stimulated emission and the threshold of generation of stimulated emission of dye molecules in the presence of metal NPs depends on the chemical nature of the dye [2-4].

[1] Aimukhanov A.K., Ibrayev N.Kh., Ishchenko A.A., Kulinich A.V., "Effect of silver and gold nanoparticles on the spectral and luminescent properties of a merocyanine dye," Theor. Exp. Chem. **54**, 369 (2019).

[2] Aimukhanov A. K., Ibrayev N.Kh., "Influence of gold nanoparticles on the properties of stimulated emission of 6-amino-1h-phenalen-1-one in the pores of anodized aluminum oxide," J. Lum. **124**, 216 (2018).

[3] Aimukhanov A. K., Ibrayev N.Kh., Esimbek A.M., "Properties of stimulated emission of the PM567 dye in pores of anodized aluminum oxide," Rus. Phys. J. **60**, 1667 (2018).

[4] Ibrayev N.Kh., Aimukhanov A.K., "Influence of plasmon resonance in silver nanoparticles on the properties of stimulated emission of 1,3,5,7,8-pentamethyl-2,6-diethylpyrromethene-difluoroborate molecules in film of porous aluminum oxide," Opt. and Laser Technol. **115**, 246 (2019).

[5] Ibrayev N., Ishchenko A., Afanasyev D., Zhumabay N., "Active laser medium for near-infrared spectral range based on electron-unsymmetrical polymethine dye and silver nanoparticles" Appl. Phys. B (2019) (*in Press*).

Higher-order derivative gravity and Black Holes

Anuar Idrissov
Nazarbayev University
e-mail: anuar.idrissov@nu.edu.kz

Abstract: Modifications of Einstein's theory of gravitation have been extensively considered over the last decade, in connection to both cosmology and quantum gravity. Higher-curvature and higher-derivative gravity theories constitute the main examples of such modifications. These theories exhibit, in general, more degrees of freedom than those found in standard General Relativity. In this work we review via both formal arguments the most relevant methods to unveil the gravitational degrees of freedom of a given model, discussing the merits and pitfalls of the various approaches. We also want to shed a light on black holes application of higher order gravities. Since black holes are the most fundamental objects in a theory of gravity, and they provide powerful probes for studying some of the more subtle global aspects of the theory. In the end, we summarize the whole discussions and provide with some insight into the future directions for developments of the higher-order derivative gravity and black holes.

[1] Renormalization of Higher Derivative Quantum Gravity - Stelle, K.S. Phys.Rev. D16 (1977)
[2] Classical Gravity with Higher Derivatives - Stelle, K. S. Gen.Rel.Grav. 9 (1978)
[3] Higher-order theories of gravity: diagnosis, extraction and reformulation via non-metric extra degrees of freedom—a review - Belenchia, Alessio et al. Rept.Prog.Phys. 81 (2018) no.3, 036001
[4] Black Holes in Higher-Derivative Gravity - Lu, H. *et al.* Phys.Rev.Lett. 114 (2015) no.17, 171601

Analysis of the dependence of the structural parameters of membranes based on NOA and anode current on the parameters of the production process

B.E. Alpysbayeva, Korobova N.E.[3], M.F. Kadir, M.T. Yskak, M.S. Batalova

al-Farabi Kazakh National University[1], Laboratory engineering profile of al-Farabi Kazakh National University[2], Almaty, Republic of Kazakhstan

National Research University MIET[3], Zelenograd, Russian Federation

E-mail: balausa.alpysbayeva@kaznu.kz

Abstract: Anodic alumina has a unique nanoscale cellular structure, high mechanical strength, unique dielectric and optical properties. The unique porous structure, such parameters as: diameter, length and distance between adjacent pores of which it is possible to vary in the course of the synthesis, allows the use of films of porous aluminum oxide as a variety of nanomaterials. This paper presents experimental data on the structure of porous anodic alumina and the dependence of the anodic current on the parameters of the production process. The change in the growth rate of POA films as a function of the anodization time was studied.

1. Introduction

Among the porous membranes, PAOA-based membranes, formed by the method of electrochemical anodizing of aluminum foil, are of the greatest interest. Membranes obtained by electrochemical anodization are highly ordered structures with parallel vertical pores [1, 2].The unique porous structure, the parameters (diameter, length and distance between adjacent pores) of which can be varied during the synthesis process allows the use of films of porous aluminum oxide as inorganic membranes, templating material for the synthesis of nanowires or nanotubes with a controlled diameter and high geometric anisotropy, as well as 2D photonic crystals and biosensors [3,4,5]. Geometric parameters of porous alumina depend on the formation conditions: voltage, anode current, time and temperature.

Aluminum foil (99.999%) with a thickness of 0.5 mm was used as the starting material for the synthesis of films of porous aluminum oxide. In order to increase the size of aluminum crystallites, remove micro stresses and subsequently achieve better ordering of Al pores, the substrate was annealed in air for 10 hours at 160 °C and then for 20 hours at a temperature of 450 ° C (heating rate in both cases was 1 °C/min) muffle furnace. Then, the oxide layer formed on the foil surface was removed by electrochemical polishing of aluminum in a mixture of 40g CrO_3 + 210 ml H_3PO_4 (concentrated acid) + 45 ml H_2O at a temperature of 80°C. The membranes based on porous alumina were obtained by a two-stage anodizing process in 0.4 M oxalic acid at a temperature of 4–19 ° C. With an increase in the magnitude of the voltage, the thickness of the porous film, which grows in the same time, increases; the growth rate of the film grows sublinearly. With increasing voltage value, the initial value of the anode current also increases (Figure 1).

a - at T = 19 ° C; b - at T = 4 ° C

Fig. 1. Graph of anode current versus anodization time

As can be seen from Figure 1, the anode current in the anodization process gradually decreases, which, as already noted, indicates the beginning of pore formation and further stabilization of the anode current occurs when the pores grow deep into the oxide film. According to the data obtained on the dependence of the anode current on the time of the anodization process, it can be concluded that the maximum current value at room temperature is higher than at low temperature, and this can be traced for all voltage values. Measurement errors do not exceed the allowed values.

References

[1] W. Lee, R. Ji, U.G. Sele, K. Nielsch, “Fast fabrication of long-range ordered porous alumina membranes by hard anodization”, Nature materials. 2006. V. 5 P. 741 – 747.

[2] Y. Du, W.L. Cai, C.M. Mo, J. Chen, L.D. Zhang and X.G. Zhu, “Preparation and photoluminescence of alumina membranes with ordered pore arrays”, Applied Physics Letters. V. 74. № 20. 1999. P. 2951-2953.

[3] S. Shingubara, “Fabrication of nanomaterials using porous alumina templates”, Journal of Nanoparticle Research. vol. 5, 2003, pp. 17–30.

[4] L. Velleman, G. Triani, P.J. Evans, J.G. Shapter, D. Losic, “Structural and chemical modification of porous alumina membranes”, *Microporous Mesoporous Mater.* 2009, *126*, 87–94.

[5] M. Batalova, B. Alpysbayeva, N. Korobova, M. Kadir, M. Yskak, Zh. Kalkozova, “Structural Features of Nanoporous Aluminum Oxide Membranes Using Atomic Force Microscopy”, 2019 IEEE Conference in Russian, 1999-2002.

Study of variations in ground-level radiation background from natural terrestrial radionuclides and their influence on the occurrence of cancer risks among the population

Dyachkov V.V.[1], Zaripova Yu.A.[1], Yushkov A.V.[1], Shakirov A.L.[1], Bigeldiyeva M.T.[1], Dyussebayeva K.S.[2], Abramov K.E.[1]

[1] *National Nanotechnology Laboratory of Open Type, Almaty, Kazakhstan;*
[2] *Kazakh National University named al-Farabi, Almaty, Kazakhstan;*
E-mail: slava_kpss@mail.ru

Nowadays, special attention of public and international institutions is given to reasoning and creating ways to ensure the safety of the population from natural radioactive radon. Radiologically, radon is the predominant source of exposure to the public. The contribution of radon to the total radiation dose of people reaches more than 50%. The study of the mechanisms of alpha radiation of radon on biological organisms and the study of the concentration of radon and its daughter decay products in the habitable human environment is the main urgent task and the subject of study of this problem by this team of authors over 10 years. Within the framework of the previous and present projects, the authors obtained the following results on the study of variations in the prism background radiation from natural terrestrial radionuclides and their influence on the occurrence of cancer risks among the population.

To study the effect of natural alpha radiation from radon isotopes on biological organisms, a series of experiments were conducted to register radon emanation in the vicinity of tectonic faults and to collect relevant data on the incidence of lung cancer in people living in their immediate vicinity [1]. Mechanisms have been proposed that lead to the occurrence of such diseases.

The authors measured radon activity over a long period of time from 2016 to 2018 with a measurement frequency of 2 hours and revealed diurnal, seasonal variations. For the first time, in addition to the well-known daily variations, periodic 4-day variations in the emanation of soil radon were experimentally detected, measured, and determined. Experiments were carried out on the content of beta radionuclides of the daughter products of the decay of radon contained in the soil of the surface layer of the earth at various places in Almaty. The result of these experiments was a map of the beta contamination of the city of Almaty [2].

Based on the complex study of sources, diffusion and accumulation of radon and its DPR, a concept was developed based on the ventilation system of the building [3].

The work was supported by the state grant financing of basic research (project No. IRN AP05131884)

1. Khamdieva O.H., Biyasheva Z.M., Zaripova Yu.A., Dyachkov V.V., Yushkov A.V. Tectonic faults influence that reinforce radon emanation and cancer lung risk // 41st FEBS Congress, Molecular and Systems Biology for a Better Life Journal, 283 (Supplement S1), 03-08 September, 2016, Ephesus/Kuşadasi, Turkey, pp. 254 – 255
2. Dyachkov V.V., Zaripova Yu.A., Yushkov A.V., Shakirov A.L., Biyasheva Z.M., Bigeldiyeva M.T., Dyussebayeva K.S., Abramov K.E. A Study of the Accumulation Factor of the Daughter Products of Radon Decay in the Surface Layer Using Beta Spectrometry // Physics of Atomic Nuclei, 81 (10), 2018, pp. 1509 – 1514
3. Dyachkov V.V., Zaripova Yu.A., Yushkov A.V., Shakirov A.L. Building ventilation system. Patent for useful model. № 2017/0623.2.

Investigating bound entangled two-qutrit states via the best separable approximation

Ayatola Gabdulin, Aikaterini Mandilara
Department of Physics, School of Science and Technology, Nazarbayev University, 53 Qabanbay Batyr Avenue, Astana 010000, Kazakhstan
E-mail: *ayat.gabdulin@gmail.com*

Abstract: We use the linear programming algorithm introduced in [1] to perform Best Separable Approximation [2] on random sets [3] of density matrices representing bipartite systems of two qutrits. It is known that for this case a small volume of PPT (bound) entangled states exist, and these states form layers on the outer surface of polytope of separable states. We devise a method for estimating from our numerical results the thickness of these layers as well as the percentage of the surface of the separable polytope covered by these. We compare these results with studies in bipartite systems of dimension 12 and we draw preliminary conclusions on the growth of volume of bound entangled bipartite states with the dimension of the Hilbert space.

[1] V. M. Akulin, G. A. Kabatyanski, A. Mandilara, "Essentially entangled component of multipartite mixed quantum states, its properties, and an efficient algorithm for its extraction," Phys. Rev. A 92, 042322 (2015).
[2] M. Lewenstein and A. Sanpera, "Separability and Entanglement of Composite Quantum Systems," Phys.Rev.Lett. 80, 2261-2264 (1998).
[3] K. Zyczkowski, K. A. Penson, I. Nechita and B. Collins, "Generating random density matrices," J. Math. Phys. 52, 062201 (2011).

Cost-effective Synthesis of Photocatalytic Active ZnO Nanoplates

Y.U. Kedruk[1], L.V. Gritsenko[1,2], G. Cicero[3], Kh.A. Abdullin[2]

[1]*Kazakh National Research Technical University after K.I. Satpayev, Satpayev str., 22, Almaty, Kazakhstan*

[2]*National nanotechnology laboratory of open type at al-Farabi Kazakh National University, al-Farabi ave., 71, Almaty, Kazakhstan*

[3]*Department of Applied Science and Technology, Politecnico di Torino, Corso Duca degli Abruzzi, 24, 10129 Turin, Italy*

Author e-mail address: janegirl10@mail.ru

Abstract: Recently, photocatalysis is widely used in the creation of renewable energy sources, as well as for cleaning the environment. In this work cost-effective hydrothermal synthesis of ZnO powders was developed. The effect of the concentration of the basic solution components on the morphology and structural properties of the synthesized samples was studied. A correlation between the morphology of the synthesized zinc oxide powders and their photocatalytic activity was established.

Lately, the process of photocatalytic degradation is becoming increasingly important as an effective technology for the treatment of wastewater containing stable and hazardous organic substances [1-3]. This process has several advantages compared to other cleaning methods, such as complete mineralization, no waste disposal problems, low cost and no need for extremely mild conditions for temperature and pressure [2]. At the moment, a significant amount of information has been accumulated about the process of photocatalytic mineralization in terms of reactions and mechanism, degradation of individual compounds, comparison of various photocatalysts, etc. [3, 4]. Also photocatalytic processes using semiconductor nanoparticles in terms of the removal of organic matter, the destruction of cancer cells, bacteria and viruses was developed [5]. Therefore, the development of photocatalytic materials exhibiting a high intensity of photoinduced molecular transformations and reactions on the surface is highly relevant.

ZnO nanopowders were synthesized by a low-cost hydrothermal method at room temperature. The growth solution contained zinc acetate dihydrate $(CH_3COO)_2Zn\times2H_2O$ and sodium hydroxide NaOH dissolved in distilled water. The study of the obtained samples by electron microscopy showed that an increase in the alkali concentration of the growth solution with the remaining synthesis parameters unchanged causes a decrease in the geometric parameters of the synthesized ZnO powders. Changing the NaOH concentration in grows solution allows us to synthesize ZnO powders with different morphologies such as large pointed elongated particles, small particles of irregular spherical shape, as well as in the form of thin nanoplates (Fig. 1). The results of the X-ray diffraction study showed that all synthesized ZnO samples demonstrate the hexagonal structure of wurtzite.

All prepared samples demonstrate high photocatalytic activity, which is superior to commercial zinc oxide powders. It was noted that photocatalytic degradation of Rhodamine-B (RhB) proceeds faster in the presence of ZnO nanoplates, synthesized at a higher concentration of NaOH during low-temperature, cost-effective synthesis, due to a higher specific surface of these structures.

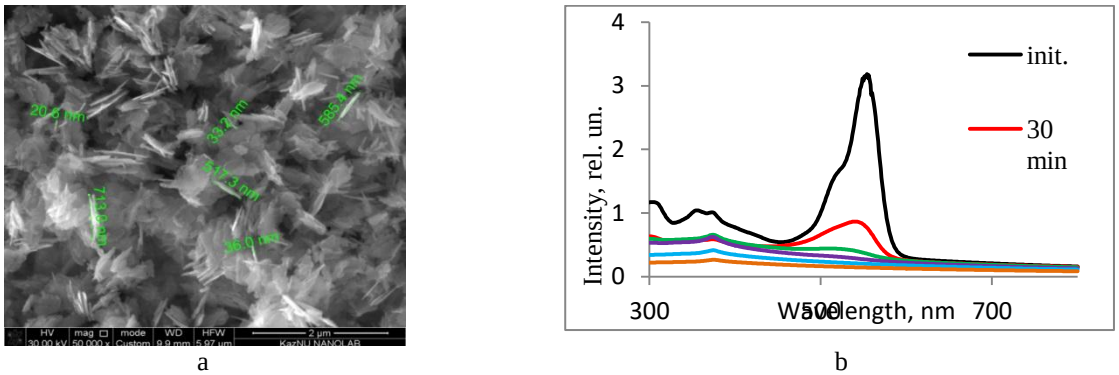

a b

Fig. 1. ZnO sample, synthesized in an aqueous solution at room temperature for 15 minutes;
a - the morphology, b - changes in the optical density spectra of an aqueous solution of RhB with a ZnO sample with UV light for 150 minutes

This work was supported by grant AP05130100 of Ministry of Education and Science of the Republic of Kazakhstan.

References

[1] Mills A., Davies R.H. and Worsley D., "Water purification by semiconductor photocatalysis", Chem. Sos. Revs. 22:417–425 (1993).
[2] Legrini O., Oliveros E. and Braun A.M., "Photochemical processes for water treatment", Chem. Rev. 93:671–698 (1993).
[3]Pelizzetti E., Minero C., Borgarello E. and Tinucci L., "Photo- catalytic activity and selectivity of titania colloids and particles prepared by the sol–gel technique: photooxidation of phenol and atrazine", Langmuir 9: 267-3001(1993).
[4] Lisenbigler A.L., Guangquan L. and Yates J.T., "Photocatalysis on TiO_2 surfaces: principles, mechanisms, and selected results", Chem. Rev. 95: 735–758(1995).
[5] Mills A., Punte L. and Stephan M., "An overview of semiconductor photocatalysis", J. Phosochem. Photobiol. A 108: l–35 (1997).

Noether symmetry approach in teleparallel gravity with fermionic field for anisotropic universe

Myrzakulov Kairat, Kenzhalin Duman

L.N. Gumilyov Eurasian National University, Eurasian International Centre for Theoretical Physics and Department of General and Theoretical Physics, Nur-Sultan 010008, Kazakhstan

E-mail: krmyrzakulov@gmail.com

Abstract: In the present work, we consider a model with a fermionic field that is non-minimally coupled to teleparallel gravity for Bianchi type I universe. We found exact solutions which describing late accelerating expansion.

In the present work, we consider a model with a fermionic field that is non-minimally coupled to gravity in the framework of teleparallel gravity for Bianchi type I universe [1-3]. Here we obtained the corresponding field equations.

$$\frac{\dot{A}\dot{B}}{AB}+\frac{\dot{A}\dot{C}}{AC}+\frac{\dot{C}\dot{B}}{CB}-\frac{1}{2F}V=0, \tag{1}$$

$$\frac{\ddot{B}}{B}+\frac{\ddot{C}}{C}+\frac{\dot{B}\dot{C}}{BC}+\frac{\dot{F}}{F}\left(\frac{\dot{B}}{B}+\frac{\dot{C}}{C}\right)+\frac{1}{2F}\left(\frac{i}{2}\left(\bar{\psi}\gamma^{0}\dot{\psi}-\dot{\bar{\psi}}\gamma^{0}\psi\right)-V\right)=0, \tag{2}$$

$$\frac{\ddot{A}}{A}+\frac{\ddot{C}}{C}+\frac{\dot{A}\dot{C}}{AC}+\frac{\dot{F}}{F}\left(\frac{\dot{A}}{A}+\frac{\dot{C}}{C}\right)+\frac{1}{2F}\left(\frac{i}{2}\left(\bar{\psi}\gamma^{0}\dot{\psi}-\dot{\bar{\psi}}\gamma^{0}\psi\right)-V\right)=0, \tag{3}$$

$$\frac{\ddot{A}}{A}+\frac{\ddot{B}}{B}+\frac{\dot{A}\dot{B}}{AB}+\frac{\dot{F}}{F}\left(\frac{\dot{A}}{A}+\frac{\dot{B}}{B}\right)+\frac{1}{2F}\left(\frac{i}{2}\left(\bar{\psi}\gamma^{0}\dot{\psi}-\dot{\bar{\psi}}\gamma^{0}\psi\right)-V\right)=0 \tag{4}$$

Here we use Noether symmetry approach for determine forms of the coupling and potential function of fermionic field as $F=F_0\Psi$ and $V=V_0\psi$. Finally, we found exact solutions for these functions as de Sitter solutions.

References

[1] Cai Y-F., Capozziello S., De Laurentis M., Saridakis E.N. "F(T) teleparallel gravity and cosmology" Reports on Progress in Physics, Vol. 79, p. 106901(2016.)

[2] Myrzakulov R. "Accelerating universe from F(T) gravity" The European Physical Journal C. Vol. 71, p. 1752 (2011).

[3] Kucukakca Y. "Teleparallel dark energy model with a fermionic field via Noether symmetry" The European Physical Journal C. Vol. 74, No. 10. p. 3086 (2014).

Metric $F(R)$ gravity with tachyon field

Myrzakulov Nurgissa, Darigozova Azhar, Meirbekov Bekdaulet

L.N. Gumilyov Eurasian National University, Eurasian International Centre for Theoretical Physics and Department of General and Theoretical Physics, Nur-Sultan 010008, Kazakhstan

E-mail: nmyrzakulov@gmail.com

Abstract: A model for a homogeneous and isotropic Universe whose gravitational sources are a pressureless matter field and a tachyon field non-minimally coupled to the $F(R)$ gravity is analyzed. Gravitational field equation for our model is derived.

1. Introduction

In the context of scalar fields the models with tachyon fields minimally coupled to the $F(R)$ received a considerable attention. The tachyon field has its roots in string theory, but it can be introduced in a simple manner as a generalization of the Lagrangian density of a relativistic particle, i.e., $L = -m\sqrt{1-\dot{q}^2} \rightarrow L_\varphi = -V(\varphi)\sqrt{1-\partial^\mu\varphi\partial_\mu\varphi}$, in the same way that the quintessence could be considered as a generalization of the Lagrangian density for a non-relativistic particle, namely, $L = \frac{\dot{q}^2}{2} - V(q) \rightarrow L_\varphi = \frac{\partial^\mu\varphi\partial_\mu\varphi}{2} - V(\varphi)$. In this work it is discussed the role of the tachyon field within a cosmological framework and the search for any relationship of the tachyon field to its root in string theory is not considered.

2. Model and field equations

The action for a tachyon field non-minimally coupled to the $F(R)$ is written as

$$S = \int\sqrt{-g}\ d^4x\ \{h(\varphi)R - V(\varphi)\sqrt{1-\partial_\mu\varphi\partial^\mu\varphi}\} + S_m, \tag{1}$$

Equation of motion are

$$\frac{\ddot{a}}{a} = -\frac{\rho + 3p}{12Fh} \tag{2}$$

where

$$p = -V\sqrt{1-\dot{\varphi}^2} + hF - F_R Rh + 4HF_R h'\dot{\varphi} + F_R h''\dot{\varphi}^2 + F_R h'\ddot{\varphi} \tag{3}$$

$$\rho = \rho_\varphi + \rho_m,\ \rho_\varphi = 6HF_R h'\dot{\varphi} + Fh + F_R Rh + \frac{V}{\sqrt{1-\dot{\varphi}^2}} \tag{4}$$

3. Concluding remarks

In this paper we consider tachyon field non-minimally coupled to the $F(R)$ gravity. Equation of motion for our model is derived.

4. References

[1] Souza de C. Rudinei., Kremer G.M. “Constraining nonminimally coupled tachyon fields by the Noether symmetry” Classical and Quantum gravity 26, 135008 (2009).

Cylindrical solutions in gravity's rainbow

Myrzakulov Yerlan, Bekkhozhayev Saidkhozha, Yergaliyeva Gulmira
L.N. Gumilyov Eurasian National University, Eurasian International Centre for Theoretical Physics and Department of General and Theoretical Physics, Nur-Sultan 010008, Kazakhstan
E-mail: ymyrzakulov@gmail.com

Abstract: In this work, we study the various cylindrical solutions (cosmic strings) in gravity's rainbow scenario. We discuss the possible Kasner, quasi-Kasner and non-Kasner exact solutions of the field equations. In this framework, we find that quasi-Kasner solutions cannot be realized in gravity's rainbow.

1. Introduction

In this work, we first briefly review the basics of energy-dependent Einstein field equations described by a specific rainbow functions. Following the basic properties of cosmic strings, we write the metric of the cosmic string in gravity's rainbow. Implementation the metric of the cosmic string in gravity's rainbow to the Einstein field equations leads to a set of differential equations in terms of rainbow function. In order to realize the exact solutions of these differential equations, we consider the two parametric metric solution (so-called Kasner solution, which is an unique exact solution for the Einstein equations with cylindrical symmetry). In addition to that we also discuss the possibility of the quasi-Kasner and non-Kasnersolutions. In this regard, we find that the quasi-Kasner solutions cannot be realized in gravity's rainbow [1].

2. Realization of Kasner's solution in gravity's rainbow

In this section, to find the exact solution, we focus, in particular, Kasner's solution in gravity's rainbow. The two parametric metric, so-called Kasner solution, is an unique exact solution for the Einstein equations with cylindrical symmetry in GR (Kasner 1921, 1925; Kramer et al. 1980). This is given by following line element:

$$ds^2 = (kr)^{2a}dt^2 - dt^2 - \beta^2(kr)^{2(b-1)}r^2d\varphi^2 - (kr)^{2c}dz^2 \tag{1}$$

here k defines an appropriate length scale and β is a constant and it is related directly to the deficit angle of the conical space-time.

3. Concluding remarks

In this work, we have investigated the static cylindrical solutions for Einstein's field equations in gravity's rainbow. The cosmic string metric is supposed to be static (i.e. with vanishing off diagonal components and time independent) and cylindrically symmetric. In this setting, we have discussed cosmic strings in energy-dependent background. The fields equations following this metric lead to various energy-dependent differential equations. In order to solve these differential equations, we have considered the possibility of Kasner's, quasi-Kasner and non-Kasner solutions. It is well-known that the Kasner solutions are two parametric metric and unique exact solutions for the Einstein equations with cylindrical symmetry. It is shown that the quasi-Kasner solutions cannot be realized in gravity's rainbow. Also, we have found that the gravity's rainbow cosmic strings follow same behavior (singularities) to that of standard GR theory.

4. References

[1] Momeni D.,· Upadhyay S.,· Myrzakulov Y.,· Myrzakulov R. "Cosmic string in gravity's rainbow" Astrophysics and Space Science 362, 148 (2017).
[2] Kasner E. "Geometrical Theorems on Einstein's Cosmological Equations", American Journal of Mathematics, Vol. 43, No. 4, pp. 217-221 (1921).
[3] Kasner E. "Solution of the Einstein equations involving functions of only one variable", Trans. American Math. Soc., 27, pp. 155-162.
[4] Kramer D., Stephani H., MacCallum M., Hoenselaers C., Herlt E. "Exact Solutions of Einstein's Field Equations", Cambridge Monographs on Mathematical Physics, 2nd Edition (2003).

The age of the Universe in Einstein-Maxwell model with g-essence

Razina O., Tsyba P., Meirbekov B., Azimbay L., Kenzhaliev D., Mukasheva A., Zhassybaeva M.

Eurasian International Center for Theoretical Physics and Department of General and Theoretical Physics Eurasian National University, Nur-Sultan

E-mail: razina_ov@enu.kz

Abstract: Based on the proposed model, we analyzed the age of the universe. For the fixed value of Ω_m, the age of the Universe depends on n. According to observational data, the age of the universe should be ~13.5 Gyr., which corresponds to $n = \frac{2}{3}$, and in our model for the realization of the possibility of accelerated expansion of the universe, the condition $n > 1$ must be satisfied. Thus, the age of the universe of the investigated model is more than ~13.5 Gyr.

We consider the accelerated expansion of the universe in the context of Einstein-Maxwell model with g-essence [1]. Lets then start from equation $q = -1 + \frac{1}{n}$. and $q(z) = \frac{1+z}{H}\frac{dH}{dz} - 1$, find the Hubble parameter as a function of the redshift z as

$$H(z) = nH_0(1+z)^{\frac{1}{n}}, \tag{1}$$

where $a_0/a = 1 + z$ with a_0 and H_0 being the values of the parameter at the present epoch. Within the flat universe, dark energy picture, to the Friedmann equations give the expansion rate as

$$H^2(z)/H_0^2 = \Omega_m(1+z)^3 + \delta H^2/H_0^2, \tag{2}$$

where now we encapsulate any modification to the Friedmann equation of general relativity in the last term, $\Omega_m = \rho/\rho_{0c}$, $\rho_{0c} = 3H_0^2$. Also, defining the effective EOS, denoted by $w_{eff}(z)$, as

$$w_{eff}(z) = -1 + \frac{1}{3}\frac{d\ln\delta H^2}{d\ln(1+z)}, \tag{3}$$

we can calculate $w_{eff}(z)$ using equations (1)-(3) with the result

$$w_{eff} = -1 + \frac{1}{3}\frac{\frac{n}{2}(1+z)^{\frac{2}{n}} - 3\Omega_m(1+z)^3}{n^2(1+z)^{\frac{2}{n}} - \Omega_m(1+z)^3}. \tag{4}$$

For $n = 2$ and $\Omega_m = 0.33$ we have $w_{eff} \leq -1$, which is the characteristic of one type of dark energy, the so-called phantom and from equation (4), for $n \to +\infty$, we have $w_{eff} \to -1$.

To continue we consider the age of the universe in Einstein-Maxwell model with g-essence. Thus, the age of the matter dominated Universe in FLRW models is given by

$$t_0 = \frac{2}{3}\frac{1}{\sqrt{1-\Omega_m}}H_0^{-1}\ln\left[\frac{1+\sqrt{1-\Omega_m}}{\sqrt{\Omega_m}}\right], \tag{5}$$

where $H_0^{-1} = 9.8 \times 10^9 h^{-1}$ years and the dimensionless parameter h, according to present data, is about 0.7. Hence, in the flat matter dominated universe with $\Omega_{total} = 1$ the age of the universe would be only $t_0 = \frac{2}{3}H_0^{-1} =$ 9.3 Gyr. This value, even taking into account the uncertainty in the measurement of H_0, contradicts the independent restrictions on the age of the universe ~13.5 Gyr. We obtain the age of the universe by taking matter in the Friedmann equations as follows

$$t_0 = n\frac{1}{\sqrt{1-\Omega_m}}H_0^{-1}\ln\left[\frac{1+\sqrt{1-\Omega_m}}{\sqrt{\Omega_m}}\right]. \tag{6}$$

For a flat, matter dominated Universe with $\Omega_m = 0.33$ and $n = \frac{2}{3}$ we have a prediction for the age of the Universe of about 13.2 Gyr. It seems that the age of the universe in our model is longer than the FLRW model. Figure 1 shows the behavior of the age parameter, t_0, as a function of Ω_m for different values of n.

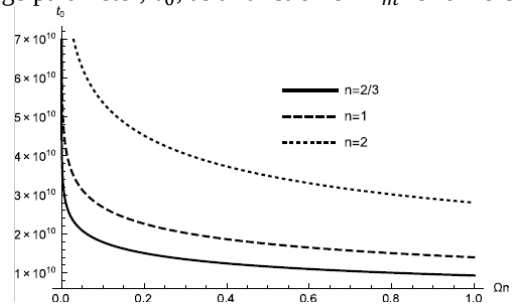

Fig. 1. t_0 as a function of Ω_m for $n = 2/3$ (solid line), $n = 1$ (dashed line) and $n = 2$ (dotted line). Figure shows that for a fixed value of Ω_m the predicted age of the universe is longer for larger values of n.

[1] Razina O., Tsyba P., Meirbekov B., Myrzakulov R., "Cosmological Einstein-Maxwell model with g-essence," Int. J. Mod. Phys. D **28,** 1950126 (2019).

Luminescent properties of nanocrystalline TiO_2 films

Serikov T.M, Ibrayev N.K.
Institute of Molecular Nanophotonics, E.A. Buketov Karaganda State University, Karaganda, Republic of Kazakhstan,
E-mail: niazibrayev@mail.ru

Spectral and kinetic properties of photoluminescence of films obtained from TiO_2 nanoparticles and nanotubes are investigated. Films of titanium dioxide (Sigma Aldrich) nanoparticles were made by the method of "doctor-blading". Titanium dioxide nanotubes are synthesized by electrochemical anodizing. Further, the films were subjected to heat treatment at a temperature of 773K and 1273K. The excitation was carried out by a nitrogen laser (λgen=337 nm) at the residual pressure of the cryostat . At room temperature, no luminescence was observed for all samples. When cooling the films up to T=160 K in the wavelength range of 400 – 800 nm, a wide band of luminescence is registered with maxima at 510 and 540 nm (Fig. 1A) that correspond to anatase modification. When the substrate temperature decreases up to 90 K, the intensity of the glow increases [1].

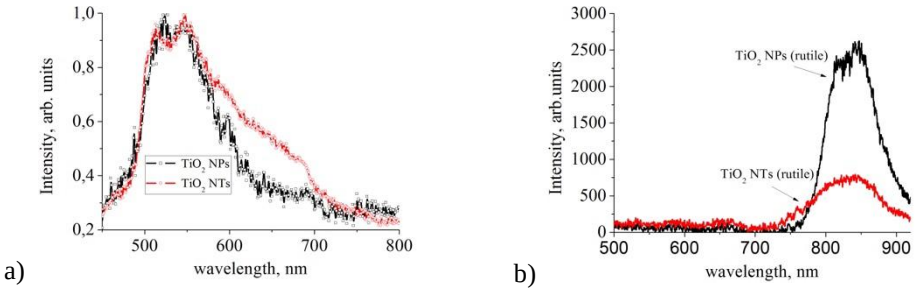

a) b)

Fig. 1. Luminescence spectras of the film annealed at 773K (a) and 1273 K(b)

The nature of this luminescence is associated with defects located in the near-surface region of crystallites, and possibly associated with possible defect states: autolocalized excitons STE (self–trapped excitons) and Ti3+. Comparison of the luminescence spectra shows that the luminescence intensity of nanotubes in the region of 600-700 nm is higher than in the case of nanoparticles. The Gaussian approximation established that the observed luminescence spectra are formed by three bands with maxima at 510, 540 and 600 nm, that is, three luminescence centers (defective levels) located at different depths in the band gap. Annealing of samples at T=1273 K leads to a long-wave shift of the photoluminescence band with a maximum wavelength of 850 nm, which corresponds to the rutile structure (Fig. 1b). For all observed defective luminescence centers, the luminescence decay kinetics were measured and the lifetimes of the excited States of the defective centers were calculated from the exponential part of the damping curves, the results of which are shown in table 1.

Table 1–Duration of films luminescence of TiO2 nanoparticles and nanotubes

Example	Excitation wavelength			
	510 nm	540 nm	600 nm	850
Nanoparticles (773 K)	τ=6,25 ms	τ=3,19 ms	τ= 6,7 ms	τ= 7,5 ms
Nanotubes (773 K)	τ=2,50	τ=0,8 ms	τ=6,3 ms	τ= 8 ms

Serikov T.M, Ibrayev N.K., Nuraje N., Savilov S.V., Lunin V.V. LuInfluence of surface properties of the titanium dioxide porous films on the characteristics of solar cells // Russian chemical bulletin.– № 66, T. 4.–P. 614-621.

Refractive indexes and properties of thin cryovacuum deposition films of organic molecules

A. Aldiyarov[1], D. Sokolov[1], A.Nurmukan[1], A.Kolomiitseva

Al-Farabi Kazakh National University, Institute of Experimental and Theoretical Physics, 71 al-Farabi Ave., 050040 Almaty, Republic of Kazakhstan

Author e-mail address: yasnyisokol@gmail.com

Abstract: As objects of research in recent decades, cryovacuum deposits, formed from the simplest organic gaseous substances are increasingly being selected [1]. One of the widely used classes of substances in this respect are alcohols and Freon's [2-4], which offer a line of structurally identical substances with different molecular sizes and masses. Such a choice is caused by chance within a particular family study the effect of the degree of complexity of the molecules on the properties of the glassy state [5], including their kinetic stability, as well as astrophysical interest in connection with the frequent detection of these substances in outer space [6].

The hydrogen-bonded and organic substances - ethanol, carbon tetrachloride, Freon 134a etc. are presented. The choice of temperature range of research from 16 K to 150 K is due to the presence of structural transformations for these substances.

Mechanisms of glassy states of matter, their connection with the basic properties of the resulting glasses are a set of questions, the answers to which will allow bettering understanding the nature of the formation as a completely deposited state. Having in mind that the concept of the glassy state applies not only to amorphous, but also to the liquid crystal, and even crystalline materials with any type of disorder, the known water glass freezing transition is just one example of a class "glass transition" due to loss of balance, which should occur quite often in condensed matter [7-8]. The same circumstance significantly expands the number of objects of investigation glass-forming states and methods for their preparation and subsequent analysis.

As for the methods for obtaining glass-like materials, in recent decades, the method of physical cryogenic deposition from the gas phase to the cooled substrate has been widely used [9-10], which makes it possible to control the necessary phase-formation conditions-substrate temperature and gas phase pressure (condensation rate). This, in turn, allows the experimental verification of a number of theoretical models for the formation of disordered condensed states. In particular, it can be a test of the model of Ramos [9], in which the influence of the anisotropic structure of molecules on the formation of organic glasses of varying degrees of stability is discussed. The mobility and residence time of molecules in the adsorption layer are considered as the main factors, which is determined by the temperature of the substrate and the rate of cryodeposition, the parameters that can most accurately be maintained in experiments when the samples are obtained precisely by the method of physical cryovacuum condensation. The experimental setup and the measurement procedure were described by us earlier [11].

The substances like a methane and nitrous oxide was additionally chosen for obtain optical properties.

2. References

[1] M.D.Ediger "Perspective: Highly stable vapor-deposited glasses", The journal of chemical physics 147, 210901 (2017).
[2] A. Drobyshev, A. Aldiyarov, A. Nurmukan, D. Sokolov, A. Shinbayeva, "Structure transformations in thin films of CF3-CFH2 cryodeposites. Is there a glass transition and what is the value of Tg?", Applied Surface Science. V.466, pp 196-200, (2018)
[3] A. Drobysheva, A. Aldiyarov, A. Nurmukan, D. Sokolov, and A. Shinbayeva, "IR Studies of Thermally Stimulated Structural Phase Transformations in Cryovacuum Condensates of Freon 134a", Low Temperature Physics 44, 831 (2018).
[4] A. Drobyshev, A. Aldiyarov, D. Sokolov, A. Shinbayeva, and N. Tokmoldin, Low Temperature Physics/Fizika Nizkikh Temperatur, v. 43, No. 10, pp. 1521–1524, (2017).
[5] S. Ramos, M. Oguni, K. Ishii, and H. Nakayama, "Character of devitrification, viewed from enthalpic paths, of the vapor-deposited ethylbenzene glasses," J. Phys. Chem. B 115, 14327–14332 (2011).
[6] R.L. Hudson, P.A. Gerakines, M.H. Moore, "Infrared spectra and optical constants of astronomical ices: II. Ethane and ethylene", Icarus 243, 148–157, (2014).
[7] Andrea Cavagna, Physics Reports 476, 51 (2009).
[8] H. Suga, S. Seki, J. Non-Cryst. Solids 16, 171 (1974).
[9] Aldiyarov A.; Aryutkina M.; Drobyshev A., Low Temp. Phys. 35, 251 (2009).
[10] Hudson, R. L.; Loeffler, M. J.; Gerakines, P. A., J. Chem. Phys. 146, 024304 (2017).
[11] A. Aldiyarov, M. Aryutkina, A. Drobyshev and V. Kurnosov, Low Temp. Phys. 37, 524 (2011).

Cosmological solutions in F(T) gravity with Chaplygin gas model

A. Zhadyranova, S. Nurkasymova, O. Razina, P. Tsyba

Eurasian International Center for Theoretical Physics and Department of General and Theoretical Physics, Eurasian National University, Nur-Sultan, 010008, Kazakhstan)

E-mail: pyotrtsyba@gmail.com

Abstract: The presence of spinor fields is considered in the framework of some extensions of telepar-
allel gravity, where the Weitzenb¨ ock connection is assumed. Some well-known models as the Chaplygin gas and its generalizations are reconstructed in terms of a spinor field in the framework of teleparallel gravity.

As a first example, let us consider the original Chaplygin gas, whose equation of state (EoS) is defined as [1]:

$$\boldsymbol{p = -\frac{A}{\rho}}$$

where $\boldsymbol{A}$ is a positive constant. The cosmological model based on the Chaplygin gas was proposed for the first time as an alternative to the quintessences models for dark energy. Let us assume a potential for the spinor field which has the special form $\boldsymbol{V = V(\bar{\psi}, \psi)}$ where $\boldsymbol{u = \bar{\psi}\psi}$ is a scalar, and no other matter contribution. Then, in terms of the scale factor $\boldsymbol{a}$, has the following solution:

$$H = \pm 3^{\frac{1}{2}}(A + Ba^{-6})^{\frac{1}{4}},$$

$$\rho = (A + Ba^{-6})^{\frac{1}{2}}, p = -A(A + Ba^{-6})^{-\frac{1}{2}},$$

$$\psi_j = c_j a^{-\frac{3}{2}} e^{-iD}, \psi_l = c_l a^{-\frac{3}{2}} e^{iD}, j = 1,2, l = 3,4,$$

$$V = (A + Ba^{-6})^{\frac{1}{2}}.$$

Here $\boldsymbol{B, c_j, c_l, c}$ are constants, being $\boldsymbol{c = c_1^2 + c_2^2 + c_3^2 + c_4^2}$ and

$$D = \mp 0.5\sqrt{3}Bc^{-1}a^{-2}(A + Ba^{-6})^{-\frac{3}{4}}.$$

Whereas the scale factor is given by:

$$\boldsymbol{t = \frac{1}{6\sqrt[4]{A}}\left(\ln\frac{\sqrt[4]{A + Ba^{-6}} + \sqrt[4]{A}}{\sqrt[4]{A + Ba^{-6}} - \sqrt[4]{A}} - 2\arctan\sqrt[4]{1 + A^{-1}Ba^{-6}}\right)}$$

And the EoS parameter yields:

$$\boldsymbol{\omega = -1 + \frac{B}{B + Aa^6}}.$$

Finally the expressions for the potential, and the kinetic term can be expressed in terms of $\boldsymbol{u}$:

$$\boldsymbol{V = \sqrt{A + Bc^{-2}u^2}},$$

$$\boldsymbol{Y = Ba^{-6}\left(A + Ba^{-6}\right)^{-\frac{1}{2}}},$$

$$\boldsymbol{u = ca^{-3}}.$$

In the work, the teleparallel theory of gravity in the framework of which is obtained, the models proposed in the framework of this theory can be described by the state equations of the Chaplygin gas type.

References

[1] R. Myrzakulov, D. Saez-Gomes, P. Tsyba Cosmological solutions in F(T) gravity with the presence of spinor fields. International Journal of Geometric Methods in Modern Physics Vol. 12 (2015) 1550023 (14 pages)

Excitation spectra and UV luminescence of industrial YAG:Ce based phosphors

Aida Tulegenova[1], Victor Lisitsyn[2]
[1]*al-Farabi Kazakh National University,Almaty, 050040, Kazakhstan*
[2]*National Research Tomsk Polytechnic University, Tomsk, 634050, Russia*
E-mail: *tulegenova.aida@gmail.com*

The nature of the processes that converting the excitation energy into visible light by phosphors for LEDs has been studied completely insufficiently. The main difficulty in studying these processes thing is impossible to ensure high accuracy of reproduction of the results of the synthesis of multicomponent materials, which are YAG:Ce -based phosphors. The dependence on the synthesis conditions was demonstrated in a number of papers [1-2]. The study of processes stimulated by optical excitation in the phosphor can be facilitated by the study of additional luminescence bands to the main one, which are appear in the ultraviolet region of the spectrum.

The influence of optical radiation flux in the region of 290 and 210 nm leads to the appearance of luminescence in YAG: Ce based phosphors in the range from 300 to 450 nm. Figure 1 shows the luminescence spectra measured in the ultraviolet region upon excitation by radiation of a xenon lamp at 260 nm. In the spectrum there are two overlapping bands with maxima in the region of 315 and 380 nm.

Such spectra of ultraviolet luminescence are observed in the studied phosphors and upon excitation by radiation of chips at 265 and 275 nm. The luminescence spectra bands positions in all the studied phosphors are the same, but the ratio of their intensities is significantly different.

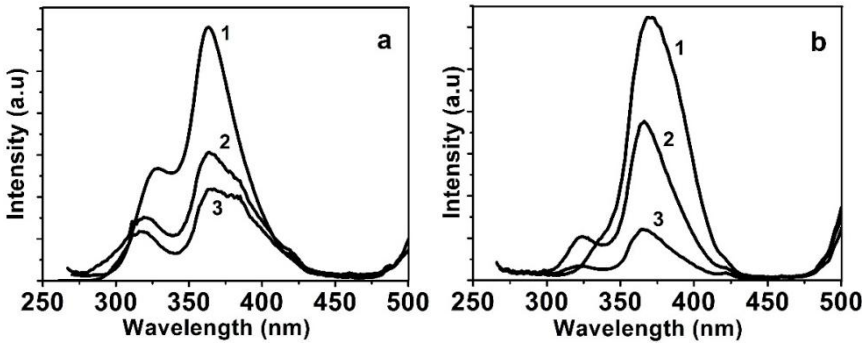

Fig.1. UV luminescence spectra of phosphors, a-AWS (1), L-2083 (2), MG 397 (3), b-YAG-05 (1), YAG-02 (2), YAG-04 (3) when excited at 260 nm

The presented research results allow the following conclusions. The luminescence centers responsible for ultraviolet luminescence are entered during the synthesis of phosphors, regardless of the initial composition of the charge. The luminescence centers responsible for the 315 and 380 nm bands are different, but are created under the same conditions.

References

[1] Lisitsyn V.M., Stepanov S.A., Valiev D.T., Vishnyakova E.A., Abdullin K.A., Markhabaeva A.A., Tulegenova A.T. Kinetic characteristics of the luminescence decay for industrial yttrium-gadolinium-aluminium garnet based phosphors, IOP Conference Series: Materials Science and Engineering. V. 110, 5 (2016)

[2] Lisitsyn V.M., Soshchin N.P., Yu Yangyang, Stepanov S.A., Lisitsyna L.A., Tulegenova A.T., Abdullin Kh. A. Photoluminescence characteristics of YAG:Ce, Gd based phosphors with different prehistories. Russian Physics Journal. V. 60, 865 (2017)